

Overview of the spin structure function g_1 at arbitrary x and Q^2

B.I. Ermolaev

Ioffe Physico-Technical Institute, 194021 St.Petersburg, Russia

M. Greco

Department of Physics and INFN, University Rome III, Rome, Italy

S.I. Troyan

St.Petersburg Institute of Nuclear Physics, 188300 Gatchina, Russia

In the present paper we summarize our results on the structure function g_1 and present explicit expressions for the non-singlet and singlet components of g_1 which can be used at arbitrary x and Q^2 . These expressions combine the well-known DGLAP-results for the anomalous dimensions and coefficient functions with the total resummation of the leading logarithmic contributions and the shift of $Q^2 \rightarrow Q^2 + \mu^2$, with $\mu/\Lambda_{QCD} \approx 10$ (≈ 55) for the non-singlet (singlet) g_1 respectively. In contrast to DGLAP, these expressions do not require the introduction of singular parameterizations for the initial parton densities. We also apply our results to describe the experimental data in the kinematic regions beyond the reach of DGLAP.

PACS numbers: 12.38.Cy

I. INTRODUCTION

As it is well-known, the spin structure function g_1 is introduced through the following conventional parametrization of the spin-dependent part $W_{\mu\nu}^{spin}$ of the hadronic tensor of the Deep Inelastic lepton- hadron Scattering:

$$W_{\mu\nu}^{spin} = iM_h \varepsilon_{\mu\nu\lambda\rho} \frac{q_\lambda}{Pq} \left[S_\rho g_1(x, Q^2) + \left(S_\rho - q_\rho \frac{Sq}{q^2} \right) g_2(x, Q^2) \right] \quad (1)$$

where we have used the standard notations: P is the hadron momentum, M_h is the hadron mass, S is the hadron spin, q is the virtual photon momentum. Traditionally, $-q^2 \equiv Q^2 > 0$ and $x = Q^2/2Pq$. The scalar functions $g_1(x, Q^2)$ and $g_2(x, Q^2)$ are called the spin structure functions. Both of them contribute to the asymmetry between the DIS cross sections when the lepton and hadron spins are antiparallel and parallel. In particular, g_1 describes such asymmetry when both spins are longitudinal, i.e. they lie in the plane formed by P and q . Obviously, in order to calculate the structure functions $g_1(x, Q^2)$ and $g_2(x, Q^2)$ in the framework of QCD, one should know the QCD behaviour at large and small momenta of virtual particles, i.e. one should be able to account for the perturbative and non-perturbative effects. At present this is impossible, so the standard description involves the factorization hypothesis: $W^{spin}_{\mu\nu}$ is represented as a convolution:

$$W_{\mu\nu}^{spin} = \widetilde{W}_{\mu\nu}^q \otimes \Psi_q + \widetilde{W}_{\mu\nu}^g \otimes \Psi_g \quad (2)$$

where Ψ_q and Ψ_g are the probabilities to find a polarized quark or gluon in the polarized hadron, while $\widetilde{W}_{\mu\nu}^{q,g}$ describe the DIS of the quarks and gluons. There is no model-independent theoretical description of the probabilities Ψ_q and Ψ_g in the literature because QCD at small momenta is not known. On the contrary, $\widetilde{W}_{\mu\nu}^q$ and $\widetilde{W}_{\mu\nu}^g$ can be calculated with the methods of Perturbative QCD, by summing the contributions of the involved Feynman graphs. So, the standard procedure is to replace Ψ_q and Ψ_g by the initial parton densities δq and δg . Both of them are found by fitting the experimental data at large x and not very large momenta Q^2 ($Q^2 = \mu^2 \sim 1 \text{ GeV}^2$). Therefore,

$$g_1 = g_1^q \otimes \delta q + g_1^g \otimes \delta g. \quad (3)$$

It is well-known that in the Born approximation

$$g_1^{Born} = (e_q^2/2)\delta(1-x) \otimes \delta q \quad (4)$$

where e_q is the electric charge of the quark interacting with the virtual photon. Accounting for the QCD radiative corrections to g_1^{Born} and other DIS structure functions, especially by trying to perform a complete resummation of

the corrections, has been the subject of great interest in recent years. Surely, such resummation cannot be performed precisely, so it would be important to resum, in the first place, the most essential corrections. They are different for different values of x and Q^2 . For example for describing g_1 in the region of $x \sim 1$ and large Q^2 , the contributions $\sim \ln^k x$ are negligibly small compared to $\ln^k(Q^2/\mu^2)$. In contrast, $\ln^k x$ becomes quite important at $x \ll 1$ and should be accounted for.

The goal of obtaining an universal description of the structure function g_1 , which could be used for arbitrary x and arbitrary Q^2 would be appealing both for theorists and experimentalists. Most generally, one encounters various kinematic regions where the DIS structure functions have been thoroughly studied. The first kinematic region is the so-called hard region **A** of large x and large Q^2 :

$$\mathbf{A}: \quad w \gtrsim Q^2 \gg \mu^2, \quad x \lesssim 1 \quad (5)$$

where $w = 2pq$ and μ^2 is the starting point of the Q^2 -evolution. Usually, the value of μ is chosen ≈ 1 GeV or so. Through the paper we use the standard notations: q is the virtual photon momentum, p is the initial parton momentum, and $x = Q^2/w$. The region **A** was described first by the LO DGLAP evolution equations obtained in Ref. [1]:

$$\begin{aligned} \frac{d\Delta q}{dt} &= P_{qq} \otimes \Delta q + P_{qg} \otimes \Delta g, \\ \frac{d\Delta g}{dt} &= P_{gq} \otimes \Delta q + P_{gg} \otimes \Delta g \end{aligned} \quad (6)$$

where we have used the standard notation $t = \ln(Q^2/\mu^2)$ and P_{ik} (with $i, k = q, g$) are the splitting functions. Δq and Δg are the evolved (with respect to Q^2) parton distributions. The splitting functions P_{ik} in the DGLAP evolution equations (6) include the QCD coupling α_s . In order to account for the running α_s -effects, one should define the argument of α_s . The DGLAP-prescription is

$$\alpha_s = \alpha_s(Q^2). \quad (7)$$

Through the paper we will address the parametrization (7) as the DGLAP-parametrization. Eqs. (6) describe the Q^2 -evolution of the parton distributions from $Q^2 = \mu^2$, with $\mu \sim 1$ GeV, to larger Q^2 . When general solutions to Eqs. (6) are obtained, one needs to specify appropriate initial conditions. Conventionally, the initial conditions to Eqs. (6) are

$$\Delta q|_{t=0} = \delta q, \quad \Delta g|_{t=0} = \delta g, \quad (8)$$

with $\delta q, \delta g$ being called the initial parton densities. They are found by fitting the experimental data at $Q^2 = \mu^2$. After Δq and Δg have been fixed, the DIS structure functions, including g_1 , are found by convoluting them with the coefficient functions C_q, C_g :

$$g_1(x, Q^2) = C_q(x/y) \otimes \Delta q(y, Q^2) + C_g(x/y) \otimes \Delta g(y, Q^2). \quad (9)$$

The Mellin transformations of P_{ik} are called the anomalous dimensions. The splitting functions P_{ik} and coefficient functions C_k for the unpolarized DIS were calculated with LO accuracy in Ref. [1]. The LO expressions for P_{ik} and C_k for the polarized DIS were obtained in Ref. [2]. Later, the LO expressions of Refs [1, 2] for P_{ik} and C_k were complemented by the NLO results[3]. A detailed review on that subject can be found in Ref. [4]. From pure theoretical grounds, this approach should not be used outside the region **A**. However, introducing special fits[5, 6] for the initial parton densities DGLAP has been extended to the region **B** of large Q^2 and small x :

$$\mathbf{B}: \quad w \gg Q^2 \gg \mu^2, \quad x \ll 1. \quad (10)$$

Indeed the parameterizations for $\delta q, \delta g$ of Ref. [5, 6] contain singular factors x^{-a} , and used in Eq. (8), they provide g_1 with a fast growth at small x . As a result, combining the LO evolution equations of Ref. [1] and NLO DGLAP results of Ref. [3] with the standard fits of Ref. [5, 6] it has been possible to describe the available experimental data on g_1 in regions **A** and **B**, i.e. for large Q^2 and arbitrary x . In the present paper we refer to this as the Standard Approach (SA). In addition to regions **A** and **B**, there are two more interesting kinematic regions:

$$\mathbf{C}: \quad 0 \leq Q^2 \lesssim \mu^2, \quad x \ll 1, \quad (11)$$

$$\mathbf{D}: \quad 0 \leq Q^2 \lesssim \mu^2, \quad x \lesssim 1. \quad (12)$$

Besides a purely theoretical interest, the knowledge of g_1 in the regions **C** and **D** is needed because they correspond to the kinematic region investigated experimentally by the COMPASS collaboration. Obviously, the regions **C** and **D** are beyond the reach of SA. Strictly speaking, the same could be said about the region **B**: In fact the expressions for P_{ik} are obtained (see Refs. [1, 3] for detail) under the assumption of the ordering

$$\mu^2 < k_{1\perp}^2 < k_{1\perp}^2 < \dots < Q^2 \quad (13)$$

where $k_{i\perp}$ are the transverse momenta of virtual ladder partons and they are numbered from the bottom of the ladders to the top. Once this ordering is kept one is led inevitably to neglect the double-logarithmic (DL) contributions $\sim \alpha_s \ln^2(1/x)$ and other contributions independent of Q^2 . Such contributions are small in the region **A** where they are correctly neglected in the SA. However, they become essential in the region **B**. In order to account for them, the DGLAP-ordering of Eq. (13) should be replaced by the other ordering:

$$\mu^2 < \frac{k_{1\perp}^2}{\beta_1} < \frac{k_{1\perp}^2}{\beta_2} < \dots < w \quad (14)$$

where β_j are the longitudinal Sudakov variables¹ for the virtual parton momenta k_j as follows:

$$k_j = -\alpha_j(q + xp) + \beta_j p + k_{j\perp} . \quad (15)$$

In order to account for such logarithmic contributions, Eq. (14) should be implemented by the ordering for β_i :

$$1 > \beta_1 > \beta_2 > \dots > \mu^2/w . \quad (16)$$

This ordering does not exist in DGLAP because in this approach $\beta_i \geq x \sim 1$. The ordering (14,16) was first introduced in Ref. [8] in the context of QED but it applies in QCD as well. Replacing the ordering (13) by Eqs. (14, 16) makes possible to sum up all DL contributions, regardless of their argument, to all orders in α_s , i.e. to perform calculations in the double-logarithmic approximation (DLA). Explicit expressions for g_1 in DLA were obtained in Ref. [10]. The drawback of those expressions is that α_s is kept fixed at an unknown scale. The effect of running α_s were taken into account in Ref. [11]. The parametrization of α_s in Refs. [11] differs from the DGLAP- parametrization. The theoretical grounds for this new parametrization were given in Ref. [12] and a numerical comparison with the standard parameterizations can be found in Ref. [13]. On the other hand, the reason why, in spite of the lack of the resummation of quite important contributions, the SA turned out to be working well in the region **B** remained unclear until in Refs. [14, 15] we proved that the factors x^{-a} in the DGLAP-fits for the initial parton densities mimic the total resummation of the leading logarithms of x . Besides, in Ref. [14] we suggested to combine the DGLAP- results for g_1 with the results of Ref. [11] in order to obtain a unified description of g_1 in the regions **A** and **B**, without singular initial parton densities. A prescription for extending g_1 into regions **C** and **D** was given in Ref. [16].

In the present paper we present a unified description of g_1 valid in all of the regions **A-D**. The paper is organized as follows: in Sect. II we briefly remind the DGLAP-description of g_1 . For the sake of simplicity we consider in more detail, throughout the paper, the non-singlet component of g_1 , and summarize the singlet results only. As the expressions for g_1 involve convolutions, they look simpler when an integral transform has been applied. The conventionally used transform is the Mellin one. However, in the small- x , region, it is more convenient the use of the Sommerfeld-Watson transform, whose asymptotics partly coincides with the Mellin transform. This formalism is the content of Sect. III. Before dealing explicitly with g_1 , we consider in Sect. IV the appropriate treatment of the QCD coupling and compare it with the DGLAP-parametrization. The total resummation of the leading logarithms of x is quite essential in the small- x region **B**. We discuss it in Sect. V by composing and solving appropriate Infrared Evolution Equations (IREE). Such equations involve new anomalous dimensions and coefficient functions and contain the total resummation of the leading logarithms of x . The singlet and non-singlet anomalous dimensions are calculated in Sect. VI. The non-singlet coefficient function is obtained in Sect. VII and is used to write down the explicit expression for the non-singlet g_1 in the region **B**. The singlet g_1 in the region **B** is obtained in Sect. VIII. In Sect. IX the small- x asymptotics of the non-singlet g_1 is discussed, whereas the singlet asymptotics is considered in Sect. X. Both asymptotic results are of the Regge type and their intercepts are found not so small. This may lead to the wrong conclusion that the IREE method cannot be applied safely to g_1 . In order to make this point clear, we discuss the applicability of our method in Sect. XI. In Sect. XII we compare our results for g_1 in the region **B** to the DGLAP expressions. We show that DGLAP works well in the region **B** only because of the singular factors present

¹ Sudakov variables were introduced in Ref. [7]

in the parameterizations for the initial parton densities. On the other hand, when such fits are used, g_1^{DGLAP} also behaves asymptotically as a sum of Reggeon contributions. The Regge behaviour in the two approaches is discussed in Sect. XIII. Combining the total resummation of the logarithms with the DGLAP results, we give in Sec. XIV the interpolation expressions describing g_1 in the unified region $\mathbf{A} \oplus \mathbf{B}$. Furthermore we show in Sects. XV and XVI how it is possible to describe g_1 in the small- Q^2 regions \mathbf{C} and \mathbf{D} and arrive thereby to the interpolation expressions for g_1 which can be used in the whole region $\mathbf{A} \oplus \mathbf{B} \oplus \mathbf{C} \oplus \mathbf{D}$. In particular the small- Q^2 regions \mathbf{C} and \mathbf{D} are described by a shift of Q^2 . Such shift is a source of new power Q^2 - corrections and we discuss them in Sect. XVII. Due to the experimental investigation of the singlet g_1 by the COMPASS collaboration, in Sect. XVIII we give an interpretation to the recent COMPASS data. Finally Sect. XIX contains our concluding remarks.

II. DGLAP -EXPRESSIONS FOR g_1

The Standard Approach to g_1 is based on the DGLAP evolution equations and also involves some standard parameterizations for the initial parton densities δq and δg . As the notations for the anomalous dimensions, the coefficient functions and the fits for the parton densities vary widely in the literature, we explain below the notation we use through the present paper.

We will denote $g_1^{NS \ DGLAP}$ and $g_1^{S \ DGLAP}$ the non-singlet and singlet parts of g_1 when the SA is invoked. As the expressions for g_1 involve convolutions, it is convenient to write them down in the Mellin integral form. In particular, the non-singlet g_1 is:

$$g_1^{NS \ DGLAP}(x, Q^2) = (e_q^2/2) \int_{-\infty}^{\infty} \frac{d\omega}{2i\pi} (1/x)^\omega C^{NS \ DGLAP}(\omega, \alpha_s(Q^2)) \delta q(\omega) \exp \left[\int_{\mu^2}^{Q^2} \frac{dk_\perp^2}{k_\perp^2} \gamma^{NS \ DGLAP}(\omega, \alpha_s(k_\perp^2)) \right] \quad (17)$$

where $C^{NS \ DGLAP}(\omega, \alpha_s(Q^2))$ is the non-singlet coefficient function, $\gamma^{NS \ DGLAP}(\omega, \alpha_s(Q^2))$ is the non-singlet anomalous dimension and $\delta q(\omega)$ is the initial quark density in the Mellin (momentum) space. With the one-loop accuracy (NLO) (see e.g. Ref. [3]), the expression for $C^{NS \ DGLAP}$ is

$$C^{NS \ DGLAP} = C_{LO}^{NS \ DGLAP} + \frac{\alpha_s(Q^2)}{2\pi} C_{NLO}^{NS \ DGLAP}, \quad (18)$$

with

$$C_{LO}^{NS \ DGLAP} = 1, \quad C_{NLO}^{NS \ DGLAP} = C_F \left[\frac{1}{n^2} + \frac{1}{2n} + \frac{1}{2n+1} - \frac{9}{2} + \left(\frac{3}{2} - \frac{1}{n(1+n)} \right) S_1(n) + S_1^2(n) - S_2(n) \right]. \quad (19)$$

Similarly, with two-loop accuracy,

$$\gamma^{NS \ DGLAP} = \frac{\alpha_s(Q^2)}{2\pi} \gamma^{(0)}(n) + \left(\frac{\alpha_s(Q^2)}{2\pi} \right)^2 \gamma^{(1)}(n) \quad (20)$$

where

$$\gamma^{(0)}(n) = C_F \left[\frac{1}{n(1+n)} + \frac{3}{2} - S_2(n) \right]. \quad (21)$$

We have used the standard notations $S_{1,2}$ in Eqs. (19,21):

$$S_1(n) = \sum_{j=1}^{j=n} \frac{1}{j}, \quad S_2(n) = \sum_{j=1}^{j=n} \frac{1}{j^2}. \quad (22)$$

They are defined for integer n . Their generalization for arbitrary n is well-known:

$$S_1(n) = \mathbf{C} + \psi(n-1), \quad S_2(n-1) = \frac{\pi^2}{6} + \psi'(n), \quad (23)$$

with \mathbf{C} being the Euler constant. The standard fits for the initial parton densities include the normalization constants $N_{q,g}$, the power factors x^{-a} , with $a > 0$ and more complicated structures; for example,

$$\delta q(x) = N_q x^{-\alpha} (1-x)^\beta (1+\gamma x^\delta) \equiv N_q x^{-\alpha} \varphi(x). \quad (24)$$

All parameters N_q , α , β , γ , δ in Eq. (24) are fixed by fitting the experimental data at large x and $Q^2 \approx 1 \text{ GeV}^2$.

The expressions for g_1^S *DGLAP* are similar but more involved and we do not discuss them in detail in the present paper. For the sake of simplicity through the paper we use g_1 non-singlet for illustration, when it is possible, but we present the final expressions for both the non-singlet and singlet explicitly.

III. SOMMERFELD-WATSON TRANSFORM

As it is well known, the DGLAP expressions for g_1 involve convolutions and in our approach we use them too. The standard way is to use an appropriate integral transform. Traditionally, the SA uses the Mellin transform. We will proceed slight differently. Our goal is to obtain expressions for g_1 at small x and will start by considering the spin-dependent forward Compton amplitude $T_{\mu\nu}$ related to $W_{\mu\nu}^{spin}$ as follows:

$$W_{\mu\nu}^{spin} = \frac{1}{2\pi} \Im T_{\mu\nu} \quad (25)$$

where the symbol \Im means the discontinuity (imaginary part) of $T_{\mu\nu}$ with respect to the invariant total energy $s = (p+q)^2$ of the Compton scattering. At large s , when hadron masses can be neglected,

$$s \approx 2pq(1-x) \equiv w(1-x), \quad (26)$$

so $s \approx w$ at small x . The amplitude $T_{\mu\nu}$ can be parameterized similarly to $W_{\mu\nu}^{spin}$:

$$T_{\mu\nu} = iM_h \varepsilon_{\mu\nu\lambda\rho} \frac{q_\lambda}{pq} \left[S_\rho T_1(x, Q^2) + \left(S_\rho - q_\rho \frac{Sq}{q^2} \right) T_2(x, Q^2) \right] \quad (27)$$

so that

$$g_1 = \frac{1}{2\pi} \Im T_1, \quad g_2 = \frac{1}{2\pi} \Im T_2. \quad (28)$$

We call $T_{1,2}$ the invariant amplitudes. Exploiting the factorization, $T_{1,2}$ can be represented as the convolution of the perturbative and non-perturbative contributions (cf. Eq. (3)). In particular,

$$T_1 = T_q \otimes \tilde{\delta}q + T_g \otimes \tilde{\delta}g \quad (29)$$

where $\tilde{\delta}q$ and $\tilde{\delta}g$ are related to δq and δg through Eq. (28). In the Born approximation (cf. Eq. (4)),

$$T_q^{Born} = e_q^2 \frac{s}{w - Q^2 + i\epsilon}, \quad T_g^{Born} = 0. \quad (30)$$

From the mathematical point of view, Eq. (29) as well as the DGLAP equations (6) and the expressions (9) for g_1 are convolutions, so an appropriate integral transform can be used. On the other hand, the phenomenological Regge theory (see e.g. [17]) states that in order to study accurately the scattering amplitudes at high energies, one should use the Sommerfeld-Watson (SW) transform[18]. The asymptotic form of the SW transform partly coincides with the Mellin transform and often this form is especially convenient to account for the logarithmic radiative corrections. The SW transform is actually related to the signature invariant amplitudes $T^{(\pm)}$ defined, in the context of DIS, as follows:

$$T^{(+)} = \frac{1}{2} [T(s, Q^2) + T(-s, Q^2)], \quad T^{(-)} = \frac{1}{2} [T(s, Q^2) - T(-s, Q^2)] \quad (31)$$

so that

$$T(s, Q^2) = T^{(+)} + T^{(-)}, \quad T(-s, Q^2) = T^{(+)} - T^{(-)}. \quad (32)$$

Let us demonstrate that the signature of the Compton invariant amplitude T_1 in Eq. (27) is negative. Using Eq. (32), we can represent T_1 in Eq. (27) as the sum of the signature amplitudes $T_1^{(\pm)}$. In order to satisfy the Bose statistics,

$T_{\mu\nu}$ should be invariant to the permutation of the incoming and outgoing photons in Eq. (27), i.e. to the replacement combining $\mu \rightleftharpoons \nu$ and $q \rightleftharpoons -q$. On the other hand, in the limit of large s , where the SW transform makes sense, the proton spin remains unchanged under such replacement because $S_p \approx P_p/M$ whereas $s \approx 2pq \rightarrow -s$. It immediately allows one to conclude that the amplitude $T_1^{(+)}$ should not be present in Eq. (27). Therefore,

$$g_1(x, Q^2) = \frac{1}{\pi} \Im T_1^{(-)}(s, Q^2) . \quad (33)$$

The Compton amplitudes with the positive signature contribute to the structure functions F_1 and F_2 describing the unpolarized DIS. The calculation of the non-singlet component of F_1 and the non-singlet g_1 is quite similar, so in the present paper we consider g_1^{NS} in detail and give the results for F_1^{NS} in Appendix A. In order to account for the logarithmic contributions it is convenient to use the asymptotic SW transform for amplitudes $T^{(\pm)}$ in the following form:

$$T^{(\pm)} = \int_{-\imath\infty+\delta}^{\imath\infty+\delta} \frac{d\omega}{2\pi\imath} \left(\frac{s}{\mu^2}\right)^\omega \xi^{(\pm)}(\omega) F^{(\pm)}(\omega, y) \quad (34)$$

where $y = \ln(Q^2/\mu^2)$ and ξ are the signature factors:

$$\xi^{(\pm)} = -[e^{-\imath\pi\omega} \pm 1]/2 \approx [1 \pm 1 + \imath\pi\omega]/2 . \quad (35)$$

The integration line in Eq. (34) runs parallel to $\Im\omega$ and δ should be larger than the rightmost singularity of $F^{(\pm)}(\omega, y)$. Quite often in the literature δ in Eq. (34) is dropped. In the phenomenological Regge theory, the mass scale μ in Eq. (34) should obey $\mu^2 \ll s$, otherwise it is arbitrary. We are going to specify it later in the context of g_1 . The integration contour in Eq. (34), which includes the line parallel to the imaginary ω -axis, as stated above, must be closed up to the left. Then the contour includes all ω -singularities of $F^{(\pm)}(\omega, y)$. As Eq. (34) partly coincides with the standard Mellin transform, it is often addressed as the Mellin transform and we will do the same through the paper. Nevertheless, we will use the inverse transform to Eq. (34) in its proper form:

$$F^{(\pm)}(\omega, y) = \frac{2}{\pi\omega} \int_0^\infty d\rho e^{-\omega\rho} \Im T^{(\pm)}(s/\mu^2, y) \quad (36)$$

where we have denoted $\rho = \ln(s/\mu^2)$. Eqs. (36) and (C2) are supposed to be used at large s ($s \gg \mu^2$) where the bulk of the integrals comes from the region of small ω ($\omega \ll 1$). Obviously, Eq. (36) does not coincide with the standard Mellin transform. Finally Eqs. (25,27,31) lead to

$$g_1 = \frac{1}{2} \int_{-\imath\infty}^{\imath\infty} \frac{d\omega}{2\pi\imath} \left(\frac{s}{\mu^2}\right)^\omega \omega F^{(-)}(\omega, y) . \quad (37)$$

IV. TREATMENT OF α_s AT LARGE AND SMALL x

The rigorous knowledge on α_s is provided by the renormalization group equation (RGE) According to it, the total resummation of the leading radiative corrections to the Born value of α_s leads to the well-known expression

$$\alpha_s = \frac{1}{b \ln(-s/\Lambda^2)} \quad (38)$$

where $\Lambda \equiv \Lambda_{QCD}$ and $b = (11N - 2n_f)/12\pi$, with $N = 3$ and n_f being the number of involved flavors. Eq. (38) is the asymptotic expression valid at $|s| \gg \Lambda^2$. It is often addressed as the leading order expression for α_s and is obtained with the total resummation of the leading, single-logarithmic contributions. Corrections to Eq. (38) are also available in the literature² but we will not use them in the present paper because in practice the accuracy of the total resummations of the other radiative corrections, usually accounted for with various evolution equations, never exceeds the single-logarithmic accuracy. The minus sign at s in Eq. (38) is related to the analyticity: $\alpha_s(s)$ should be

² For recent progress in RGE see e.g. the review [19].

real at negative s , but when s is positive, $\alpha_s(s)$ acquires an imaginary part. Conventionally, $\alpha_s(s)$ at positive s is understood as the value of α_s on the upper side of the s -cut. Therefore, $-s = s \exp(-i\pi)$ and

$$\alpha_s(s) = \frac{1}{b} \frac{1}{[\ln(s/\Lambda^2) - i\pi]} = \frac{1}{b} \left(\frac{\ln(s/\Lambda^2) + i\pi}{\ln^2(s/\Lambda^2) + \pi^2} \right). \quad (39)$$

Expressions (38,39) are perturbative and asymptotic. In order to be consistent with the applicability of the perturbative QCD, μ defined in Eqs. (13,14) should be large enough:

$$\mu \gg \Lambda. \quad (40)$$

An alternative way is to modify Eq. (38) in order to be able to investigate α_s at $s \lesssim \Lambda^2$. For example, there is the so called Analytic Perturbation Theory (APT) suggested in Ref. [20]. It is based on subtracting from Eq. (38) its pole contribution at $s = -\Lambda^2$. In the vicinity of the pole

$$\alpha_s(s) = \frac{1}{b \ln \left((\Lambda^2 + |s| - \Lambda^2)/\Lambda^2 \right)} \approx \frac{1}{b} \left[\frac{\Lambda^2}{|s| - \Lambda^2} + \frac{1}{2} \right] + O(|s| - \Lambda^2). \quad (41)$$

The result of the subtraction is called the effective coupling and is used instead of α_s . Such a coupling can be used at any value of s . The recent results in this approach can be found in Refs. [21]. However, APT does not allow one to get rid of the cut-off μ when the Sudakov contributions of the higher-loop Feynman graphs are involved. So, in the present paper we do not follow this approach.

Now let us discuss how α_s is incorporated into the expressions for the amplitude A of the forward annihilation of the quark-antiquark pair into another pair. The generalization to the scattering of gluons can be obtained easily. We assume that the external quarks are almost on-shell, with virtualities $\sim \mu^2$, keeping $\mu^2 \ll s$. In the Born approximation, the amplitude A_{Born} is given by the following expression (see Fig. 1):

$$A_{Born} = -4\pi\alpha_s C^{(col)} \frac{\bar{u}(-p_2)\gamma_\mu u(p_1)\bar{u}'(p_1)\gamma_\mu u'(-p_2)}{s + i\epsilon} \equiv \frac{\bar{u}(-p_2)\gamma_\mu u(p_1)\bar{u}'(p_1)\gamma_\mu u'(-p_2)}{s} M_f^{Born}(s) \quad (42)$$

where $s = (p_1 + p_2)^2$. In Eq. (42) and through the paper we use the Feynman gauge for intermediate gluons. According

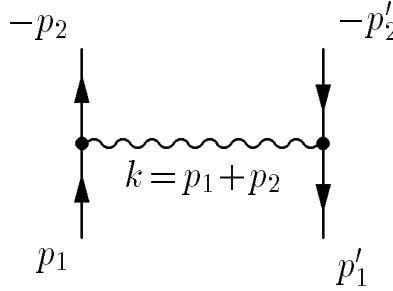


FIG. 1: The Born amplitude A_{Born} .

to Appendix A, the quark color factor $C^{(col)} = C_F = (N^2 - 1)/2N$ for the t -channel color singlet and $C^{(col)} = -1/2N$ for the vector (octet) representation. Through the paper we mostly discuss the color singlet amplitude. We address $M^{Born}(s)$ as the invariant amplitude for this process in the Born approximation:

$$M^{Born}(s) = -4\pi\alpha_s C^{(col)} \frac{s}{s + i\epsilon}. \quad (43)$$

By definition, α_s in the Born approximation is a constant. The radiative correction to M_f^{Born} can be divided into two groups:

- (i) The corrections contributing to α_s .
- (ii) The other corrections.

Leaving the corrections to (ii) for the next Sects. we consider now the effect of (i). They transform the fixed α_s in Eqs. (42,43) into the running coupling. It is possible to fix the argument of α_s , using the arguments of Ref. [22].

Incorporating the radiative corrections from (i) to A_{Born} leads, in particular, to insert the quark bubbles into the (horizontal) propagator of the intermediate gluon. In the logarithmic approximation, each quark bubble brings the contribution $\sim n_f \ln s$. The gluon logarithmic contributions, each $\sim N$, come from more involved graphs but eventually all contributions lead to the factor $b = (11N - 2n_f)/(12\pi)$ which multiplies the overall logarithm. Obviously, the argument of this logarithm coincides with the argument of the logarithm from the fermion bubble contribution and it is s . The total resummation of the leading radiative corrections from group (i) converts the fixed α_s of Eq. (42) into the well-known expression of Eq. (38) and therefore converts the Born invariant amplitude M^{Born} of Eq. (43) into $M^{(0)}$:

$$M^{(0)}(s) = -4\pi\alpha_s(s)C^{(col)}\frac{s}{s+i\epsilon}. \quad (44)$$

In order to apply the Mellin transform to $M^{(0)}$, we allow for the shift $s \rightarrow s - \mu^2$, with $s \gg \mu^2$, in Eq. (44). Then we can write

$$M^{(0)}(s) = \int_{-\infty}^{\infty} \frac{d\omega}{2\pi i} \left(\frac{s}{\mu^2}\right)^\omega F^{(0)}(\omega), \quad (45)$$

with

$$F^{(0)}(\omega) = 4\pi C^{(col)} \frac{A(\omega)}{\omega} \quad (46)$$

where $A(\omega)$ corresponds to $\alpha_s(s)$ in the ω -space :

$$A(\omega) = \frac{1}{b} \left[\frac{\eta}{\eta^2 + \pi^2} - \int_0^\infty \frac{d\rho e^{-\omega\rho}}{(\rho + \eta)^2 + \pi^2} \right]. \quad (47)$$

In Eq. (47) we have denoted $\eta = \ln(\mu^2/\Lambda_{QCD}^2)$. The first term in Eq. (47) corresponds to the cut of the bare gluon propagator while the second term comes from the cut of $\alpha_s(s)$. They have opposite signs because of the famous anti-screening in QCD, which is the basis of the asymptotic freedom for α_s . In the literature $M_f^{(0)}$ and $F_f^{(0)}$ are often called Born amplitudes (and we also follow this tradition) in spite of the fact that they include the leading radiative correction from group (i). The radiative corrections to $M_f^{(0)}$, i.e. the corrections from the group (ii), are often included by using evolution equations. Such equations involve convolutions of $M_f^{(0)}$, so they look simpler in the ω -space. We discuss this in detail in the next Section and focus now on the parametrization of α_s in the parton ladders. As the treatment of α_s for the color singlet M_0 and octet M_V amplitudes is the same, we will not specify the channel below.

First we remind that the well-known result $\alpha_s = \alpha_s(Q^2)$ in the DGLAP equations follows from the parametrization

$$\alpha_s = \alpha_s(k_\perp^2) \quad (48)$$

in every rung of the ladder Feynman graphs, where the ladder (vertical) partons can be either quarks or gluons. The notation k_\perp in Eq. (48) stands for the transverse components of momenta k of the vertical partons (quarks and gluons). The theoretical grounds for this parametrization can be found in refs. [23, 24, 25]. The analysis of the parametrization of α_s directly for the DGLAP equations was discussed in details in Ref. [26]. In Ref. [12] we had shown that the arguments of Ref. [26] in favor of using the parametrization (48) in DGLAP can be used at large x only. Later, in Ref. [27] we made a more detailed investigation on this issue and showed that the parametrization (48) is always an approximation regardless of value of x . As the matter of fact, $\alpha_s(k_\perp^2)$ should be replaced by the effective coupling α_s^{eff} given by the following expression:

$$\begin{aligned} \alpha_s^{eff} &= \alpha_s(\mu^2) + \frac{1}{\pi b} \left[\arctan\left(\frac{\pi}{\ln(k_\perp^2/\beta\Lambda^2)}\right) - \arctan\left(\frac{\pi}{\ln(\mu^2/\Lambda^2)}\right) \right] \\ &= \alpha_s(\mu^2) + \frac{1}{\pi b} \left[\arctan\left(\pi b \alpha_s(k_\perp^2/\beta)\right) - \arctan\left(\pi b \alpha_s(\mu^2)\right) \right], \end{aligned} \quad (49)$$

where the longitudinal Sudakov variable β is defined in Eq. (15). However when the starting point μ^2 of the Q^2 -evolution obeys the strong inequality

$$\mu^2 \gg \Lambda^2 e^\pi \approx 23\Lambda^2, \quad (50)$$

α_s^{eff} can be approximated by the much simpler expression:

$$\alpha_s^{eff} \approx \alpha_s(k_\perp^2/\beta). \quad (51)$$

If additionally x is large, $\alpha_s^{eff} \approx \alpha_s(k_\perp^2)$. For practical use, the inequality in Eq. (50) can be expressed in terms of the discrepancy $R(\mu)$ defined as

$$R(\mu) = \frac{|(1/\pi b) \arctan(\pi/\ln(\mu^2/\Lambda^2)) - \alpha_s(\mu^2)|}{\alpha_s(\mu^2)}. \quad (52)$$

A simple calculation shows that $R(\mu)$ rapidly grows when μ decreases, ranging, for example, from $R(\mu) = 5\%$ at $\mu^2 = 28 \text{ GeV}^2$ to $R(\mu) = 10\%$ at $\mu^2 = 2.5 \text{ GeV}^2$ and $R(\mu) = 50\%$ at $\mu^2 = 0.9 \text{ GeV}^2$. As the DGLAP starting point of the Q^2 -evolution is typically chosen close to 1 GeV^2 , the latter example shows that the DGLAP parametrization Eq. (48) has an error of 50 % at such low scale. This statement is true for all DIS structure functions. In order to derive Eq. (49) we consider now the parametrization of α_s in the integral expressions for the DIS structure functions. Here we partly follow the approach of Ref. [26]. To this aim we consider the forward Compton amplitude $T(x, Q^2)$ related to the structure functions by Eq. (28). Obviously, this equation is true for all DIS structure functions, so we drop here the signature superscript in T as unessential. One can show (and in this paper we will do it in the context of DGLAP and our Infrared Evolution Equations) that T obeys the following Bethe-Salpeter equation:

$$T(x, Q^2) = T^{Born} + i \int \frac{d^4 k}{(2\pi)^4} \frac{2wk_\perp^2}{(k^2 + i\epsilon)^2} M((q+k)^2, k^2, Q^2) 4\pi \frac{\alpha_s((p-k)^2)}{(p-k)^2 + i\epsilon}. \quad (53)$$

The integral term in Eq. (53) is shown in Fig. 2. The notation $M((q+k)^2, k^2, Q^2)$ in Eq. (53) corresponds to the

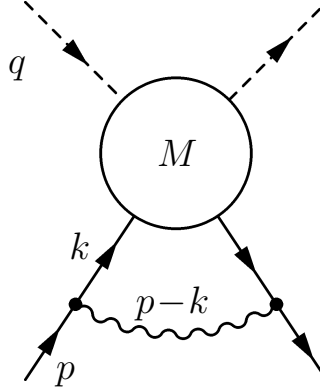


FIG. 2: The integral contribution in Eq. (53). The w -cut is implied, though is not shown explicitly.

blob in Fig. 2. Besides the amplitude T , it can also include a kernel (splitting functions). The inhomogeneous term T^{Born} is T in the Born approximation. To be specific, we consider the case when the horizontal parton in Fig. 2 is the virtual gluon with momentum $p-k$ whereas the vertical partons, with momentum k , can be either quarks or gluons. When they are quarks, $k^2 + i\epsilon$ should be replaced by $k^2 - m_q^2 + i\epsilon$, with m_q being the quark mass, but this shift does not play any role for our consideration below. The factor $2wk_\perp^2$ in Eq. (53) appears as a result of the simplification of the spin structure of the ladder Feynman graph in Fig. 2. We use the Sudakov parametrization (15) for momentum k of the vertical partons. In terms of the Sudakov variables α, β, k_\perp ,

$$k^2 = -w\alpha\beta - k_\perp^2, \quad 2qk = w\alpha + w\beta, \quad 2pk = -w\alpha. \quad (54)$$

where $w = 2pq$. It is convenient to introduce a new variable $m^2 = (p-k)^2$ instead of α . Therefore,

$$\alpha = \frac{m^2 + k_\perp^2}{w(1-\beta)}, \quad k^2 = -\frac{\beta m^2 + k_\perp^2}{1-\beta}. \quad (55)$$

Using Eqs. (54,55), we can rewrite Eq. (53) in a simpler way:

$$T(x, Q^2) = T^{Born} + \frac{i}{4\pi^2} \int_{\mu^2}^w dk_\perp^2 \int_{\beta_0}^1 d\beta \int_{-\infty}^{\infty} dm^2 \frac{w(1-\beta)k_\perp^2}{[m^2\beta + k_\perp^2 - i\epsilon]^2} M((q+k)^2, (\beta m^2 + k_\perp^2), Q^2) \frac{\alpha_s(m^2)}{m^2 + i\epsilon}. \quad (56)$$

The integration over β and k_\perp^2 in Eq. (56) runs over the region

$$\beta_0 < \beta < 1, \quad \mu^2 < k_\perp^2 < w. \quad (57)$$

The value of β_0 follows from the requirement of positivity of the invariant energy $(q+k)^2$ of the blob in Fig. 2:

$$\beta_0 \approx x + \frac{k_\perp^2}{w - m^2}. \quad (58)$$

Let us notice that the m^2 -dependence in Eq. (58) can be neglected to the leading logarithmic accuracy that we keep through this paper.

A. Integration in Eq. (56) at fixed α_s

Let us consider first the calculation of Eq. (56) under the approximation of fixed α_s . From the analysis of the ladder Feynman graphs (see e.g. the review [9]) one can see that DL contribution comes from the region of large k_\perp^2 where

$$-k^2 \approx k_\perp^2 \gg k_\parallel^2 = \beta m^2. \quad (59)$$

It allows to neglect the dependence of M on βm^2 in Eq. (56). It is convenient to integrate Eq. (56) over m^2 , using the Cauchy theorem. The singularities of the integrand are: the double pole from the vertical propagators

$$\beta m^2 + k_\perp^2 - \imath\epsilon = 0 \quad (60)$$

and the simple pole from the horizontal gluon propagator

$$m^2 + \imath\epsilon = 0. \quad (61)$$

The integration contour can be equally closed up or down. Traditionally (see e.g. Ref. [9]) the integration contour is closed down which involves taking the residue at the simple pole (61), so we arrive at the following result:

$$T(x, Q^2) = T^{Born} + \frac{\alpha_s}{2\pi} \int_{\mu^2}^w \frac{dk_\perp^2}{k_\perp^2} \int_{\beta_0}^1 d\beta (1 - \beta) M(\beta, Q^2, k_\perp^2). \quad (62)$$

Obviously, when x is large enough, one can change the upper limit of the integration over k_\perp^2 for Q^2 . Similarly, $\beta_0 \approx x$. Extracting the Born factor $1/\beta$ from M we can write

$$M(\beta, k_\perp^2) = (1/\beta) PT \quad (63)$$

where P is a kernel. To specify it, let us provide T with the quark and gluon subscripts through the replacement T by T_r (with $r = q, g$). It leads to specifying PT in Eq. (63): $PT = P_{rr'} T_{r'}$. At last, assuming that we have used the planar gauge allows to identify $(1 - \beta)P_{rr'}$ with the standard LO DGLAP splitting functions. Differentiation of Eq. (62) with respect to the upper limit of the k_\perp^2 -integration (which is Q^2 at large x) leads to the standard integro-differential DGLAP equations for the Compton amplitudes T_q, T_g .

B. Integration in Eq. (56) with running α_s

When α_s is running, it is also convenient to use the Cauchy theorem for integrating Eq. (56) over m^2 . The integration contour can again be closed down. However, the spectrum of singularities in the lower semi-plane now includes the pole (61) and the cut of α_s running along the real axis:

$$\mu^2 < m^2 - \imath\epsilon < +\infty. \quad (64)$$

Therefore, instead of Eq. (62) we arrive at the more complicated expression:

$$T(x, Q^2) = T^{Born} + \frac{1}{2\pi} \int_{\mu^2}^w dk_\perp^2 \int_{\beta_0}^1 d\beta (1 - \beta) \left[\frac{\alpha_s(\mu^2)}{k_\perp^2} M(\beta, Q^2, k_\perp^2) + \int_{\mu^2}^\infty \frac{dm^2}{m^2} M(\beta, Q^2, \beta m^2 + k_\perp^2) \Im \alpha_s(m^2) \frac{k_\perp^2}{(\beta m^2 + k_\perp^2)^2} \right]. \quad (65)$$

where we have not used the assumption of Eq. (59). The second term in the rhs of Eq. (65) is the result of taking the residue in the pole (61) and the third term corresponds to accounting for the cut (64). Eq. (65) demonstrates explicitly that it is impossible to factorize α_s , i.e. to integrate $\alpha_s(m^2)$ over m^2 , without making the approximation of Eq. (59). When this approximation has been made, we immediately obtain

$$T(x, Q^2) = T^{Born} + \frac{1}{2\pi} \int_{\mu^2}^w \frac{dk_{\perp}^2}{k_{\perp}^2} \int_{\beta_0}^1 d\beta (1 - \beta) M(\beta, Q^2, k_{\perp}^2) \alpha_s^{eff}, \quad (66)$$

with α_s^{eff} given by Eq. (49). Indeed, in this case the integral over m^2 in Eq. (66) is

$$I = \frac{1}{b} \int_{\mu^2}^{k_{\perp}^2/\beta} \frac{dm^2}{m^2} \frac{1}{\ln^2(m^2) + \pi^2} = \frac{1}{\pi b} \left[\arctan\left(\frac{\pi}{\ln(\mu^2/\Lambda^2)}\right) - \arctan\left(\frac{\pi}{\ln(k_{\perp}^2/\beta)}\right) \right]. \quad (67)$$

Obviously, the term π^2 in the integrand in Eq. (67) can be neglected when μ obeys Eq. (50). It leads to the approximative expression of Eq. (51) for α_s^{eff} . The approximation $\beta m^2 \ll k_{\perp}^2$ was also made in Ref. [26] for the integration Eq. (56) over m^2 in the case of running α_s . However, the integration contour in that paper was closed up in order to take the residue of the double pole at $k^2 = \beta m^2 + k_{\perp}^2 = 0$, which contradicts the assumption of Eq. (59) made in Ref. [26]. Taking this residue automatically led to the wrong conclusion that $\alpha_s^{eff} = \alpha_s(-k_{\perp}^2/\beta)$ regardless of the value of μ . This error was found and corrected in Ref. [27].

V. DESCRIPTION OF g_1 IN THE REGION **B**: TOTAL RESUMMATION OF THE LEADING LOGARITHMS

The region **B** is defined in Eq. (10). As it includes small x and large Q^2 , both logs of $1/x$ and Q^2 are equally important in this region and should be summed up. The most important logarithmic contributions to g_1 in region **B** are the double-logarithmic (DL) ones, i.e. the terms

$$\sim \alpha_s^n \ln^{2n-k}(1/x) \ln^k(Q^2/\mu^2), \quad (68)$$

with $k = 0, 1, \dots, n$, so they should be accounted for in the first place. Then the sub-leading, single-logarithmic (SL), contributions can also be taken into account etc. Therefore, an appropriate evolution equation for g_1 in region **B** should account for the evolution both with respect to x and Q^2 while DGLAP controls the Q^2 -evolution only and cannot sum up the logarithms of x . In addition, the running coupling effects in Eq. (68) should be taken into account. To this end, a special attention should be given to the parameterizations of α_s in region **B** and we will use here the results of Sect. IV. In order to resum DL contributions we use the alternative method of the Infrared Evolution Equations (IREE), first suggested by L.N. Lipatov (see Ref. [28]). Then it was applied to the elastic scattering of quarks in Ref. [29] and in Ref. [30], with the generalization to inelastic processes (radiative e^+e^- annihilation). Since then the IREE method has been applied to various problems and a brief review of the applications can be found in Ref. [31]. It is convenient to compose IREE for the Compton amplitudes $T^{(-)}$ related to g_1 by Eq. (33).

A. The essence of the method

As we have mentioned above, the DGLAP -ordering of Eq. (13) makes impossible to collect all DL contributions, regardless of their arguments, to all powers in α_s . In order to account for them, the ordering of Eq. (13) should be changed as in Eq. (14). This leads to the infrared (IR) singularities emerging from the graphs with soft gluons. In order to regulate them an IR cut-off μ should be introduced and therefore the result of such calculation becomes μ -dependent. The fermion (quark) ladders contributing e.g. to the non-singlet components of the DIS structure functions do not need an IR cut-off as long as the quark masses are accounted for. But in order to treat them similarly to the graphs with soft gluons, one can choose $\mu \gg$ masses of involved quarks. After that the quark masses can be dropped and the only remaining mass scale is μ . Generally, the value of μ is arbitrary, with one important exception: in order to use the perturbative QCD, μ should obey Eq. (40).

On one hand, such flexibility can be used to resum DL contributions through the use of evolution equations with respect to μ , which is the basis of our approach.

On the other hand, after such a resummation has been done, we arrive to a result which depends on this indefinite

parameter³. Of course, the problem of fixing the IR cut-off is not a new one. It has been known since long time ago, appearing first in QED, where μ is replaced in the final expressions by a suitable mass or energy scales. However, in the context of QCD this problem becomes more involved. Indeed, besides regulating the IR divergencies, μ acts also as a border line between Perturbative and Non-Perturbative QCD. Of course such a border is totally artificial from the point of view of the physics of hadrons.

Below we will discuss how we fix the value of μ for the non-singlet (where $\mu = 1$ GeV approximately) and singlet ($\mu = 5.5$ GeV) components of the structure function g_1 .

The last point deserving a discussion concerns the possible dependence of our results on the way of introducing the IR cut-off: basically, different ways can lead to different results as it was shown explicitly in Ref. [32]. However, such a discrepancy appears far beyond the leading logarithmic approximation (LLA), that we keep through this paper. We will discuss now the technical details of our approach.

B. The IREE for $T^{(-)}$ in DLA

We will consider, from now on, the invariant amplitude $T_1^{(-)}$, defined in Eqs. (27) and (31) and related to the structure function g_1 by Eq. (33). To simplify our notations, we drop both the subscript and superscript at $T_1^{(-)}$ and denote $T \equiv T_1^{(-)}$. When the cut-off μ is used for calculating Feynman graph contributions to T , this amplitude acquires the additional dependence:

$$T = T(w, Q^2, \mu^2). \quad (69)$$

This amplitude is in the left-hand side of the equation in Fig. 3. Beyond the Born approximation, T depends on its

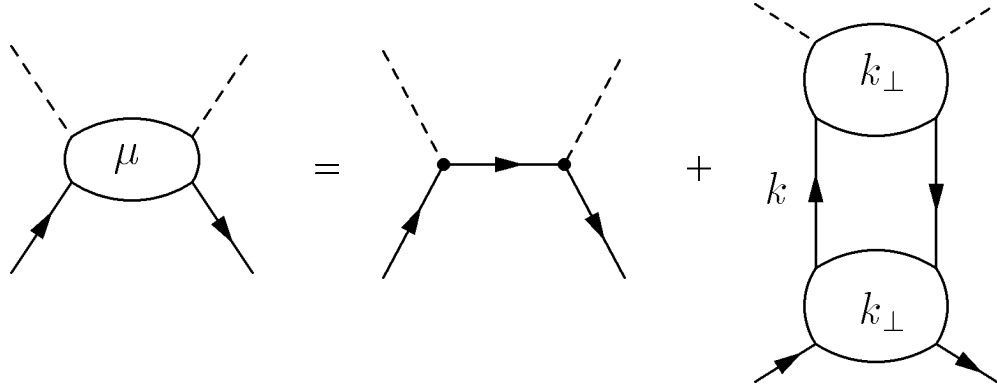


FIG. 3: The IREE for the Compton amplitude $T^{(-)}$.

arguments through their logarithms, so we can parameterize it in terms of logarithms:

$$T = T\left(\ln(w/\mu^2), \ln(Q^2/\mu^2)\right) \equiv T(\rho, y). \quad (70)$$

Therefore,

$$-\mu^2 \frac{\partial T}{\partial \mu^2} = \frac{\partial T}{\partial \rho} + \frac{\partial T}{\partial y}. \quad (71)$$

Eqs. (70) and (71) are the left-hand sides of the IREE for T (see Fig. 3) in the integral and differential form respectively. The right-hand side of the IREE includes, in the first place, the Born amplitude $T_{Born}^{(-)}$ given by Eq. (30). It corresponds to the second term in Fig. 3. In general, the other terms of IREE are obtained by factorizing the DL contributions

³ We remind that DGLAP is free of this problem due to the different ordering of Eq. (13).

of the softest partons. It is well-known that the DL contributions are technically obtained from the integration over both longitudinal and transverse momenta, each integration bringing a logarithm. Logarithmic contributions from the integration over each transverse momentum come from the kinematic regions where those momenta differ from each other: $k_{i\perp} \gg k_{j\perp}$. This implies that the set of virtual partons (quarks and gluons) always contains a parton with minimal transverse momentum. In other words, the transverse phase space can be represented as the sum of sub-regions D_i , each of them contains the parton with a minimal transverse momentum. We address such a parton as the softest parton even if its energy is not small and denote k_\perp its transverse momentum. The IR divergence arising by integrating dk_\perp/k_\perp can be regulated with the IR cut-off μ :

$$k_\perp > \mu. \quad (72)$$

Of course, μ should obey Eq. (40) to guarantee applicability of the Pert. QCD. It was shown in Ref. [8] that in QED the DL contributions can be of two different kinds:

(A): the Sudakov DL contributions coming from soft non-ladder partons;

(B): non-Sudakov DL contributions calculated first in Ref. [8]. They arise from ladder Feynman graphs. This classification stands also for QCD. The DL contributions of the softest partons from groups (A) and (B) are factorized differently.

Factorization of the softest gluon from group A:

The DL contributions from the softest non-ladder gluons can be factorized by using the QCD -generalization[30, 33, 34] of the Gribov factorization theorem (often called the Gribov bremsstrahlung theorem) of the soft photons obtained in Ref. [35]. According to it, the non-ladder gluon having the minimal k_\perp and being polarized in the plane formed by the external momenta can be factorized, i.e. its propagator is attached to the external lines only. When the Feynman gauge is used, the softest gluon propagator connects all available pairs of the external lines. The integration over other transverse momenta have k_\perp as the lowest integration limit. Such a factorization deals with k_\perp only and does not involve longitudinal momenta. Obviously, there is no way to attach the softest gluon propagator to the external lines of amplitude $T^{(-)}$ with the DL accuracy⁴.

Factorization of the softest partons from the group B:

Both the DGLAP-ordering in Eq. (13) and the ordering in Eq. (14) imply that one can always find a ladder (vertical) parton (quark or gluon) with minimal transverse momentum. However, there is a difference between the two cases: the softest parton in (13) is always the lowest parton at the ladder whereas in (14) the softest gluon can be anywhere in the ladder, from the bottom to the top. Therefore, it corresponds to the factorization of the lowest ladder rung in the DGLAP ordering (13), and the factorization of an arbitrary ladder rung under (14). The latter option corresponds to the last term in Fig. 3. By definition, in both cases the integration over k_\perp involves μ as the lowest limit whereas integrations over other $k_{i\perp}$ are μ -independent.

Now we can compose the IREE for T in the integral form. The lhs is just T while the rhs consists of the Born contribution and the term obtained by using the factorization B, therefore we arrive at the following IREE

$$T_r(\rho, y) = T_{r \text{ Born}} + i \int \frac{d^4 k}{(2\pi)^4} \frac{2wk_\perp^2}{(k^2 + i\epsilon)^2} T_{r'}((q+k)^2, Q^2, k^2) M_{r'r}((p-k)^2, k^2) \quad (73)$$

where any of r, r' denotes q or g ; the factor $2wk_\perp^2$ comes by simplifying the spin structure; The negative signature amplitudes $M_{r'r}$ of the $2 \rightarrow 2$ -forward scattering of partons correspond to the lower blobs in the rhs of Fig. 3. This will account for the total resummation of the leading logarithms as we'll see in detail in the next Sect. When the DGLAP-ordering (13) is used instead of (14), only the lowest ladder rung can be factorized and therefore $M_{r'r}^{(-)}$ are in this case given by the DL part of the LO DGLAP splitting functions. In other words, we arrive in this case to Eq. (53). Applying the operator $-\mu^2 \partial / \partial \mu^2$ to Eq. (73) it converts the lhs into Eq. (71). On the other hand Eq. (30) shows that the Born contribution in the rhs of Eq. (73) vanishes under the differentiation because it does not depend on μ . Using the SW transform as in Eq. (34) we rewrite Eq. (73) in terms of the amplitudes F_r , related to T_r through Eq. (34):

$$\omega F_r(\omega, y) + \frac{\partial F_r(\omega, y)}{\partial y} = \frac{1}{8\pi^2} F_{r'}(\omega, y) L_{r'r}(\omega) \quad (74)$$

⁴ We will use this kind of factorization in the next Sect. for calculating the lower blob in Fig. 3

where $L_{r'r}$ is related to $M_{r'r}$ by the transform Eq. (34). The derivation of Eq. (74) from Eq. (73) is given in detail in Ref. [11]. The general technique of simplifying the convolution in Eq. (73) is given in Appendix C. It is useful to rewrite Eq. (74) in terms of the flavor singlet, T^S , and non-singlet, T^{NS} , components of the Compton amplitude $T_r^{(-)}$:

$$\frac{\partial F^{NS}(\omega, y)}{\partial y} = \left(-\omega + \frac{1}{8\pi^2} L_{qq}(\omega) \right) F^{NS}(\omega, y), \quad (75)$$

and

$$\begin{aligned} \frac{\partial F_q^S(\omega, y)}{\partial y} &= \left(-\omega + \frac{1}{8\pi^2} L_{qq}(\omega) \right) F_q^S(\omega, y) + \frac{1}{8\pi^2} F_g^S(\omega, y) L_{gq}(\omega), \\ \frac{\partial F_g^S(\omega, y)}{\partial y} &= \left(-\omega + \frac{1}{8\pi^2} F_q^S(\omega, y) L_{qg}(\omega) \right) F_g^S(\omega, y) + \frac{1}{8\pi^2} L_{gg}(\omega) F_g^S(\omega, y). \end{aligned} \quad (76)$$

It is also convenient to introduce the amplitudes H_{ik} related to L_{ik} as follows:

$$H_{ik} = \frac{1}{8\pi^2} L_{ik}. \quad (77)$$

F^S , and F^{NS} are related to the singlet and non-singlet components of g_1 with Eq. (37). Eqs. (75,76) are written in the DGLAP-like form, with the derivative with respect to Q^2 , but actually they combine the evolution with respect to Q^2 and w .

Let us consider how to incorporate the single-logarithmic corrections from group (ii) of Sect. IV into Eqs. (75,76).

C. Inclusion of single-logarithmic contributions into Eq. (74)

Technically, the DL contributions appear from the integrals over the loop momenta k_i of the following form:

$$\sim \int \frac{dk_{i\perp}^2}{k_{i\perp}^2} \frac{d\beta_i}{\beta_i} \varphi(p_r, k_j), \quad (78)$$

where we have used notations p_r for external momenta and presumed that $j \neq i$. The function $\varphi(p_r, k_j)$ is independent of k_i , which follows from imposing the strong inequalities giving rise to the DL integration region:

$$k_{i\perp} \ll k_{j\perp}, \quad \beta_i \ll \beta_j. \quad (79)$$

When, for example, linear terms in k_i are present in φ , one of the integrations in Eq. (78) does not give rise to a logarithm and as a consequence a single-logarithmic (SL) contributions appears. This takes place in the integration region where the strong inequalities (79) do not apply. In particular, when the inequality $k_{i\perp} \ll k_{j\perp}$ is not fulfilled there is not a single soft parton in this region and therefore the method we use cannot account for such contributions. On the other hand, replacing the DL inequality $\beta_i \ll \beta_j$ by the single-logarithmic one, $\beta_i < \beta_j$ is not essential for the method and these SL contributions can be taken into account. This replacement converts Eqs. (75,76) into

$$\omega F^{NS}(\omega, y) + \frac{\partial F^{NS}(\omega, y)}{\partial y} = \frac{1}{8\pi^2} (1 + \lambda_{qq}\omega) h_{qq}(\omega) F^{NS}(\omega, y), \quad (80)$$

and

$$\begin{aligned} \omega F_q^S(\omega, y) + \frac{\partial F_q^S(\omega, y)}{\partial y} &= (1 + \lambda_{qq}\omega) h_{qq}(\omega) F_q^S(\omega, y) + (1 + \lambda_{gq}\omega) h_{gq}(\omega) F_g^S(\omega, y), \\ \omega F_g^S(\omega, y) + \frac{\partial F_g^S(\omega, y)}{\partial y} &= (1 + \lambda_{qg}\omega) h_{qg}(\omega) F_q^S(\omega, y) + (1 + \lambda_{gg}\omega) h_{gg}(\omega) F_g^S(\omega, y) \end{aligned} \quad (81)$$

with $\lambda_{rr'}$ given by the following expressions:

$$\lambda_{qq} = 1/2, \quad \lambda_{qg} = -1/2, \quad \lambda_{gq} = -2, \quad \lambda_{gg} = -13/24 + n_f/(12N), \quad (82)$$

obtained with one-loop calculations in the planar gauge. The new amplitudes h_{ik} are defined similarly to H_{ik} and account not only for the total resummation of the DL contributions but also contain the resummation of the SL contributions. Therefore Eqs. (80,81) account for the resummation of the leading (DL) together with sub-leading (SL) contributions to the w -evolution and for the resummation of the leading (DL) contributions to the Q^2 -evolution. For this reason they can be considered as the generalization of the DGLAP equations to the region (B). In contrast to the well-developed technology of resummation of double logarithms, no regular methods for the total resummation of SL contributions are presently available in the literature.

VI. IREE FOR THE AMPLITUDES H_{ik} AND h_{ik}

The expressions for the parton amplitudes H_{ik} and h_{ik} in Eqs. (75-81) can be found by explicitly solving the IREE for them. Such equations were obtained and discussed in detail first in Ref. [10] where α_s was kept fixed, while the running coupling effects were implemented in Ref. [11]. The technique for solving the IREE for the anomalous dimensions is similar to the one for amplitudes T^S , so we give below just a short comment on it. As it was done before for the Compton amplitudes, we begin with the IREE for amplitudes $M_{ik}(\rho)$ related to the Mellin amplitudes $H_{ik}(\omega)$ through Eq. (34). The amplitudes $L_{ik}(\rho)$ do not depend on Q^2 , so the left-hand side of the IREE for $H_{ik}(\omega)$ does not involve derivatives and is equal to $\omega H_{ik}(\omega)$. The invariant amplitudes M in the Born approximation were introduced in Eq. (44). It was shown that in the ω -space all of them are $\sim 1/\omega$, so we can write

$$H_{ik}^{Born} = a_{ik}/\omega, \quad (83)$$

with

$$a_{qq} = \frac{A(\omega)C_F}{2\pi}, \quad a_{qg} = \frac{A'(\omega)C_F}{\pi}, \quad a_{gq} = -\frac{n_f A'(\omega)}{2\pi}, \quad a_{gg} = \frac{4NA(\omega)}{2\pi}, \quad (84)$$

where we have used the standard notations $C_F = (N^2 - 1)/2N = 4/3$, n_f is the number of the quark flavors, A is defined in Eq. (47) and

$$A'(\omega) = \frac{1}{b} \left[\frac{1}{\eta} - \int_0^\infty \frac{d\rho e^{-\omega\rho}}{(\rho + \eta)^2} \right]. \quad (85)$$

The reason for the replacement of $A(\omega)$ by $A'(\omega)$ is that the argument of α_s in L_{qq} and L_{gq} is space-like, so the coupling does not lead to π -terms. The next term in the rhs of the IREE are the convolutions of the anomalous dimensions appearing as the convolution in Eqs. (75,76). At last, the rhs contains the contribution from the factorization of the soft (Sudakov) gluons. We account for this contribution approximately (see Ref. [11]) for more details. Eventually we arrive at the system of IREE for the singlet anomalous dimensions H_{ik} represented in Fig. 4. In the case of the non-singlet anomalous dimension, all gluon contributions in Eq. (86) should be dropped. Rewriting Fig. 4 in a detailed form, we arrive at the system of the algebraic non-linear equations for H_{ik} :

$$\begin{aligned} \omega H_{qq} &= b_{qq} + H_{qq}H_{qq} + H_{qg}H_{gq}, & \omega H_{qg} &= b_{qg} + H_{qq}H_{qg} + H_{qg}H_{gg}, \\ \omega H_{gq} &= b_{gq} + H_{gq}H_{qg} + H_{gg}H_{gq}, & \omega H_{gg} &= b_{gg} + H_{gq}H_{qg} + H_{gg}H_{gg}. \end{aligned} \quad (86)$$

where we have denoted

$$b_{ik} = a_{ik} + V_{ik}, \quad (87)$$

with a_{ik} given by Eq. (84). Then

$$V_{ik} = \frac{m_{ik}}{\pi^2} D(\omega), \quad (88)$$

$$m_{qq} = \frac{C_F}{2N}, \quad m_{gg} = -2N^2, \quad m_{gq} = n_f \frac{N}{2}, \quad m_{qg} = -NC_F, \quad (89)$$

and

$$D(\omega) = \frac{1}{2b^2} \int_0^\infty d\rho e^{-\omega\rho} \ln((\rho + \eta)/\eta) \left[\frac{\rho + \eta}{(\rho + \eta)^2 + \pi^2} + \frac{1}{\rho + \eta} \right]. \quad (90)$$

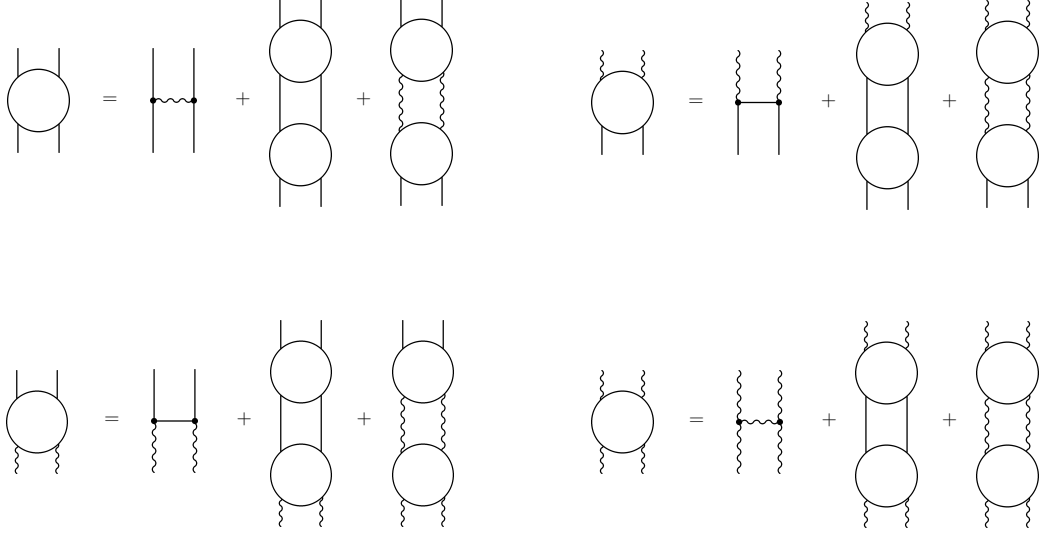


FIG. 4: The IREE for singlet amplitudes H_{ik} . The solid lines correspond to quarks and the wavy lines denote gluons.

Let us add a comment on the terms V_{ik} . They appear from those graphs in Fig. 4 where the softest virtual gluon is factorized, i.e. its propagator is attached to the external lines in all possible ways. The blob obtained after the factorization is not a color singlet but an octet in the t (vertical) channel because the factorized gluon bears the color and belongs to an octet representation of the color group $SU(3)$. So, these new amplitudes $M_{ik}^{(8)}$ should be calculated independently. It is not a big deal for the non-singlet g_1 which involves $M_{qq}^{(8)}$ only, but becomes a serious technical problem when all $M_{ik}^{(8)}$ are involved (see Ref. [10]). Fortunately, all $M_{ik}^{(8)}$ rapidly decrease with energy, and then is possible to approximate them by their Born values with a few per cent accuracy as was suggested in Ref. [36].

Eqs. (86), similarly to Eqs. (75,76), combine the total resummation of DL contributions and the running coupling effects but do not include other SL contributions. The part of SL contributions accounted through Eq. (82) can be easily incorporated into Eqs. (86), leading to the following equations:

$$\begin{aligned}\omega h_{qq} &= b_{qq} + (1 + \lambda_{qq}\omega)h_{qq}h_{qq} + (1 + \lambda_{qg}\omega)h_{qg}h_{gq}, \\ \omega h_{qg} &= b_{qg} + (1 + \lambda_{qg}\omega)h_{qg}h_{qg} + (1 + \lambda_{gg}\omega)h_{gg}h_{gg}, \\ \omega h_{gq} &= b_{gq} + (1 + \lambda_{gq}\omega)h_{gq}h_{gq} + (1 + \lambda_{qq}\omega)h_{qq}h_{qq}, \\ \omega h_{gg} &= b_{gg} + (1 + \lambda_{gg}\omega)h_{gg}h_{gg} + (1 + \lambda_{qg}\omega)h_{qg}h_{gq}.\end{aligned}\tag{91}$$

Now we present the expressions for the non-singlet case. Dropping all gluon contributions in Eq. (91), we immediately arrive to the equation for the non-singlet amplitude \tilde{h}_{qq} :

$$\omega \tilde{h}_{qq} = b_{qq} + (1 + \lambda_{qq}\omega)(\tilde{h}_{qq})^2\tag{92}$$

with the obvious solution

$$\tilde{h}_{qq} = \frac{[\omega - \sqrt{\omega^2 - B_{NS}}]}{2(1 + \lambda_{qq}\omega)}\tag{93}$$

where

$$B_{NS} = 4(1 + \lambda_{qq}\omega)b_{qq}.\tag{94}$$

Unfortunately, the system of non-linear algebraic equations in Eq. (91) can be solved analytically only if all λ_{ik} are dropped. In this case the solution to the system is

$$\begin{aligned}H_{qq} &= \frac{1}{2}\left[\omega - Z + \frac{b_{qq} - b_{gg}}{Z}\right], & H_{qg} &= \frac{b_{qg}}{Z}, \\ H_{gq} &= \frac{1}{2}\left[\omega - Z - \frac{b_{qq} - b_{gg}}{Z}\right], & H_{gg} &= \frac{b_{gg}}{Z}\end{aligned}\tag{95}$$

where

$$Z = \frac{1}{\sqrt{2}} \sqrt{(\omega^2 - 2(b_{qq} + b_{gg})) + \sqrt{(\omega^2 - 2(b_{qq} + b_{gg}))^2 - 4(b_{qq} - b_{gg})^2 - 16b_{gg}b_{qq}}} . \quad (96)$$

The non-linear algebraic equations in Eq. (92) and Eq. (86) have more than one solution, however the solution chosen in Eqs. (93,95) obeys the matching condition

$$\tilde{h}_{qq} \rightarrow a_{qq}/\omega, \quad H_{ik} \rightarrow H_{ik}^{Born} = a_{ik}/\omega \quad (97)$$

at $\omega \rightarrow \infty$, with a_{ik} given by Eq. (84). In other words, this matching condition in Eq. (97) implies that these amplitudes are represented at low energies by their Born values. Indeed, from Eq. (34) high energies correspond to small ω and vice versa.

VII. SOLUTION TO THE IREE (80) FOR g_1 NON-SINGLET

As soon as the expressions for h_{qq} are obtained, one can easily find the general solution to the linear differential equation (80) for the Mellin amplitude F^{NS} . As the procedure between the non-singlet and singlet cases has a purely technical difference, we consider in detail the former case and proceed to the singlet case in a much shorter way.

A. General solution to the non-singlet equation (80)

Obviously, the general solution to Eq. (80) is

$$F^{NS} = \tilde{F}^{NS}(\omega) e^{-\omega y + y(1 + \lambda\omega)\tilde{h}_{qq}} \quad (98)$$

and therefore

$$T^{NS}(x, Q^2) = \int_{-\imath\infty}^{\imath\infty} \frac{d\omega}{2\imath\pi} \left(w/\mu^2\right)^\omega \tilde{F}^{NS}(\omega) e^{-\omega y + y(1 + \lambda_{qq}\omega)\tilde{h}_{qq}} = \int_{-\imath\infty}^{\imath\infty} \frac{d\omega}{2\imath\pi} (1/x)^\omega \tilde{F}^{NS}(\omega) e^{y(1 + \lambda_{qq}\omega)\tilde{h}_{qq}} \quad (99)$$

with $\tilde{F}^{NS}(\omega)$ being arbitrary. In order to specify it, we use the matching condition

$$T^{NS}(x, Q^2) = \tilde{T}^{NS}(w/\mu^2) \quad (100)$$

when $y = 0$. The new amplitude $\tilde{T}^{NS}(w/\mu^2)$ describes again the forward Compton scattering off the same quark, however the virtual photon has now a virtuality $\approx \mu^2$. The IREE for $\tilde{T}^{NS}(w/\mu^2)$ should be obtained independently.

B. Composing the IREE for $\tilde{T}^{NS}(w/\mu^2)$.

The IREE for $\tilde{T}^{NS}(w/\mu^2)$ is similar to the IREE for $T^{NS}(x, Q^2)$, Eq. (73). It has the same structure and involves the same amplitude M_{qq} . Still, it differs from Eq. (73) because of two following points:

- (a) $\tilde{T}^{NS}(w/\mu^2)$ does not depend on Q^2 , so the differential IREE for it does not involve $\partial/\partial y$;
- (b) the Born amplitude $\tilde{T}_{Born}^{NS}(w/\mu^2)$ can be obtained from $T^{NS}(x, Q^2)$, putting $Q^2 = \mu^2$, so its contribution does not vanish under differentiation with respect to μ . Then introducing the Mellin amplitude $\tilde{F}^{NS}(\omega)$ related to $\tilde{T}^{NS}(w/\mu^2)$ through the transform (34), we arrive at the following IREE:

$$\omega \tilde{F}^{NS}(\omega) = (e_q^2/2) + (1 + \lambda_{qq}\omega)\tilde{h}_{qq}\tilde{F}^{NS}(\omega). \quad (101)$$

and therefore

$$\tilde{F}^{NS}(\omega) = \frac{(e_q^2/2)}{\omega - (1 + \lambda_{qq}\omega)\tilde{h}_{qq}(\omega)} \quad (102)$$

C. Expression for g_1^{NS} in the Region B

Combining Eqs. (102, 98) and (37) and convoluting the perturbative expression with the initial quark density immediately leads to

$$\begin{aligned} g_1^{NS} &= \frac{e_q^2}{2} \int_{-\infty}^{\infty} \frac{d\omega}{2\pi i} \left(\frac{w}{\mu^2} \right)^\omega \frac{\omega \delta q(\omega)}{\omega - (1 + \lambda_{qq}\omega) \tilde{h}_{qq}(\omega)} e^{-\omega y + y \tilde{h}_{qq}} \\ &= \frac{e_q^2}{2} \int_{-\infty}^{\infty} \frac{d\omega}{2\pi i} \left(\frac{1}{x} \right)^\omega \frac{\omega \delta q(\omega)}{\omega - (1 + \lambda_{qq}\omega) \tilde{h}_{qq}(\omega)} e^{y \tilde{h}_{qq}} \end{aligned} \quad (103)$$

where $\delta q(\omega)$ is the initial quark density in ω -space. Confronting Eq. (103) to Eq. (17) it is clear that

$$h_{NS}(\omega) = (1 + \lambda_{qq}\omega) \tilde{h}_{qq}(\omega) = (1/2) \left[\omega - \sqrt{\omega^2 - B_{NS}(\omega)} \right] \quad (104)$$

is the new non-singlet anomalous dimension. It contains the total resummation of DL contributions together with the running α_s effects and a part of SL contributions as explained in the previous Sect. Similarly,

$$C_{NS} = \frac{\omega}{\omega - (1 + \lambda_{qq}\omega) \tilde{h}_{qq}(\omega)} = \frac{\omega}{\omega - h_{NS}(\omega)} = \frac{2\omega}{\omega + \sqrt{\omega^2 - B_{NS}(\omega)}} \quad (105)$$

is the new non-singlet coefficient function. It is expressed through the anomalous dimension and therefore incorporates the same kind of logarithmic contributions. Eventually we arrive at the final expression for g_1^{NS} in the region **B** of large Q^2 and small x :

$$g_1^{NS}(x, Q^2) = \frac{e_q^2}{2} \int_{-\infty}^{\infty} \frac{d\omega}{2\pi i} x^{-\omega} C_{NS}(\omega) \delta q(\omega) e^{h_{NS}(\omega) \ln(Q^2/\mu^2)}. \quad (106)$$

VIII. SOLUTION TO THE IREE (76) FOR THE SINGLET g_1

Eq. (76) for g_1^S can be solved in a similar way as the IREE for g_1^{NS} . First a general solution should be obtained and then constrained with a boundary condition. The general solution is easy to obtain:

$$\begin{aligned} F_q &= e^{-\omega y} \left[C^{(+)} e^{\Omega_{(+)} y} + C^{(-)} e^{\Omega_{(-)} y} \right], \\ F_g &= e^{-\omega y} \left[C^{(+)} \frac{X + \sqrt{R}}{2H_{qg}} e^{\Omega_{(+)} y} + C^{(-)} \frac{X - \sqrt{R}}{2H_{qg}} e^{\Omega_{(-)} y} \right] \end{aligned} \quad (107)$$

where

$$X = H_{gg} - H_{qq} \quad (108)$$

and

$$R = (H_{gg} - H_{qq})^2 + 4H_{qg}H_{gq}. \quad (109)$$

We remind that the anomalous dimensions H_{ik} are found in Eq. (95). The exponents $\Omega_{(\pm)}$ are also expressed in terms of H_{ik} :

$$\Omega_{(\pm)} = \frac{1}{2} \left[H_{qq} + H_{gg} \pm \sqrt{(H_{gg} - H_{qq})^2 + 4H_{qg}H_{gq}} \right]. \quad (110)$$

Finally the quantities $C^{(+)}$ and $C^{(-)}$ have to be specified.

In order to constrain Eq. (107) we use the matching condition at $Q^2 = \mu^2$:

$$\begin{aligned} F_q(\omega, Q^2 = \mu^2) &= C^{(+)} + C^{(-)} = \tilde{F}_q(\omega), \\ F_g(\omega, Q^2 = \mu^2) &= C^{(+)} \frac{X + \sqrt{R}}{2H_{qg}} + C^{(-)} \frac{X - \sqrt{R}}{2H_{qg}} = \tilde{F}_g(\omega). \end{aligned} \quad (111)$$

The new Mellin amplitudes $\tilde{F}_{q,g}(\omega)$ correspond to the forward Compton scattering, when the photon virtuality is μ^2 . They should be found independently. We again proceed by using new IREE for them. They have a structure similar to Eq. (76). The difference is that the new equations do not contain derivatives with respect to y and account for the Born contributions

$$\tilde{F}_q^{Born} = \frac{\langle e_q^2 \rangle}{\omega}, \quad \tilde{F}_g^{Born} = 0, \quad (112)$$

where $\langle e_q^2 \rangle$ is the standard notation for the averaged e_q^2 . So, the IREE for amplitudes $\tilde{F}_{q,g}$ are

$$\begin{aligned} \omega \tilde{F}_q^S &= \langle e_q^2 \rangle h_{qq}(\omega) \tilde{F}_q^S(\omega) + h_{gq}(\omega) \tilde{F}_g^S(\omega, y), \\ \omega \tilde{F}_g^S &= h_{qg}(\omega) \tilde{F}_q^S(\omega) + h_{gg}(\omega) \tilde{F}_g^S(\omega) \end{aligned} \quad (113)$$

and the solution to Eq. (113) is

$$\begin{aligned} \tilde{F}_q^S &= \langle e_q^2 \rangle \frac{\omega - H_{gg}}{\omega^2 - \omega(H_{qq} + H_{gg}) + (H_{qq}H_{gg} - H_{qg}H_{gq})}, \\ \tilde{F}_g^S &= \langle e_q^2 \rangle \frac{H_{gq}}{\omega^2 - \omega(H_{qq} + H_{gg}) + (H_{qq}H_{gg} - H_{qg}H_{gq})}. \end{aligned} \quad (114)$$

Combining Eqs. (114) and (111), we obtain the explicit expressions for $C^{(\pm)}$:

$$\begin{aligned} C^{(+)} &= \langle e_q^2 \rangle \frac{2H_{gq}H_{qg} - (X - \sqrt{R})(\omega - H_{gg})}{2\sqrt{R}[\omega^2 - \omega(H_{qq} + H_{gg}) + (H_{qq}H_{gg} - H_{qg}H_{gq})]}, \\ C^{(-)} &= \langle e_q^2 \rangle \frac{-2H_{gq}H_{qg} + (X + \sqrt{R})(\omega - H_{gg})}{2\sqrt{R}[\omega^2 - \omega(H_{qq} + H_{gg}) + (H_{qq}H_{gg} - H_{qg}H_{gq})]}. \end{aligned} \quad (115)$$

Introducing the initial quark and gluon densities δq and δg respectively and using Eq. (37), we finally arrive at the following expression for g_1^S in region **B**:

$$\begin{aligned} g_1^S(x, Q^2) &= \frac{1}{2} \int_{-\infty}^{\infty} \frac{d\omega}{2\pi i} \left(\frac{1}{x} \right)^\omega \left[\left(C^{(+)} e^{\Omega_{(+)y}} + C^{(-)} e^{\Omega_{(-)y}} \right) \omega \delta q(\omega) + \right. \\ &\quad \left. \left(C^{(+)} \frac{(X + \sqrt{R})}{2H_{qg}} e^{\Omega_{(+)y}} + C^{(-)} \frac{(X - \sqrt{R})}{2H_{qg}} e^{\Omega_{(-)y}} \right) \omega \delta g(\omega) \right]. \end{aligned} \quad (116)$$

where $\delta q(\omega)$ and $\delta g(\omega)$ are the initial quark and gluon densities in the ω -space. Comparing Eq. (116) to Eq. (6) it follows that $C_q^{(\pm)}(\omega)$ and $C_g^{(\pm)}(\omega)$ are the singlet coefficient functions calculated in LLA. The exponents $\Omega_{(\pm)}$ are expressed in terms of H_{ik} in the same way as the DGLAP exponents are related to the DGLAP anomalous dimensions. So, we conclude that H_{ik} are the anomalous dimensions for g_1^S in LLA. The application of the expressions for g_1 in Eqs. (106,116) and the study of their impact on the Bjorken sum rule can be found in Ref. [39].

IX. ASYMPTOTICS OF THE NON-SINGLET g_1 IN THE REGION **B**

The expressions Eqs. (106,116) represent g_1 in the region **B**. Before discussing them in detail, we consider first their asymptotics at fixed $Q^2 \gg \mu^2$ and $x \rightarrow 0$. Strictly speaking, such asymptotics can be obtained by applying the saddle-point method. When the small- x behaviour is proved to be of the Regge type (power-like), one can use a short cut by finding the position of the leading (rightmost) singularity in the ω -plane. Of course, such singularities can be different for g_1^{NS} and g_1^S and should be found independently. In the present Sect. we consider the small- x asymptotics of the non-singlet g_1 .

A. Asymptotic scaling

Let us assume that the initial quark density δq in Eq. (106) is non-singular in x at $x \rightarrow 0$, so it does not contribute to the small- x asymptotics. Then by applying the saddle-point method to Eq. (106) one deals with the non-singlet coefficient function and the anomalous dimension only. In this case the stationary point is (see Appendix E for details)

$$\omega_0 = \sqrt{B_{NS}} \left[1 + (1 - \kappa)^2 (y/2 + 1/\sqrt{B_{NS}})^2 / (2 \ln^2 \xi) \right], \quad (117)$$

with

$$\kappa = d\sqrt{B}/d\omega|_{\omega=\omega_0} \quad (118)$$

and $y = \ln(Q^2/\mu^2)$, $\xi = \sqrt{Q^2/(x^2\mu^2)}$.

It immediately leads to the Regge asymptotics for the non-singlets:

$$g_1^{NS} \sim \frac{e_q^2}{2} \delta q(\omega_0) \Pi_{NS} \xi^{\omega_0/2}, \quad (119)$$

with

$$\Pi_{NS} = \frac{\left[2(1-\kappa)\sqrt{B_{NS}}\right]^{1/2} (y/2 + 1/\sqrt{B_{NS}})}{\pi^{1/2} \ln^{3/2} \xi}. \quad (120)$$

When in Eq. (117) $y \ll 2/\sqrt{B_{NS}(\omega)}$ (let us notice in advance that at $\omega = \Delta_{NS}$ it means that $y \ll 150 \mu^2$), the value of ω_0 does not depend on y at all. Therefore Eq. (119) can be rewritten as:

$$g_1^{NS}(x, Q^2) \sim (e_q^2/2) \delta q(\omega_0) c_{NS} T_{NS}(\xi) \quad (121)$$

with

$$T_{NS}(\xi) = \xi^{\omega_0/2} / \ln^{3/2} \xi. \quad (122)$$

The factor c_{NS} is

$$c_{NS} = \left[2(1-\kappa)/(\pi\sqrt{B_{NS}})\right]^{1/2} \quad (123)$$

and does not depend on y . Eq. (121) predicts the scaling behavior for the non-singlet structure functions: in the region $Q^2 \ll 150 \mu^2$, with $T^{(\pm)}$ depending on one argument ξ instead of x and Q^2 independently. Therefore in this region

$$g_1^{NS} \sim \tilde{g}_1^{NS} \equiv \Pi_{NS}(\omega_0) \delta q(\omega_0) (Q^2/x^2 \mu^2)^{\omega_0/2} \quad (124)$$

at $x \rightarrow 0$, with ω_0 being the largest root of Eq. (125):

$$\omega^2 - B_{NS} = 0. \quad (125)$$

We call the result of Eq. (124) **asymptotic scaling**: g_1^{NS} asymptotically depends on one variable Q^2/x^2 only, instead of two variables x and Q^2 . The DGLAP prediction for the asymptotics of g_1^{NS} in Eq. (132) is quite different. Below we compare these results in detail

According to the results of Ref. [14] (see also Appendix E), in the opposite case, when $Q^2 \gtrsim 150 \mu^2$, the rightmost and non-vanishing at $w \rightarrow \infty$ stationary point is again given by Eq. (125) but the pre-exponential factor Π_{NS} essentially depends on y , so the asymptotic scaling in this region holds for g_1^{NS}/y .

Let us notice that the sign of the non-singlet asymptotic behaviour is positive when $\delta q(\omega_0)$ is positive and coincides with the sign of g_1^{NS} in the Born approximation. In other words, both the x and Q^2 -evolutions do not affect the sign of g_1^{NS} . Now we focus on solving Eq. (125).

B. Estimate for the non-singlet intercept

In a more detailed form, equation Eq. (125) is

$$\begin{aligned} \omega^2 - (1 + \lambda_{qq}\omega) \left[\left(\frac{2C_F}{\pi b} \right) \left(\frac{\eta}{\eta^2 + \pi^2} - \int_0^\infty \frac{d\rho e^{-\omega\rho}}{\rho^2 + \pi^2} \right) + \right. \\ \left. \left(\frac{2C_F}{\pi b} \right)^2 \frac{1}{4NC_F} \int_0^\infty d\rho e^{-\omega\rho} \ln((\rho + \eta)/\eta) \left(\frac{\rho + \eta}{(\rho + \eta)^2 + \pi^2} + \frac{1}{\rho + \eta} \right) \right] = 0 \end{aligned} \quad (126)$$

where we have used the notation $\eta = \ln(\mu^2/\Lambda^2)$. Let us remind that in the case of fixed α_s Eq. (126) is much simpler and can be solved analytically:

$$\omega^2 - \frac{2\alpha_s C_F}{\pi} - \left(\frac{2\alpha_s C_F}{\pi}\right)^2 \frac{1}{\omega^2 4N C_F} = 0, \quad (127)$$

with the obvious solution ω_0^{DL} given by the following expression[10]:

$$\omega_0^{DL} = (2\alpha_s C_F/\pi)^{1/2} \sqrt{\frac{1}{2} \left[1 + \left(1 + \frac{4}{N^2 - 1} \right)^{1/2} \right]}. \quad (128)$$

In contrast, Eq. (126) cannot be solved analytically. Besides, there is a big qualitative difference between the cases of fixed and running α_s . Although the IR cut-off μ is used for regulating the IR divergencies in both cases, Eq. (127) is free of any μ -dependence whereas Eq. (126) is obviously μ -dependent and therefore the solution ω_0 also depends on μ : $\omega_0 = \omega_0(\mu)$. The value of μ is restricted by Eq. (40) only. As a result, we arrive at the solution to Eq. (126) in the form of the curve plotted in Fig. 5. Eq. (126) shows that ω_0 depends on μ through η , therefore ω_0 depends on the

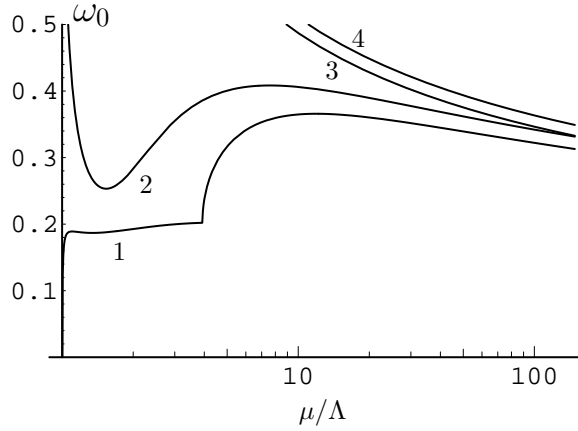


FIG. 5: Dependence of the intercept ω_0 on infrared cutoff μ : 1– for F_1^{NS} ; 2– for g_1^{NS} ; 3– and 4– for F_1^{NS} and g_1^{NS} respectively without account of π^2 -terms. The structure function F_1^{NS} is discussed in the Appendix B.

ratio μ/Λ and on n_f . Besides the η -dependence, ω_0 is not sensitive to the value of Λ . The plot in Fig. 5 shows that the curve $\omega_0 = \omega_0(\mu)$ rapidly grows at $\mu \lesssim \Lambda$, however this region contradicts Eq. (40), so the perturbative expression (38) for α_s cannot be used at so small μ . Both Eq. (126) and the plot in Fig. 5 are consistent in the region (40) only and should not be considered out of this region. Eq. (126) has one maximum in region (40):

$$\Delta_{NS} \equiv \max[\omega_0] = \omega_0(\mu_{NS}) = 0.42 \quad (129)$$

at

$$\mu = \mu_{NS} \equiv \Lambda e^{2.3} \approx 10\Lambda. \quad (130)$$

For the sake of simplicity we chose in Ref. [11] $n_f = 3$ and $\Lambda = 0.1$ GeV. It would have been more realistic to choose $\Lambda = 0.5$ GeV, and Eq. (130) shows that such a change of Λ leads to multiply by a factor of 5 the values of μ for the singlet and non-singlet obtained in Ref. [11]. Comparison of the curves 1 and 2 in Fig. 5 to the curves 3 and 4 shows that the important role played by the π^2 -terms in α_s (i.e. respecting the analyticity) for producing a maximum in the curves 2 and 4. Furthermore in the vicinity of this maximum, the power expansion

$$\omega_0(\mu) = \omega_0(\mu_{NS}) + \frac{d\omega_0(\mu_{NS})}{d\mu}(\mu - \mu_{NS}) + \frac{1}{2} \frac{d^2\omega_0(\mu_{NS})}{d\mu^2}(\mu - \mu_{NS})^2 + \dots \quad (131)$$

does not contain the linear term, so $\omega_0(\mu_{NS}) \equiv \Delta_{NS}$ is much less dependent on μ than all other points on the curves 1 and 2. This remarkable feature allows us to identify Δ_{NS} as the best candidate⁵ for the perturbative estimate of the genuine intercept of the non-singlet g_1 . According to the prediction of the Regge approach, the genuine intercept should be a constant, with no other dependence. However, Eq. (126) and its solution (129) account for the leading logarithmic contributions only and leave aside sub-leading perturbative contributions and possible non-perturbative ones, so it is hardly possible to identify (129) with the genuine intercept. Nevertheless, it turned out that our estimate (129) is in a good agreement with the results of Ref. [37] obtained by fitting all available experimental data. This leads to a very interesting conclusion: by some unknown reason all sub-leading and non-perturbative contributions to the non-singlet intercept happen to be either small or irrelevant at $\mu = \mu_{NS}$, so that the LLA prediction (129) proves to be a good estimate for the non-singlet intercept. Motivated by this result, we call μ_{NS} the Optimal non-singlet mass scale. However, it is worth stressing that this scale is an artefact of our approach and should disappear when non-perturbative contributions (also dependent on the same scale) would be accounted for. To conclude, let us notice that the Regge form of the small- x asymptotics of g_1 is the direct consequence of the total resummation of logarithms of x and cannot appear at fixed orders in α_s . This small- x asymptotics depends on Q^2 only through the factor $(Q^2/\mu^2)^{\Delta_{NS}/2}$ (see Eq. (124)). In particular it means that the intercept Δ_{NS} has no dependence on Q^2 . On the other hand, the well-known DGLAP small- x asymptotics

$$g_1^{NS \text{ DGLAP}} \sim \exp \left[\sqrt{\frac{2C_F}{\pi b}} \ln(1/x) \ln \left(\frac{\ln(Q^2/\Lambda^2)}{\ln(\mu^2/\Lambda^2)} \right) \right]. \quad (132)$$

can also be obtained (see Appendix F for detail) with the saddle-point method providing the initial parton densities are not singular at $x \rightarrow 0$ (In Sect. XII we consider the alternative case presently used in the Standard Approach for the analysis of experimental data at small x). The DGLAP -asymptotics (132) clearly does not exhibit the Regge behavior. The same is true for the case where the anomalous dimensions and coefficient functions are calculated in high but fixed orders in α_s which would correspond to the NN..NLO DGLAP accuracy (see Appendix G for detail). In principle, one might think that a generalization of Eq. (132) could lead to the Regge asymptotics, however with the intercept depending on Q^2 . We show now that there are no theoretical grounds for such a scenario. Indeed, it follows from Eq. (F7) that the Q^2 -dependence in Eq. (132) is the consequence of the use of the DGLAP -parametrization $\alpha_s = \alpha_s(k_\perp^2)$ and the DGLAP -ordering (13). As explained in detail in Appendix F, at small x this ordering should be changed by the ordering (14). Then the upper limit Q^2 in Eq. (13) in the small- x region should be modified to w (see Ref. [27] for detail). After that the DGLAP asymptotics will not depend on Q^2 but at the same time will not have a Regge-type form. The Regge asymptotics is achieved by accounting for the resummation of the leading logarithms of x . It exhibits an asymptotic behavior much steeper than the DGLAP result (132), not only with respect to x but also with respect to Q^2 . The comparison of Eq. (132) to Eq. (124) shows that $g_1^{NS \text{ DGLAP}}/g_1^{NS} \rightarrow 0$ when $x \rightarrow 0$. The question however arises: how small should x be in order to allow our asymptotic expression Eq. (124) to represent g_1^{NS} reliably? We answer this question below.

C. Applicability region of the small- x asymptotics

The asymptotic expression (124) for g_1^{NS} is obviously much simpler than the integral representation (106) and also much easier to work with. However, it is valid for very small x only. In order to determine when Eq. (124) reliably represents Eq. (106), let us study numerically the ratio

$$R_{as}^{NS}(x, Q^2) = \frac{g_1^{NS}(x, Q^2)}{\tilde{g}_1^{NS}(x, Q^2)} \quad (133)$$

at fixed Q^2 and different values of x . The result is plotted in Fig. 6. According to it, g_1^{NS} is reliably represented by its asymptotic expression $\tilde{g}_1^{NS}(x, Q^2)$ at $x \lesssim 10^{-6}$ only. So, strictly speaking, Eq. (124) should not be used at available values of x . However, in the literature one can find that Regge type ($\sim x^{-a}$) fits of the experimental data are used at much larger values of x , and such fits are reported to work well. We suggest a simple explanation to this: the phenomenological parameterizations including the Regge type fits have nothing in common with the expression in Eq. (124) obtained with the saddle-point method. In order to use such parameterizations at relatively

⁵ We are grateful to P. Castorina for this very useful observation.

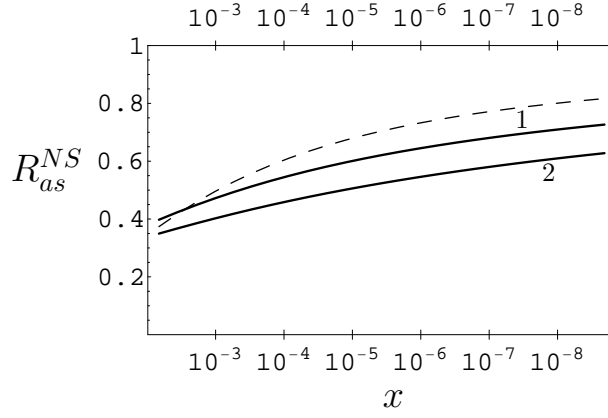


FIG. 6: Rate of the g_1^{NS} approach to asymptotics for different Q^2 : solid curve 1 for $Q = 10\mu$, solid curve 2 for $Q = 100\mu$, dashed curve for $Q = \mu$.

large values of x (at $x \gg 10^{-6}$), one can choose the exponents a in the fits greater than the genuine intercepts. An analysis of such Regge parameterizations can be found in Ref. [13]. To conclude, we also notice also that sometimes Regge parameterizations are used with intercepts depending on Q^2 : they have no theoretical ground and contradict Eq. (124).

X. SMALL- x ASYMPTOTICS OF THE SINGLET g_1 IN THE REGION B

The small- x asymptotics of g_1^S in the region **B** can be obtained quite similarly to the non-singlet case, by applying the saddle-point method to Eq. (116). The singlet asymptotics also exhibits the Regge behavior:

$$g_1^S(x, Q^2) \sim (1/x)^{\omega_0} (Q^2/\mu^2)^{\omega_0/2} [A(\omega_0)\delta q(\omega_0) + B(\omega_0)\delta g(\omega_0)] \quad (134)$$

where ω_0 is the stationary point and A , B include the asymptotic form of the coefficient functions. The position of the leading singularity corresponds the largest root of the equation

$$(\omega^2 - 2(b_{qq} + b_{gg}))^2 - 4(b_{qq} - b_{gg})^2 - 16b_{qq}b_{gg} = 0. \quad (135)$$

Similarly to the non-singlet case, the position of the singlet leading singularity depends on μ , with one maximum

$$\omega_0^S \equiv \Delta_S = 0.86 \quad (136)$$

achieved at (we choose again $n_f = 3$)

$$\mu = \mu_S \approx \Lambda e^4 \approx 55\Lambda \quad (137)$$

which gives $\mu_S/\Lambda \approx 55$ GeV when $\Lambda = 0.1$ GeV. By repeating the arguments given also in the previous Sect., we call Δ_S the singlet intercept and call μ_S the Optimal singlet mass scale. The Optimal singlet and non-singlet mass scales are quite different. Our perturbative estimate (136) is also in a very good agreement with the result obtained in Ref. [38] by fitting the experimental data. Eq. (134) shows that the asymptotic scaling is also valid for the singlet g_1 : asymptotically g_1^S depends on one argument Q^2/x^2 only. In contrast to the case of the non-singlet asymptotics (124), the interplay between δq and δg can affect the sign of g_1^S . Indeed, in the Born approximation $g_1^S > 0$ but it can be negative (positive) asymptotically depending on the sign of $A\delta q + B\delta g$ in Eq. (134).

XI. APPLICABILITY REGION OF THE IREE METHOD

In this Sect. we discuss the region of applicability of our approach and also answer a claim on a possible contradiction in our method that we have got in the past: in the IREE technology that we use to sum up the leading logarithms we work in the ω -space and systematically keep ω small. On the other hand when we calculate the non-singlet and

especially the singlet intercepts, they are found not so small. Therefore we should guarantee the validity of our method not only at small but also at large ω . We start from the conventional analysis of the double-logarithmic QCD power series (138), so we would like to stress at once that the use of (138) for analysis of QCD processes and all estimates (e.g. the one in Eq. (139)) based on it originate from the QED results (see e.g. Ref. [9]) where the running coupling effects can be neglected. They can become unreliable in QCD and therefore these conventional estimates should be replaced by more accurate estimates which we present in this Sect.

Now let us remind the basic principle of the Leading Logarithmic Approximation, and DLA in particular. The straightforward calculation of the Feynman graphs contributing to a certain quantity (for instance, to the non-singlet coefficient) yields the double-logarithmic contributions. In the n -th order of the perturbation theory they are $\sim \alpha_s^n \ln^{2n}(1/x)$. For the sake of simplicity we keep here α_s fixed and leave out other numerical parameters like $1/\pi$, color factors, etc. Accounting for the running coupling effects and sub-leading logarithmic contributions does not change the essence of the problem. The series of such contributions, for example

$$c_1 \alpha_s \ln(1/x) + c_2 \alpha_s^2 \ln^3(1/x) + c_3 \alpha_s^4 \ln^5(1/x) + \dots \quad (138)$$

converges when $\alpha_s \ln^2(1/x) < 1$ only. It brings us to a rough estimate for the lowest limit for x :

$$x > x_{min} = \exp[-1/\sqrt{\alpha_s}]. \quad (139)$$

On the other hand, it is interesting to know the result of the total resummation of the DL terms at really small $x < x_{min}$ and even at $x \rightarrow 0$. The reason is that the DL terms are not so large compared to other contributions at $x \gtrsim x_{min}$ but dominate at small x . However, the series in Eq. (138) diverges at $x < x_{min}$ and cannot be summed up in this region. The solution to this problem is well-known: in the first place the series Eq. (138) should be summed up at $x > x_{min}$ and then the result of the resummation can be analytically continued into the region $x < x_{min}$. Let us notice that the series Eq. (138) becomes divergent in region $x < x_{min}$ and is called an asymptotic series. In the ω -space the series Eq. (138), according to the relation

$$\int_{-\infty}^{\infty} \frac{d\omega}{2\pi i} e^{\omega \ln(1/x)} \frac{1}{\omega^{1+2n}} = \frac{1}{(2n)!} \ln^{2n}(1/x), \quad (140)$$

is given by:

$$\tilde{c}_1 \frac{\alpha}{\omega^2} + \tilde{c}_2 \frac{\alpha^2}{\omega^4} + \tilde{c}_3 \frac{\alpha^3}{\omega^6} + \dots \quad (141)$$

This series converges when, roughly,

$$\omega > \omega_{min} = \sqrt{\alpha_s} \quad (142)$$

whereas the DL terms becomes large at $\omega < \omega_{min}$. To be specific, let us notice that the expressions for the coefficient functions in Eqs. (105,115) represent the total sum of the DL contributions. Strictly speaking, the coefficient functions should first be calculated for large ω : $\omega > \omega_{min}$ (where the DL contributions are small) and then continued to the region of small ω . However, anticipating the analytical continuation into the small ω region, quite often a short cut is taken and we follow this way: we treat ω as small since the beginning. It gives us the reason to neglect all non-logarithmic corrections regardless of their relatively large values in the region (142). After the total resummation of the DL terms has been done, the formulae obtained are insensitive to the value of ω and therefore can be used at any x . The resummed expressions (105,115) contain new singularities ω_0 (branching points in our case but, generally, they can also be poles), which are absent in the series (141). The rightmost singularities, i.e. the intercepts (Δ_{NS} and Δ_S in our case), determine the range of convergence of the series Eq. (138) instead of $\sqrt{\alpha_s}$: the series (141) converges only if

$$\omega > \Delta, \quad (143)$$

with Δ being the intercept. However, after the total resummation in (141) has been performed, the result of the resummation can be used at arbitrary values of ω . To conclude, we note that all equations for the resummation of the leading logarithms, and in particular the IREE we have used, are not the equations for finding the intercepts. Indeed, the intercepts are the singularities and the values of ω in the IREE should be kept pretty far away from them by definition. The intercepts appear in the asymptotic expressions and therefore they should be found independently of the resummation methods, usually by applying the saddle-point method.

XII. COMPARISON OF g_1 TO g_1^{DGLAP} IN THE REGION **B**

In this Sect. we compare our results (106,116) to the DGLAP expressions for g_1 at small x . We are not going to use here the asymptotic expressions in Eqs. (124,134) or (132), but we compare the two approaches at small but finite x . First we will compare the basic ingredients of the expressions for g_1 : the anomalous dimensions and the coefficient functions. Whenever it is possible, we will consider in detail, for the sake of simplicity, the non-singlet g_1 and more briefly generalize our results to the case of g_1^S .

A. Comparison of the coefficient functions and the anomalous dimensions

Eqs. (106) and (17) have a similar structure: each integrand contains the initial parton density, the coefficient function and the exponent with the non-singlet anomalous dimension to govern the Q^2 -evolution. However, C_{NS} and h_{NS} in Eq. (106) contain the total resummation of the leading logarithms of x whereas in Eq. (17) the coefficient function and the anomalous dimension are considered to LO and NLO accuracy, namely they are given in Eqs. (18,20). Originally DGLAP was suggested for studying the region **A** of large x and large Q^2 . Due to the oscillating factor $x^{-\omega}$ in the Mellin integrals, the main contribution to g_1 in the region **B** comes from small ω . On the contrary, the main contribution in region **A** comes from large ω . At large ω , the expressions for C_{NS} and h_{NS} in Eq. (106) can be expanded into a converging series in $1/\omega$:

$$C_{NS} = 1 + \frac{A(\omega)C_F}{2\pi} \left[\frac{1}{\omega^2} + \frac{1}{2\omega} \right] + \dots, \quad (144)$$

$$h_{NS} = \frac{A(\omega)C_F}{2\pi} \left[\frac{1}{\omega} + \frac{1}{2} \right] + \dots \quad (145)$$

Obviously we observe a large discrepancy between Eqs. (144,145) and the LO DGLAP expressions in Eqs. (18,20). However, this discrepancy almost disappears when we come back to the region **B** where ω is small and therefore regular terms $\sim \omega^k$ in Eqs. (18,20) can be dropped. The remaining discrepancy is due to the different treatment of the QCD coupling. When the starting point of the Q^2 -evolution obeys Eq. (40), then $A(\omega)$ with very good approximation can be replaced by $\alpha_s(k_\perp^2/x)$, but definitely not by $\alpha_s(k_\perp^2)$. Taking into account more terms in the series and adding them to Eqs. (144,145) does not change the situation. So, we conclude that in region **B** the first and second terms of the $1/\omega$ -expansion of Eqs. (104,105) reproduce the most important LO and NLO DGLAP results in the non-singlet anomalous dimension and coefficient function, with the exception of the different treatment of the QCD coupling. Expanding Eqs. (95,115) into a series in $1/\omega$ and comparing the result to the singlet DGLAP anomalous dimensions and coefficient functions, we arrive at the same conclusion.

B. Numerical comparison of the x -evolutions in Eqs. (17) and (106)

The integrands in Eqs. (17) and (106) for the non-singlet g_1 contains also a phenomenological ingredient: the initial quark densities δq . Let us introduce the ratio

$$R_{NS} = \frac{g_1^{NS}}{g_1^{NS, DGLAP}} \quad (146)$$

and study its x -dependence at fixed Q^2 , for example at $Q^2 = 10 \text{ GeV}^2$. Obviously, this cannot be done until δq is fixed. The choice

$$\delta q(x) = N_q \delta(1-x) \quad (147)$$

corresponds to approximate the initial hadron by a quark and to neglect all influence of the hadron structure. Of course, such a choice cannot be used for phenomenological applications, but it makes possible to compare the x -evolutions in Eqs. (17) and (106). The substitution of the bare quark input into Eqs. (17) and (106) leads to the x -dependence of R_{NS} plotted in Fig. 7. This shows that the impact of the leading logarithms becomes quite sizable at $x_0 \approx 10^{-2}$. So, we arrive to a sort of puzzle:

According to the different behaviour of the x -evolution in Eqs. (17) and (106), the DGLAP -description of g_1^{NS} should have failed for $x < 10^{-2}$, but phenomenologically it is well-known that DGLAP works well at $x < 10^{-2}$. The solution to this puzzle is given below.

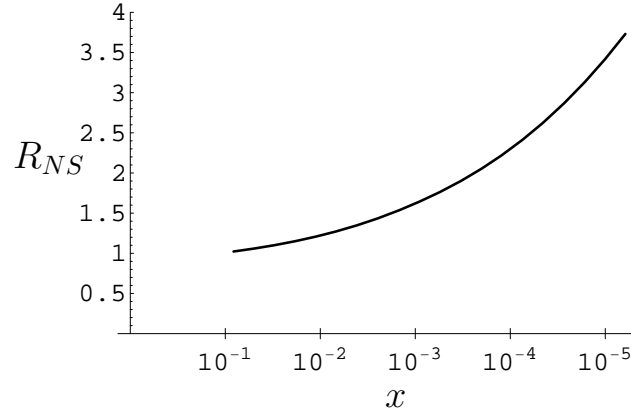


FIG. 7: Rise of R_{NS} of Eq. (146) at small x in case of bare quark input and for $Q^2 = 10 \text{ GeV}^2$.

C. The role of the initial parton densities

In order to clarify the problem, let us consider in more detail a standard fit to the initial quark density, as in Eq. (201):

$$\delta q(x) = N_q x^{-\alpha} (1 - x)^\beta (1 + \gamma x^\delta) \equiv N_q x^{-\alpha} \varphi(x).$$

with all parameters N_q , α , β , γ , δ being positive. As the fit is defined at certain fixed values of $x = x_0$ and $Q^2 = Q_0^2$, all its parameters depend on x_0 , Q_0^2 . We define N_q as the normalization. As the term $x^{-\alpha} \rightarrow \infty$ when $x \rightarrow 0$, we call it the singular term, although the fit is introduced at large x . We call φ the regular part of the fit because $\varphi \rightarrow 1$ when $x \rightarrow 0$. Once transformed into the ω -space, the fit becomes a sum of pole contributions:

$$\delta q(\omega) = N_q \left[(\omega - \alpha)^{-1} + \sum_{k=1}^{\infty} \left(m_k (\omega + k - \alpha) + \gamma (\omega + k + \delta - \alpha)^{-1} \right) \right] \quad (148)$$

where $m_k = \beta(\beta - 1) \dots (\beta - k + 1)/k!$. The first pole in Eq. (148) corresponds to the singular term x^{-a} in Eq. (24). We call it the leading pole. The other, non-leading poles in Eq. (148) originate from the interference between $\varphi(x)$ and x^{-a} . Substituting Eq. (148) into the DGLAP expression (17), we see that the contribution of the leading pole, $\tilde{g}_1^{NS \text{ DGLAP}}$ to $g_1^{NS \text{ DGLAP}}$ is (we drop the NLO contribution here)

$$\tilde{g}_1^{NS \text{ DGLAP}}(x, Q^2) = \frac{e_q^2}{2} N_q \left(\frac{1}{x} \right)^\alpha C^{NS \text{ DGLAP}}(\alpha) \left(\frac{\ln(Q^2/\Lambda^2)}{\ln(\mu^2/\Lambda^2)} \right)^{\gamma_{(0)}(\alpha)/(2\pi b)}. \quad (149)$$

Substituting the other terms of Eq. (148) into Eq. (17) it leads to a contribution quite similar to that in Eq. (149), however with $\alpha \rightarrow \alpha_k = \alpha - k$ and $\alpha - k - 1$. Obviously, $\alpha > \alpha_k$. Therefore $\tilde{g}_1^{NS \text{ DGLAP}}$ in Eq. (149) is really the leading contribution to $g_1^{NS \text{ DGLAP}}$ at small x and actually it represents the small- x asymptotics of $g_1^{NS \text{ DGLAP}}$. Confronting Eq. (149) to the very well-known expression (132) for the DGLAP asymptotics, we see that they are totally different. The singular terms are also included into the DGLAP parametrization of the singlet parton densities. It leads to the steep growth of g_1 at small x and provides the reason for the agreement between the DGLAP-description of the structure functions and the experimental data. Therefore the DGLAP success at small x is related to the use of singular fits for the initial parton densities. This is the solution to the puzzle. Now let us discuss the most important consequences of this result.

First, let us confront the asymptotics of Eqs. (149) and (124). We see that the x -dependence in these expressions is identical: both formulae exhibit the Regge (power-like) behavior. It allows us to conclude that the singular term $x^{-\alpha}$ in the standard DGLAP fits mimics the total resummation of the leading logarithms of x . Therefore, the singular factors can be dropped when the total resummation of the leading logarithms of x is accounted for. In order to show it explicitly, let us study numerically R_{NS} , using the standard DGLAP fit of Eq. (24). The results are plotted in Fig. 8. We can observe that R_{NS} is pretty close to unity only when the fit (24) is used in the expression for $g_1^{NS \text{ DGLAP}}$, whereas only the regular part, φ , of the fit is used in the resummed expression (106). All other options drive R_{NS} far away from unity at small x . So, the resummation of the leading logarithms leads to simplify the standard fits. Fig. 8

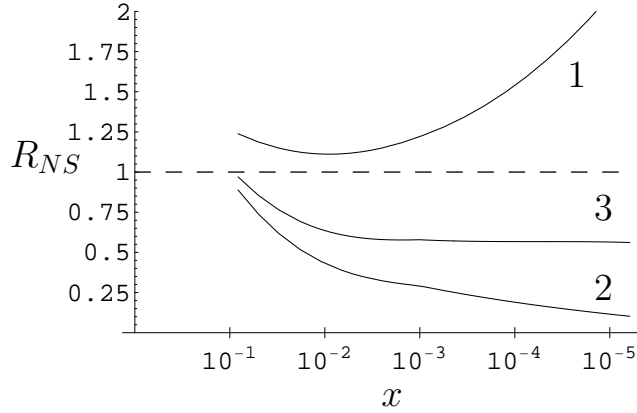


FIG. 8: Examples of the small x -behaviour of R_{NS} for different singular terms in the initial quark distribution fits of Eq. (24): $\alpha = 0$ (curve 1), $\alpha = 0.576$ (curve 2), $\alpha = 0.36$ (curve 3). All curves correspond to $Q^2 = 10 \text{ GeV}^2$, and involve only a regular part, φ , in the parametrization of the initial quark density used for g_1 of Eq. (106).

explicitly demonstrates that the singular fit (24) and the total resummation of the logarithms lead to close values of g_1 in region **B**. From a practical point of view, the use of the resummation is preferable because it allows one to construct new fits with a reduced number of parameters. From the theoretical point of view, the resummation is even more preferable. Indeed, the DGLAP intercept α in Eq. (149) depends on the starting point x_0 , Q_0^2 , where α is fixed, and such a dependence can hardly be deduced from theoretical considerations. On the contrary, the intercept Δ_{NS} in Eq. (124) is independent of the initial parton densities.

Now we would like to comment on an apparent puzzle arising first from the results of Refs. [5, 40] and then also in other subsequent publications:

On one hand, the direct comparison in Ref. [40] of the NLO DGLAP result, $g_1^{NS \text{ DGLAP}}$ to the expression for g_1^{NS} obtained in Ref. [10] in the limit of fixed α_s showed that

$$g_1^{NS}/g_1^{NS \text{ DGLAP}} \ll 1 \quad (150)$$

at the small values of x available in experiment and therefore the conclusion was made that the resummation of $\ln^k(1/x)$ can yield a small impact. On the other hand, it is clear that the small- x asymptotics (124) is much steeper than the well-known DGLAP asymptotics (132), which proves that asymptotically

$$g_1^{NS}/g_1^{NS \text{ DGLAP}} \gg 1 \quad (151)$$

and therefore the total resummation of $\ln^k(1/x)$ should be essential. So, Eqs. (150) and (151) obviously contradict each other, which is puzzling. The contradiction between Eqs. (150) and (151) has been interpreted in the literature as follows: accounting for the leading logarithms has a small impact on the small- x behavior of g_1 until the region of extremely small x is achieved.

However, a close inspection of Eqs. (24,148) for the standard fit suggests another solution to this puzzle. The point is the exponential DGLAP asymptotics (132) is changed to the Regge asymptotics of Eq. (149) as soon as a fit of the type (24) is chosen. Then, as parameters α in such fits obey

$$\alpha > \Delta, \quad (152)$$

with Δ in Eq. (152) being either the non-singlet or singlet intercept, depending on the case, the strong inequality sign in Eq. (151) should be reversed. The reason why the exponents α in the singular factors of the DGLAP fits should obey Eq. (152) is clear: indeed, we have just shown above that the asymptotic regime is actually achieved at very small x , so in order to reproduce it at values of x accessible at present experiments, the parameter α , playing the role of the intercept, should be larger than the intercepts Δ . In this connection we remind that our predictions agree

very well with results of Refs [37, 38], whereas the phenomenological value of the intercept α in Eq. (24) contradicts those results. It is clear that combining singular fits with the total resummation of logarithms also implies a double counting of the same logarithmic contributions: explicitly in the first case and implicitly in the latter, through the singular factors $x^{-\alpha}$. Furthermore, Eqs. (124) and (149) explicitly show that neither the DGLAP intercept α nor our intercept Δ_{NS} depend on Q^2 . Such a dependence, sometimes appearing in the literature as a possible generalization of Eq. (132) is an ad hoc assumption and never appears as a result of QCD calculations.

Finally, let us notice that it is commonly believed that the expression for the fit in Eq. (24) mimics the effect of the hadron structure, including basically unknown non-perturbative contributions. On the other hand, when the leading logarithms are accounted for and the initial parton densities are fitted at not too large x , the x -dependent terms in φ can be almost dropped, so the fit can be simplified down to N_q . It means that the impact of the non-perturbative contributions is greater at large x whereas in the small- x region it is reduced to a simple normalization.

XIII. REGGEON STRUCTURE OF g_1

According to the Regge theory (see e.g. Ref. [17]), any forward scattering amplitude, including the invariant Compton amplitude T related to g_1 through Eq. (33), asymptotically exhibits the Regge (power-like) behavior and can be written as a sum of such power-like terms called Reggeons. The same should be true for g_1 . In this Sect. we show that both the standard approach (SA) and our description of g_1 agree with such a representation. However, the Reggeons in these two approaches are different and the reasons for this Reggeon representation are also quite different. As usually we begin with considering in detail the non-singlet g_1 .

A. Reggeon structure of g_1 in the SA description

Eq. (148) with the standard DGLAP fit in the ω -representation can be re-written as:

$$\delta q(\omega) = \frac{r}{\omega - j} + \sum_{k=1}^{\infty} \frac{r_k}{\omega - j_k} + \sum_{k=1}^{\infty} \frac{\tilde{r}_k}{\omega - \tilde{j}_k} \quad (153)$$

where r , r_k , \tilde{r}_k and j , j_k , \tilde{j}_k are expressed through the parameters of the fit as follows:

$$j = \alpha, \quad j_k = \alpha - k, \quad \tilde{j}_k = \alpha - k - \delta, \quad (154)$$

$$r = N_q, \quad r_k = (1 + \gamma)N_q\beta(\beta - 1) \cdot (\beta - k + 1)/(k!), \quad \tilde{r}_k = \gamma N_q\beta(\beta - 1) \cdot (\beta - k + 1)/(k!). \quad (155)$$

By inserting Eq. (153) into Eq. (17), integrating over ω , and taking the residues of the poles of Eq. (153), allows us to write $g_1^{NS \text{ DGLAP}}$ in the region **B** as the following series:

$$g_1^{NS \text{ DGLAP}}(x, Q^2) = \frac{e_q^2}{2} \left[S(x, Q^2) + \sum_{k=1}^{\infty} \left(S_k(x, Q^2) + \tilde{S}_k(x, Q^2) \right) \right] \quad (156)$$

where, to the LO accuracy, the terms S , S_k , \tilde{S}_k are

$$\begin{aligned} S(x, Q^2) &= \left(\frac{1}{x} \right)^j C^{NS \text{ DGLAP}}(j) r \left(\frac{\ln(Q^2/\Lambda^2)}{\ln(\mu^2/\Lambda^2)} \right)^{\gamma_{DGLAP}(j)/(2\pi b)}, \\ S_k(x, Q^2) &= \left(\frac{1}{x} \right)^{j_k} C^{NS \text{ DGLAP}}(j_k) r_k \left(\frac{\ln(Q^2/\Lambda^2)}{\ln(\mu^2/\Lambda^2)} \right)^{\gamma_{DGLAP}(j_k)/(2\pi b)}, \\ \tilde{S}_k(x, Q^2) &= \left(\frac{1}{x} \right)^{\tilde{j}_k} C^{NS \text{ DGLAP}}(\tilde{j}_k) \tilde{r}_k \left(\frac{\ln(Q^2/\Lambda^2)}{\ln(\mu^2/\Lambda^2)} \right)^{\gamma_{DGLAP}(\tilde{j}_k)/(2\pi b)}. \end{aligned} \quad (157)$$

It is clear that the x -dependence of each of the terms S , S_k , \tilde{S}_k is Regge-like, so we call them the DGLAP Reggeons contributing to the non-singlet g_1 . The intercept j of the Reggeon S is the largest, and we call S the leading Reggeon and address S_k and \tilde{S}_k as the sub-leading Reggeons. Only the leading Reggeon has the positive intercept. All other intercepts are negative. We remind that all features of the DGLAP Reggeons are due to the assumed form of the initial quark density and are related to the phenomenological parameters of the fit (24). Obviously, one can decompose the DGLAP expression for the singlet g_1 quite similarly into a set of Reggeons.

B. Reggeon structure of Eq. (106)

Let us consider once more the limit of g_1 at $x \rightarrow 0$. In Sects. X, XI we have shown that the use of the saddle-point method to Eqs. (106,116) led to the Regge asymptotics (124,134). The intercepts Δ_{NS} and Δ_S were determined in Eqs. (129,136) as the largest roots of Eqs. (126) and (135) respectively. They are not simple poles in the ω -plane but the rightmost square-root branching points. They were found by solving numerically Eqs. (126,135). However, each of this equations can have more than one root. Applying the same argument we are able to find the additional non-singlet and singlet intercepts $\Delta_{NS}^{(k)}$ and $\Delta_S^{(k)}$, with $k = 1, 2, \dots$. Accounting for these contributions allows us to represent the non-singlet and singlet g_1 in a form similar to Eq. (156):

$$g_1(x, Q^2) \sim \frac{e^2}{2} \left[B(x, Q^2) + \sum_k B_k(x, Q^2) \right] \quad (158)$$

where the leading contribution $B(x, Q^2)$ is given by Eq. (124) for g_1^{NS} and by Eq. (134) for g_1^S . The other Reggeons $B_k(x, Q^2)$ look quite similarly. Namely, they can be obtained from Eqs. (124) and (134) with the replacement $\Delta_{NS} \rightarrow \Delta_{NS}^{(k)}$ and $\Delta_S \rightarrow \Delta_S^{(k)}$ respectively. In particular, for g_1^{NS} we have

$$B_k = \Pi(\Delta_{NS}^{(k)}) \delta q(\Delta_{NS}^{(k)}) (Q^2/x^2 \mu^2)^{\Delta_{NS}^{(k)}/2} \quad (159)$$

and Reggeons for g_1^S have the structure of Eq. (134). We call B, B_k QCD Reggeons because they are obtained from the total resummation of the leading logarithms in the QCD perturbation series. The Reggeon B has the maximal intercept compared to B_k , so we call it the leading QCD Reggeon and Reggeons B_k are the sub-leading (secondary) QCD Reggeons. It turns out that only the leading non-singlet Reggeon has the positive intercept (129) whereas the next non-singlet intercept is $\Delta_{NS}^{(1)} \approx 0$. On the contrary, there are three singlet Reggeons with positive intercepts: $\Delta_S^{(1)} = 0.55$, $\Delta_S^{(2)} = 0.35$, $\Delta_S^{(3)} = 0.21$.

C. Comparison between the DGLAP and the QCD Reggeons

The Regge theory, in the DIS context, states that the Regge (power-like) form of g_1 should be achieved at $x \rightarrow 0$ only, while g_1 looks quite differently at large x . It perfectly agrees with the features of the QCD Reggeons B, B_k obtained with the saddle-point method from the expressions for g_1 due to the QCD radiative corrections. They appear as a result of the total resummation of the QCD perturbation series and are never present to any fixed order of the perturbative expansions, including, of course, the Born term. Also they are not simple poles but square-root branching points, Their intercepts are found in terms of the basic QCD constants as the number of the colors N , the number of the flavors n_f , and Λ_{QCD} .

On the contrary, the SA Reggeons are produced by the poles present in any fixed order in α_s , including the Born approximation. They exist at any x , even at $x \sim 1$, because they are generated by the structure of the fit for δq instead of QCD radiative corrections. The intercepts of the SA Reggeons are expressed in terms of the phenomenological parameters of the fit (24) and have nothing to do with QCD calculations, so we call them input Reggeons in contrast to the QCD Reggeons B, B_k . On one hand, the existence of such Reggeons contradicts the concepts of the Regge theory, On the other hand, we have shown that the phenomenological success of DGLAP at small x is due to the singular factors $x^{-\alpha}$ in the fits for the initial parton densities which mimic the total resummation of the QCD radiative corrections. Obviously, these parameters are chosen to match the experimental data. So one should not be surprised that a truncated set of input Reggeons S, S_k, \tilde{S}_k could be close to the experiments with a good accuracy, the agreement being entirely due to the choice of their phenomenological parameters. So any theoretical interpretation of such Reggeons in the QCD context would be groundless.

XIV. DESCRIPTION OF g_1 IN THE UNIFIED REGION $\mathbf{A} \oplus \mathbf{B}$

In this Sect. we construct a description of g_1 valid in both regions **A** and **B**. Again, we focus on the non-singlet g_1 in the first place. To begin with, let us remind that in region **A**, where x is large, the non-singlet g_1 is described by the DGLAP expression Eq. (17) where both the coefficient function and the anomalous dimension are known to the NLO (two-loop) accuracy. In order to describe g_1^{NS} in the small- x region **B**, we took into account the leading logarithms of x and arrived at Eq. (106). When Eq. (106) is considered in the region **A**, the LL contributions become

small. On the other hand, non-logarithmic contributions accounted for in Eqs. (18,20) are quite important in this region. So, a possible option is to create an interpolation formula for g_1^{NS} which would coincide with Eq. (17) and Eq. (106) in regions **A** and **B** respectively. To this aim, let us define new coefficient function \tilde{C}^{NS} and anomalous dimension \tilde{C}^{NS} by combining directly the DGLAP results of Eqs. (18,20) and the LL results of Eqs. (105,104):

$$\begin{aligned}\tilde{C}^{NS} &= C^{NS} + C_{LO}^{NS \text{ DGLAP}} + \frac{A(\omega)}{2\pi} C_{LO}^{NS \text{ DGLAP}}, \\ \tilde{h}^{NS} &= h^{NS} + \frac{A(\omega)}{2\pi} \gamma^{(0)}(\omega) + \left(\frac{A(\omega)}{2\pi} \right)^2 \gamma^{(1)}(\omega).\end{aligned}\quad (160)$$

Because of the obvious double counting in Eq. (160), let us make the necessary subtractions and define C_{comb}^{NS} and h_{comb}^{NS} , which we call the combined coefficient function and anomalous dimension:

$$\begin{aligned}C_{comb}^{NS} &= \tilde{C}^{NS} - \Delta C^{NS}, \\ h_{comb}^{NS} &= \tilde{h}^{NS} - \Delta h^{NS}\end{aligned}\quad (161)$$

where ΔC^{NS} and Δh^{NS} are the first- and second- loop terms of the expansion of C^{NS} and h^{NS} into the series (see Eqs. (144,145)):

$$\begin{aligned}\Delta C^{NS} &= 1 + \frac{A(\omega)C_F}{2\pi} \left[\frac{1}{\omega^2} + \frac{1}{2\omega} \right], \\ \Delta h^{NS} &= \frac{A(\omega)C_F}{2\pi} \left[\frac{1}{\omega} + \frac{1}{2} \right].\end{aligned}\quad (162)$$

By inserting C_{comb}^{NS} and h_{comb}^{NS} in Eq. (106), we arrive at the final expression for g_1^{NS} valid in the region **A** \oplus **B**:

$$g_1^{NS}(x, Q^2) = \frac{e_q^2}{2} \int_{-\infty}^{\infty} \frac{d\omega}{2\pi i} \left(\frac{1}{x} \right)^\omega C_{comb}^{NS}(\omega) \delta q(\omega) e^{y h_{comb}^{NS}(\omega)}.\quad (163)$$

Quite similarly we obtain the combined coefficient functions $C_{comb}^{(\pm)}(\omega)$ and anomalous dimensions h_{ik}^{comb} for the singlet g_1 :

$$C_{comb}^{(\pm)} = C^{(\pm)} + C_{DGLAP}^{(\pm)} - \Delta C^{(\pm)}, \quad h_{ik}^{comb} = h_{ik} + h_{ik}^{DGLAP} - \Delta h_{ik}\quad (164)$$

where $C_{DGLAP}^{(\pm)}$ correspond to the DGLAP coefficient functions with the replacement $\alpha_s \rightarrow A(\omega)$ and h_{ik}^{DGLAP} are the DGLAP anomalous dimensions with the same replacement. The subtraction terms in Eq. (164) to the LO accuracy are:

$$\Delta h_{ik} = \frac{a_{ik}}{\omega}, \quad \Delta C^{(\pm)} = \frac{< e_q^2 >}{2\omega} \left[1 \mp \frac{a_{gg} - a_{qq}}{\sqrt{(a_{qq} - a_{gg})^2 + 4a_{qq}a_{gq}}} \right].\quad (165)$$

Replacing $C^{(\pm)}$ and h_{ik} in Eq. (116) by $C_{comb}^{(\pm)}$ and h_{ik}^{comb} , we finally obtain the expression for g_1^S valid in both regions **A** and **B**:

$$\begin{aligned}g_1^S(x, Q^2) &= \frac{1}{2} \int_{-\infty}^{\infty} \frac{d\omega}{2\pi i} \left(\frac{1}{x} \right)^\omega \left[\left(C_{comb}^{(+)} e^{\Omega_{(+)} y} + C_{comb}^{(-)} e^{\Omega_{(-)} y} \right) \omega \delta q(\omega) + \right. \\ &\quad \left. \left(C_{comb}^{(+)} \frac{(X + \sqrt{R})}{2h_{qg}^{comb}} e^{\Omega_{(+)} y} + C_{comb}^{(-)} \frac{(X - \sqrt{R})}{2h_{qg}^{comb} \Omega_{(-)}} e^{\Omega_{(-)} y} \right) \omega \delta g(\omega) \right]\end{aligned}\quad (166)$$

where $\Omega_{(\pm)}$, X and R are also expressed in terms of h_{ik}^{comb} . In the sub-region **A** of **A** \oplus **B** the main contribution in Eqs. (163,166) comes from the DGLAP terms in the coefficient functions and anomalous dimensions while the logarithmic terms are small, so that Eqs. (163,166) almost coincide with the DGLAP expressions. On the contrary, in the sub-region **B** the main role is played by the LL terms and therefore Eqs. (163,166) are pretty close to the expressions of Eqs. (106,116). Therefore Eqs. (163,166) really represent the interpolation expressions for g_1 in region **A** \oplus **B**.

XV. DESCRIPTION OF g_1 IN THE REGION **C**

The small Q^2 -region **C** is defined in Eq. 11. Contrary to the regions **A** and **B**, the SA cannot be used in region **C** at all. Indeed, the basic ingredient of SA, the DGLAP evolution equations, control the evolution with respect to $\ln(Q^2/\mu^2)$ in the regions **A**, **B** and do not apply at small Q^2 . In Ref.[16] we have proposed a method to describe g_1 at small Q^2 , which is a kinematic region studied experimentally. It turned out that our results for g_1 in region **B** can be generalized into the region **C** by introducing the shift

$$Q^2 \rightarrow \bar{Q}^2 \equiv Q^2 + \mu^2 \quad (167)$$

where μ is the infrared cut-off. Numerically, we have suggested to use the Optimal mass scales $\mu_{NS} = 1$ GeV and $\mu_S = 5.5$ GeV for the non-singlet and singlet case, respectively. The reasons for introducing those scales were given in Sect. X. Other shifts in Q^2 similar to Eq. (167) were suggested in various papers, see e.g. Refs. [41, 42]. In the literature, such shifts were introduced from phenomenological considerations whereas we suggest it from the analysis of the Feynman graphs contributing to g_1 . Let us notice that introducing this shift we go beyond the logarithmic approximation we have kept so far, so in this sense we consider our description of g_1 in the region **C** model-dependent. To begin with, let us notice that both the singlet and non-singlet component of g_1 obey the Bethe-Salpeter equation shown in Fig. 9. In the analytical form this equation is written

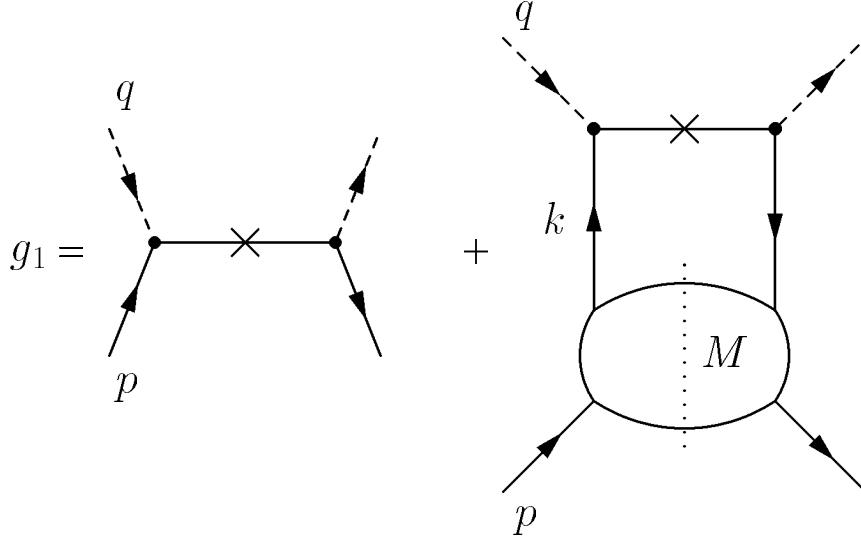


FIG. 9: The Bethe-Salpeter equation for g_1 in the region **C**.

$$g_1 = g_1^{Born} + \imath\kappa \int \frac{d^4k}{(2\pi)^4} (-2\pi\imath) \delta((q+k)^2 - m_q^2) \frac{2wk_\perp^2}{(k^2 - m_q^2)^2} \frac{E(2pk, k^2)}{2pk}, \quad (168)$$

where κ stands for the numerical factors $e^2/2$ and $< e^2/2 >$ for the non-singlet and the singlet respectively. We have skipped in Eq. (168) the convolution with the initial parton densities in order to prove the shift in Eq. (167), that the densities cannot affect. The δ -function (together with the factor $-2\pi\imath$) corresponds to the cut propagator of the upper quark with momentum k and mass m_q coupled to the virtual photon lines and the factor $2k_\perp^2$ appears after simplifying the spin structure of the equation. Similarly to Eq. (33), $E(2pk, k^2)$ in Eq. (168) is related to the invariant amplitude $M(2pk, k^2)$:

$$E(2pk, k^2) \equiv (1/2\pi) \Im M(2pk, k^2). \quad (169)$$

The invariant amplitude $M(2pk, k^2)$ describes the forward scattering of partons, with the upper partons being quarks. In other words, $M(2pk, k^2)$ can be any of $M^{NS}(2pk, k^2)$ (for g_1^{NS}) or $M_{qq}(2pk, k^2)$, $M_{q\bar{q}}(2pk, k^2)$ (for the singlet g_1). These amplitudes incorporate the total resummation of the leading logarithms. Obviously, E in Eq. (168) does not depend on Q^2 . Contrary to the parton amplitudes M_{ik} entering in Eq. (73), where k stands for the softest momenta,

the amplitudes E in Eq. (168) are essentially off-shell, and depend on two arguments: the invariant total energy $(p+k)^2 \approx 2pk$ and the virtuality k^2 which is not small now. Therefore they should be calculated independently. The amplitudes $M^{NS}(2pk, k^2)$, $M_{qg}(2pk, k^2)$, $M_{qq}(2pk, k^2)$ are considered in detail in Appendix C.

A. Infrared regularization in Eq. (168)

First, we remind that in order to account for the LL contributions in the small- x region **C**, one should use the ordering (14). This leads to the IR singularities of soft gluons and therefore an IR cut-off in the divergent propagators must be introduced. In order to treat the quarks and gluon ladders similarly, we drop the quark masses and introduce the IR cut-off in the quark and gluon ladders, providing both the ladder (vertical) partons and the soft non-ladder gluons with the fictitious mass μ , assuming that $\mu > m_{quark}$. In the previous Sects. we introduced μ in somewhat different way: according to Eq. (72), μ is the lowest limit in the integrations over k_\perp . Although it was noticed in Ref. [32] that different ways of introducing the IR cut-off lead to different results, this goes well beyond the accuracy we keep. Let us also notice that there is no need to introduce μ into the horizontal propagators of the ladder because they are IR stable. Then introducing μ Eq. (168) is modified into

$$g_1 = g_1^{Born} + \kappa \int \frac{d^4k}{(2\pi)^4} (-2\pi i) \delta((q+k)^2) \frac{2wk_\perp^2}{(k^2 - \mu^2)^2} \frac{E(2pk, k^2 + \mu^2)}{2pk}. \quad (170)$$

B. Solving the Bethe-Salpeter equation (170)

It is convenient to write Eq. (170) in terms of the Sudakov variables defined in Eq. (15). Eq. (D5) shows that the $2pk$ and k^2 -dependence for any of E^{NS} , E_{qq} , E_{qg} looks much alike, so below we consider the Bethe-Salpeter equation for g_1^{NS} only. Substituting E^{NS} into Eq. (170) and changing the order of the integrations, we arrive at

$$g_1 = g_1^{Born} + \kappa \int_{-\infty}^{\infty} \frac{d\omega}{2\pi i} \left(\frac{2pk}{k^2}\right)^\omega \omega h^{NS}(\omega) \int \frac{d\alpha}{\alpha} d\beta dk_\perp^2 \frac{wk_\perp^2}{(w\alpha\beta + k_\perp^2 + \mu^2)^2} \delta(w\beta + w\alpha - w\alpha\beta - k_\perp^2 - Q^2) \left(\frac{2pk}{k^2}\right)^\omega \left(\frac{w\alpha\beta + k_\perp^2 + \mu^2}{\mu^2}\right)^{h^{NS}}. \quad (171)$$

In the region **C** x is small, so we drop the second term in the argument of the δ -function, which is used for the integration over β . We obtain

$$g_1 = g_1^{Born} + \kappa \int_{-\infty}^{\infty} \frac{d\omega}{2\pi i} \omega h^{NS}(\omega) \int \frac{d\alpha}{\alpha} \frac{dk_\perp^2}{(\alpha Q^2 + k_\perp^2 + \mu^2)} \left(\frac{w\alpha}{\alpha Q^2 + k_\perp^2 + \mu^2}\right)^\omega \left(\frac{\alpha Q^2 + k_\perp^2 + \mu^2}{\mu^2}\right)^{h^{NS}} \quad (172)$$

The region of integration in Eq. (172) is shown in Fig. 10. It is restricted by the following limits:

(a): $w > k_\perp^2 + \mu^2 > \alpha Q^2 > 0$; (b): $w\alpha > \alpha Q^2 + k_\perp^2 + \mu^2$.

The result of the integration over this region depends on the relations between Q^2 and k_\perp^2/α . The leading contribution comes from the sub-region D in Fig. 10. Integrating over α in D leads to

$$g_1 = g_1^{Born} + \kappa \int_{-\infty}^{\infty} \frac{d\omega}{2\pi i} \omega h^{NS}(\omega) \frac{1}{\omega} \int_{Q^2}^w \frac{dk_\perp^2}{k_\perp^2 + \mu^2} \left(\frac{w}{k_\perp^2 + \mu^2}\right)^\omega \left(\frac{k_\perp^2 + \mu^2}{\mu^2}\right)^{h^{NS}}. \quad (173)$$

Replacing $k_\perp^2 + \mu^2$ by t in Eq. (173), we get

$$g_1 = g_1^{Born} + \kappa \int_{-\infty}^{\infty} \frac{d\omega}{2\pi i} h^{NS}(\omega) \int_{Q^2 + \mu^2}^{w + \mu^2} \frac{dt}{t} (w/t)^\omega (t/\mu^2)^{h^{NS}}. \quad (174)$$

In the region **C** $w \gg \mu^2$, so the upper limit of integration in Eq. (174) can be approximated by w . The lowest limit is definitely $Q^2 + \mu^2$ which proves the validity of the shift we have suggested in Eq. (167). Performing the integration over t in Eq. (174) leads to the expression of Eq. (106) but with the shifted value of Q^2 . Indeed, the integration over t yields

$$g_1 = g_1^{Born} + \kappa \int_{-\infty}^{\infty} \frac{d\omega}{2\pi i} \frac{h^{NS}}{(\omega - h^{NS})} \left[\left(\frac{w}{Q^2}\right)^\omega \left(\frac{\bar{Q}^2}{\mu^2}\right)^{h^{NS}} - \left(\frac{w}{\mu^2}\right)^{h^{NS}} \right]. \quad (175)$$

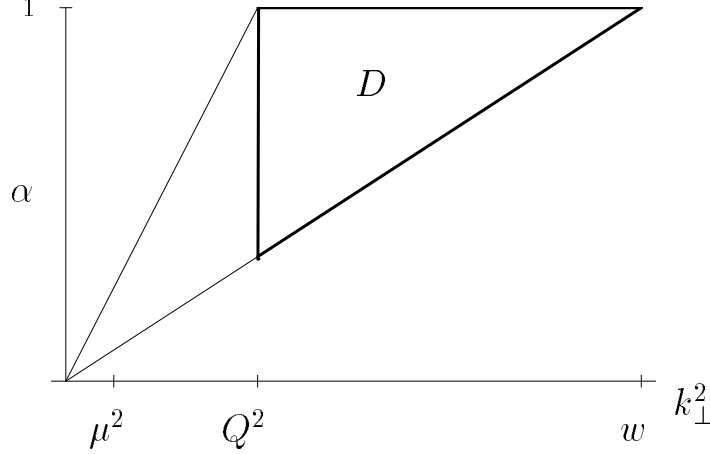


FIG. 10: The integration region in Eq. (172) .

The integration of the second term in the squared bracket yields zero, by closing the integration contour to the right of the singularity of $h^{NS}/(\omega - h^{NS})$. Using the identity

$$\frac{h^{NS}}{(\omega - h^{NS})} = -1 + \frac{\omega}{(\omega - h^{NS})} \quad (176)$$

and noticing that the first term in Eq. (176) cancels the term g_1^{Born} in Eqs. (168- 175), we arrive at the following expression:

$$g_1^{NS} = \kappa \int_{-\infty}^{\infty} \frac{d\omega}{2\pi i} \frac{\omega}{(\omega - h^{NS})} \left(\frac{1}{\bar{x}}\right)^\omega \left(\frac{\bar{Q}^2}{\mu^2}\right)^{h^{NS}} \quad (177)$$

which coincides with g_1^{NS} from Eq. (106) with the replacement $Q^2 \rightarrow \bar{Q}^2$. We have used here the shifted variable

$$\bar{x} = \bar{Q}^2/w = x + \mu^2/w \equiv x + z. \quad (178)$$

So, we have proved that our result for g_1^{NS} in region **B** can be extended to region **C** with the shift $Q^2 \rightarrow \bar{Q}^2 = Q^2 + \mu^2$.

It is not difficult to repeat the above calculations for the singlet g_1 . Eventually we conclude that our expressions (106,116) for g_1 in region **B** ($\equiv g_1^{(B)}(x, Q^2)$) can represent g_1 in the region **C** with the shifts $Q^2 \rightarrow \bar{Q}^2 = Q^2 + \mu^2$, $x \rightarrow \bar{x} = x + z$:

$$g_1^{(C)}(x, z, Q^2, \mu^2) = g_1^{(B)}(\bar{x}, \bar{Q}^2). \quad (179)$$

Obviously, Eq. (179) is valid in the unified region **B** \oplus **C**.

XVI. DESCRIPTION OF g_1 IN THE FULL REGION **A** \oplus **B** \oplus **C** \oplus **D**

In this Sect we will show that combining the shift of Q^2 introduced in Eq. (167) and the interpolation expressions of Eqs. (163-166) for g_1 in region **A**, it allows us to generalize expressions for g_1 which can be used in the full region **A** \oplus **B** \oplus **C** \oplus **D**. Let us first discuss the perturbative description of g_1 in the region **D**.

The interpolation expression for g_1^{NS} valid at large x and small Q^2 is

$$g_{1\ NS}^{(D)}(\bar{x}, \bar{Q}^2) = (e_q^2/2) \int_{-\infty}^{\infty} \frac{d\omega}{2\pi i} \left(\frac{1}{\bar{x}}\right)^\omega C_{comb}^{NS}(\omega) \delta q(\omega) e^{\bar{y} h_{comb}^{NS}(\omega)}, \quad (180)$$

where $\bar{x} = x + z$, $\bar{y} = \ln[(Q^2 + \mu^2)/\mu^2]$ and the combined coefficient function C_{comb}^{NS} and anomalous dimension h_{comb}^{NS} are given in Eq. (161).

Similarly, combining the shift and Eq. (166), the expression for the singlet g_1 in region **D** is:

$$g_{1S}^{(\mathbf{D})}(x, Q^2) = \frac{1}{2} \int_{-\infty}^{\infty} \frac{d\omega}{2\pi i} \left(\frac{1}{\bar{x}} \right)^\omega \left[\left(C_{comb}^{(+)}(\omega) e^{\Omega_{(+)} \bar{y}} + C_{comb}^{(-)}(\omega) e^{\Omega_{(-)} \bar{y}} \right) \omega \delta q(\omega) + \right. \\ \left. \left(C_{comb}^{(+)}(\omega) \frac{(X + \sqrt{R})}{2h_{comb}^{comb}} e^{\Omega_{(+)} \bar{y}} + C_{comb}^{(-)}(\omega) \frac{(X - \sqrt{R})}{2h_{comb}^{comb}} e^{\Omega_{(-)} \bar{y}} \right) \omega \delta g(\omega) \right], \quad (181)$$

Actually, Eqs. (180,181) represent g_1 not only in region **D** but also in the full region $\mathbf{A} \oplus \mathbf{B} \oplus \mathbf{C} \oplus \mathbf{D}$. Indeed, they are expressed in terms of the shifted variables \bar{x} , \bar{y} and therefore can be used at any values of Q^2 . Also they include the total resummation of the leading logarithms, so can be used in the regions **B** and **C**. Finally, they contain non-logarithmic one-loop contributions⁶ to the coefficient functions and anomalous dimensions obtained by the DGLAP-expressions, so this makes it possible to use them in the large- x regions **A** and **D**. Let us remind that the use of the shift in Q^2 drives us out of the logarithmic accuracy and also recall our suggestion is to use different values of μ for the singlet and non-singlet components of g_1 , given in Eqs. (130,137). We proceed now to the applications of the results on g_1 obtained so far..

XVII. PERTURBATIVE Q^2 -POWER CORRECTIONS

In this Section we discuss the power- $1/(Q^2)^k$ corrections to g_1 . Basically, there are various sources of such corrections but we focus only on those arising when the experimental results of g_1^{exp} are confronted to the theoretical predictions g_1^{theor} . The numerical analysis of the discrepancy between the non-singlet component of g_1^{exp} and g_1^{theor} shows (see for example Ref. [43] and Refs. therein) that

$$(g_1^{NS})^{exp} - (g_1^{NS})^{theor} \sim \sum_{k=1,2,\dots} \frac{T_k}{(Q^2)^k} \quad (182)$$

and the reason of the discrepancy is attributed to the impact of higher twists. Conventionally, the DGLAP expression of Eq. (20) is used for describing $(g_1^{NS})^{theor}$ and this is called the leading twist contribution. Naively one could expect from Eq. (182) that the impact of the power corrections should increase when Q^2 decreases, especially in the limit $Q^2 \rightarrow 0$. On the contrary, the analysis made in Ref. [43] states that, without any plausible theoretical reason, the power corrections are negligible when Q^2 decreases down to values $\sim 1 \text{ GeV}^2$.

We are going now to explain this observation and give an alternative description of the power corrections. To this aim, first let us notice that the kinematic region of g_1^{NS} studied in Ref. [43] mainly coincides with the region $\mathbf{B} \oplus \mathbf{C}$ and therefore the total resummation of the leading logarithms together with the shift of Q^2 should be included into expressions for g_1^{theor} . Eq. (179) contains both terms and therefore in the region $\mathbf{B} \oplus \mathbf{C}$

$$g_1^{NS} = \frac{e_q^2}{2} \int_{-\infty}^{\infty} \frac{d\omega}{2\pi i} \left(\frac{w}{Q^2 + \mu_{NS}^2} \right)^\omega \left(\frac{Q^2 + \mu_{NS}^2}{\mu_{NS}^2} \right)^{h^{NS}} C^{NS}(\omega) \delta q(\omega) \quad (183)$$

where $w = 2pq$ and μ_{NS} defined in Eq. (130). The terms with $Q^2 + \mu_{NS}^2$ in Eq. (183) can be expanded in the region **B**, where by definition $Q^2 > \mu_{NS}^2$, as follows:

$$\left(\frac{w}{Q^2 + \mu_{NS}^2} \right)^\omega \left(\frac{Q^2 + \mu_{NS}^2}{\mu_{NS}^2} \right)^{h^{NS}} = \left(\frac{1}{x} \right)^\omega \left(\frac{Q^2}{\mu_{NS}^2} \right)^{h^{NS}} \left[1 + \sum_{k=1} T_k^{NS}(\omega) \left(\frac{\mu_{NS}^2}{Q^2} \right)^k \right] \quad (184)$$

with

$$T_k^{NS} = \frac{(-\omega + h_{NS})(-\omega + h_{NS} - 1) \dots (-\omega + h_{NS} - k + 1)}{k!}. \quad (185)$$

⁶ The second-loop contributions can be included similarly.

Obviously, the power terms in the series of Eq. (184) have a perturbative origin and have nothing to do with the higher twists. Such terms are absent in the Standard Approach. Of course we are aware that higher twists can contribute to g_1 but we argue that the perturbative power contributions of Eq. (184) should be accounted for first, and only after a reliable estimate of the impact of the higher twists can be made. In contrast, in the region \mathbf{C} where $Q^2 < \mu_{NS}^2$, the power Q^2 -expansion takes the different form:

$$\left(\frac{w}{Q^2 + \mu_{NS}^2}\right)^\omega \left(\frac{Q^2 + \mu_{NS}^2}{\mu_{NS}^2}\right)^{h^{NS}} = \left(\frac{1}{z}\right)^\omega \left[1 + \sum_{k=1} T_k^{NS}(\omega) \left(\frac{Q^2}{\mu_{NS}^2}\right)^k\right]. \quad (186)$$

The power series in Eqs. (184,186) for large and small Q^2 are derived from the same formulae. However after the expansion has been made, they cannot be related to each other by simply varying Q^2 . Our estimate $\mu_{NS} \approx 1$ GeV gives a natural explanation to the observation made in Refs. [43] that the power Q^2 -corrections die out when Q^2 approaches values ~ 1 GeV² and do not appear at smaller values of Q^2 . Let us remind that our estimate of μ_{NS} in Eq. (130) was obtained by studying the asymptotic properties of g_1^{NS} , i.e. absolutely independently of any analysis of the power corrections. We suggest that the new source of the power contributions given by Eqs. (184,186) can sizably change the conventional analysis of the higher twists contributions to the Polarized DIS. Obviously, the power expansion of the singlet g_1 can be made quite similarly.

XVIII. APPLICATION TO THE COMPASS EXPERIMENT

Now let us discuss the application of our results to the recent COMPASS data on the singlet g_1 . We consider here the results of Refs. [16, 46]. The COMPASS experiment, carried out at the Super Proton Synchrotron at CERN, has investigated g_1 by measuring the asymmetries in the scattering of a polarized 160 GeV μ^+ -beam on polarized deuterons from a fixed ⁶LiD target (see Ref. [44]). As there is only one target, the COMPASS collaboration can measure the singlet g_1 only. Values of Q^2 at the COMPASS data are basically small: events with $Q^2 < 1$ GeV² correspond to about 90% of the total data set. From Refs. [44, 45] one can conclude that the COMPASS kinematic region for measuring g_1 , $G_{COMPASS}$, is

$$G_{COMPASS} : \quad 10^{-4} \lesssim x \lesssim 10^{-1}, \quad 10^{-1} \text{ GeV}^2 \lesssim Q^2 \lesssim 1 \text{ GeV}^2. \quad (187)$$

This makes clear that the Standard Approach cannot be used for the analysis of the COMPASS data. On the contrary, our expressions (116, 181) can be used in the COMPASS kinematic region. In the region $G_{COMPASS}$ $Q^2 \ll \mu_S^2$ and therefore in this region

$$\left(\frac{w}{Q^2 + \mu_S^2}\right)^\omega \left(\frac{Q^2 + \mu_S^2}{\mu_S^2}\right)^{\Omega_{(\pm)}} = \left(\frac{1}{z}\right)^\omega \left[1 + \sum_{k=1} T_k^{(\pm)}(\omega) \left(\frac{Q^2}{\mu_S^2}\right)^k\right], \quad (188)$$

with

$$T_k^{(\pm)} = \frac{(-\omega + \Omega_{\pm})(-\omega + \Omega_{\pm} - 1) \dots (-\omega + \Omega_{\pm} - k + 1)}{k!}. \quad (189)$$

Substituting Eq. (188) into Eq. (181) leads to the following expression:

$$g_1(x, z, Q^2) \approx g_1(z) + (Q^2/\mu_S^2) \frac{\partial g_1(z, x, Q^2)}{\partial Q^2/\mu_S^2} + O((Q^2/\mu_S^2)^2) \quad (190)$$

where $z = \mu_S^2/w$. The first term in Eq. (190) is

$$g_1(z) = \frac{\langle e_q^2 \rangle}{2} \int_{-\infty}^{\infty} \frac{d\omega}{2\pi i} \left(\frac{1}{z}\right)^\omega \left[\tilde{C}_q(\omega) \delta q + \tilde{C}_g(\omega) \delta g \right]. \quad (191)$$

As stated earlier, the combined coefficient functions $\tilde{C}_{q,g}$ include the total resummation of the leading logarithms of z and the non-logarithmic contributions $\sim \alpha_s$. They are defined as follows:

$$\tilde{C}_q = C_q + C_q^{DGLAP} - \Delta C_q, \quad \tilde{C}_g = C_g + C_g^{DGLAP} - \Delta C_g. \quad (192)$$

The terms C_q^{DGLAP} and C_g^{DGLAP} in Eq. (192) are the NLO DGLAP coefficient functions and

$$\begin{aligned} C_q &= \frac{\omega(\omega - H_{gg})}{\omega^2 - \omega(H_{gg} + H_{qq}) + H_{qq}H_{gg} - H_{qg}H_{gq}}, & \Delta C_q &= 1 + \frac{a_{qq}}{\omega^2}, \\ C_g &= \frac{\omega H_{gq}}{\omega^2 - \omega(H_{gg} + H_{qq}) + H_{qq}H_{gg} - H_{qg}H_{gq}}, & \Delta C_g &= \frac{a_{gq}}{\omega^2}. \end{aligned} \quad (193)$$

The presence of the terms $C_{q,g}^{DGLAP}$ in Eqs. (192,193), as the DGLAP coefficient functions, may sound irrelevant or strange because the DGLAP description of g_1 cannot be used in the small- Q^2 kinematics we are discussing. Nevertheless, the direct calculation of $g_1(z)$ to order $\sim \alpha_s$ yields a contributions coinciding with the NLO DGLAP coefficient functions. In other words the presence of the coefficient functions has nothing to do with the Q^2 -evolution. Eq. (190) explicitly shows that the Q^2 -dependence of g_1^S in the region $G_{COMPASS}$ should be weak, and also that g_1^S practically does not depend on x in the kinematical region $G_{COMPASS}$, even at very small x . However, its absolute value cannot be fixed from theoretical grounds. Indeed, Eq. (191) implies that sign of $g_1^S(z)$ at any given z is determined by the interplay between the quark and gluon contributions and eventually depends on $\delta q/\delta g$, which cannot be determined theoretically. At the same time, Eq. (190) predicts that the z -dependence of g_1^S is pretty far from being trivial, so the experimental investigation of this dependence would be quite interesting: it can yield information about the initial quark and gluon densities. The predictions of the essential independence of g_1^S on x made in Ref. [16], was confirmed in Ref. [45] where a flat dependence of g_1^S was found. More precisely, Ref. [45] reported that

$$g_1^S \approx 0 \quad (194)$$

in the region $G_{COMPASS}$ with small errors. Unfortunately, the COMPASS data do not allow to study the z -dependence of g_1^S in the proper way. Nevertheless, the COMPASS result (194) was used in Ref. [46] in order to obtain some rough estimates for $\delta q/\delta g$. Below we consider this issue in detail.

A. Interpretation of the COMPASS data on g_1^S

The variable $w = 2pq$ in the COMPASS experiment runs in the interval

$$30 \text{ GeV}^2 \lesssim w \lesssim 270 \text{ GeV}^2 \quad (195)$$

and therefore the range for z is

$$1 \lesssim z \lesssim 0.1. \quad (196)$$

The variable z is related to the standard variable $\nu = w/(2M)$ measured in GeV, with $M = 1 \text{ GeV}$:

$$z = \left(\frac{\mu^2}{2M} \right) \frac{1}{\nu} \approx \frac{15}{\nu}, \quad (197)$$

so the region (196) covered in the COMPASS experiment corresponds to the ν -region (in GeV)

$$15 \lesssim \nu \lesssim 150. \quad (198)$$

We remind that only the x -dependence of g_1^S was studied in the COMPASS experiment. The values of w and Q^2 were not reported in the COMPASS data, which makes impossible the straightforward application of Eq. (191) to the COMPASS results. However there are several options for the interpretation of Eq. (194) and below we consider them in detail:

Option (i):

Eq. (194) means that $g_1^S(z) = 0$ for any z from the whole interval of Eq. (196). In this case Eq. (191) implies a strong correlation between δq and δg at any ω :

$$C_q(\omega)\delta q(\omega) + C_g(\omega)\delta g(\omega) = 0. \quad (199)$$

We don't find theoretical grounds for understanding this fact and think that next option is more realistic.

Option (ii):

Eq. (194) holds in the average, namely in the region (196):

$$\langle g_1^S(z) \rangle = 0 . \quad (200)$$

Obviously, in order to fulfill the Eq. (200), $g_1(z)$ should acquire both positive and negative values in the region (196). This could be realized by an appropriate choice for the initial parton densities $\delta q(z)$ and $\delta g(z)$. In ref. [14] we suggested that in region **B** one can approximate the initial parton densities by constants. Guided by this result, we suggested in Ref. [16] to approximate $\delta q(z)$ and $\delta g(z)$ at small z by simple constants to get a rough estimate. However, in the COMPASS region (196) z is not small enough to use such a simple approximation. As the DGLAP-fits from Ref. [5] work quite well and also other parameterizations have a similar structure, we suggest a similar but regular fit :

$$\delta q(z) = N_q z(1-z)^3(1+3z), \quad \delta g(z) = N_g(1-z)^4(1+3z) . \quad (201)$$

The main difference with Ref. [5] is in the absence of the power factors z^a while the terms in the brackets in Eq. (201) and in Ref. [5] coincide (x in Ref. [5] is replaced by z in Eq. (201)). Indeed in Ref. [14], as also discussed previously, we have proved that the role played by the singular terms x^{-a} in the DGLAP fits is to mimic the total resummation of $\ln^k(1/x)$. On the other hand, we would like to keep the same ratio $\delta q/\delta g$ as in Ref. [5] and therefore we also change the power factor for δq in Eq. (201). Now it is easy to check that the fit (201) do not lead to a flat z -dependence for g_1 and cannot keep $g_1(z) = 0$ in the whole COMPASS region (187).

In more detail by substitution of Eq. (201) into Eq. (181) and performing the integration over ω numerically, with fixed and positive N_q , and varying the values of N_g , we plot our results in Fig. 11.

By a close inspection of the various configurations shown, we can easily conclude that these fits could be compatible with Eq. (200) only if $N_g > 0$ and $N_g > N_q$.

As the way of averaging g_1 over z in the COMPASS data is unknown to us, we can try another possibility, approximating

$$\langle g_1(z) \rangle \approx g_1(\langle z \rangle) = 0 , \quad (202)$$

where $\langle z \rangle = 0.25$ (i.e. $\langle \nu \rangle \approx 60$ GeV) is the mean value of z from the region (196). Then using Eqs. (181,201), keeping positive N_q and varying N_g , as shown in Fig. 11, we suggest again that N_g are positive and $N_g > N_q$.

B. Comments on the measurement of g_1 in different kinematic regions.

To conclude this Sect., let us make a brief comment on the parametrization of g_1 . In the Born approximation g_1 is given by Eq. (4) and depends on the only argument x which corresponds to the famous scaling in the DIS. The radiative corrections in the higher loops bring the violation of scaling, so g_1 acquires, additionally, the Q^2 -dependence. At this stage one can parameterize g_1 by the set of variables x , Q^2 or, alternatively, w , Q^2 , or ν , Q^2 . As it is well-known, in the target rest frame $w \equiv 2pq = 2M(E - E')$ where M is the target (nucleon) mass and E (E') is the energy of the incoming (outgoing) lepton. Then Q^2 in the same frame involves the above energies and the scattering angle θ . Therefore, both x and Q^2 depend on E' and θ and these variables are not always independent of each other. Indeed, there are experiments where the x -dependence of g_1 is measured at fixed Q^2 ; then Q^2 is varied to another value and the x -dependence is studied again. In this case x and Q^2 are really independent variables. In the opposite case of fixed w and varying Q^2 , Then $x = x(Q^2)$ and therefore these variables are not exactly independent, so it is more convenient to use w instead of x , as independent variable. These examples show that using w and Q^2 instead of the standard set x , Q^2 could be more convenient for g_1 . In particular, when Q^2 is very small, using x instead of w becomes really inconvenient. Nevertheless, the w -dependence of g_1 in the COMPASS experiments predicted in Eq. (190) can be clearly extracted from the dependence on x and Q^2 . Indeed, the variable \bar{x} defined in Eq. (178) can be written in the following form:

$$\bar{x} = \mu^2 x / Q^2 + x \approx \mu^2 x / Q^2 . \quad (203)$$

Although g_1 depends on x and on Q^2 at small Q^2 very weakly, its dependence on x/Q^2 is quite essential. Indeed Eq. (190) can be regarded as a sort of a new scaling law where g_1 depends on the variable x/Q^2 only.

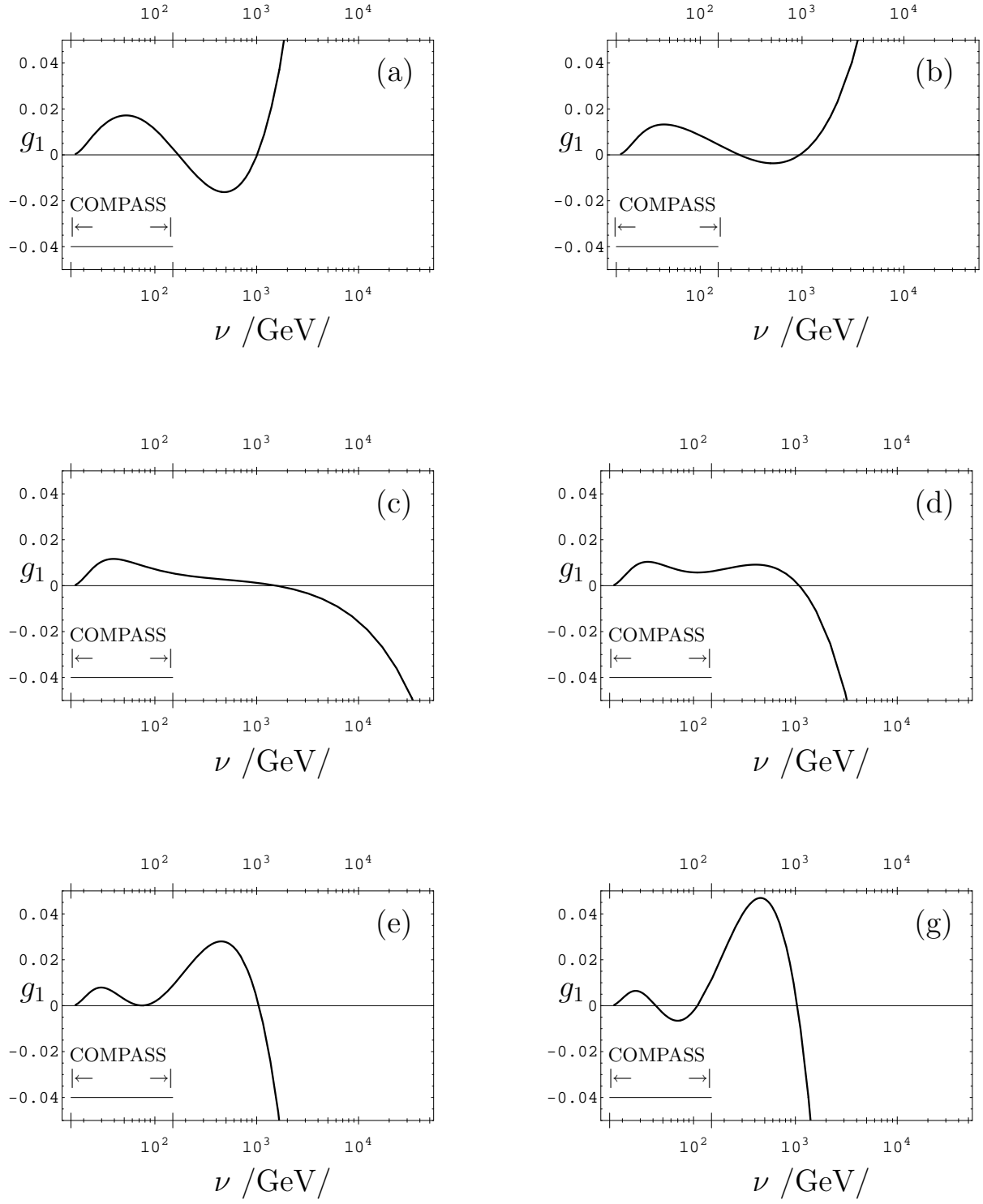


FIG. 11: The ν -dependence of $g_1(\nu)$, with δq , δg defined in Eq. (201), for $N_q = 0.5$ and different values of N_g : (a) -1.5, (b) -0.5, (c) 0, (d) 0.5, (e) 2, (g) 3.5; the COMPASS ν -region corresponds to Eq. (198) .

XIX. SUMMARY AND OUTLOOK

In the present paper we have presented an overview of our results on the spin structure function g_1 at arbitrary x and Q^2 . We have divided the whole kinematic region of x and Q^2 into the set of four regions **A** - **D** defined in Eqs. (5, 10-12) and considered g_1 in each of these regions. The region **A** is covered by the Standard Approach, based on the DGLAP evolution equations. This is briefly discussed in Sect. II. The application of the integral transforms to g_1 is given in Sect. III. In Sect. IV we have discussed in detail the parametrization of α_s and shown that the popular parametrization $\alpha_s = \alpha_s(k_\perp^2)$ is valid at large x only. Otherwise it should be replaced by the effective coupling α_s^{eff} defined in Eq. (49). When μ^2 obeys Eq. (50), α_s^{eff} can be approximated by $\alpha_s(k_\perp^2/\beta)$ (with β being the longitudinal Sudakov variable) and when, in addition, x is large, it can be simplified down to $\alpha_s(k_\perp^2)$. According to Eq. (50), the deviation of α_s^{eff} from α_s strongly depends on μ^2 . For example, when $\mu^2 = 2.5 \text{ GeV}^2$, $\alpha_s(\mu^2)/\alpha_s^{eff}(\mu^2) \approx 0.9$ but very quickly $\alpha_s(\mu^2)/\alpha_s^{eff}(\mu^2) \approx 0.5$ at $\mu^2 \approx 1 \text{ GeV}^2$, which is a typical DGLAP starting point of the Q^2 -evolution. The small- x region **B**, where the total resummation of the leading logarithms of x is essential, was considered in Sect. V. We account there for the resummation of the leading logarithms by solving an Infrared Evolution Equations (IREE), so in Sect. V the essence of the method together with the technology of IREE was discussed and the IREE for g_1 were obtained. These IREE involve new anomalous dimensions and coefficient functions. Explicit expressions for them were obtained in Sect. VI. Then the expression of Eq. (106) for the non-singlet component of g_1 in the region **B** was obtained in Sect. VII, while in Sect. VIII the result for the singlet g_1 in region **B** was given in Eq. (116). Obviously, the impact of the total resummation of logarithms of x is big at small x and becomes maximal at $x \rightarrow 0$, where the expressions in Eqs. (106,116) behave asymptotically as in Eqs. (124,134). The small- x asymptotics of the non-singlet g_1 is considered in detail in Sect. IX while Sect. X contains the asymptotics of the singlet g_1 . Both asymptotic behaviors are of the Regge type. The estimates for their intercepts are given by Eqs. (129) and (136). The small- x rise of g_1 predicted by Eqs. (124,134) is much steeper than the well-known small- x DGLAP prediction in Eq. (132). On the other hand, a numerical analysis shows that the use of the asymptotic formulae at the presently available x is not reliable, so Eqs. (106,116) should not be replaced by their asymptotic expressions of Eqs. (124,134) in the region **B**. The comparison of our results to the DGLAP-expressions for g_1 , which is impossible without fixing the initial parton densities δq and δg , shows that the impact of the resummation of the logarithms becomes essential for values smaller $x \approx 10^{-2}$. In Sect. XII, by considering in detail a standard DGLAP fit (24) for the initial parton densities, we have shown that the singular factors in the fits mimic the total resummation of the logarithms and provide the rise of g_1 at small x which is observed in the experimental data. On the other hand, when the total resummation of the logarithms is taken into account, the singular factors in the fits can be dropped. This allows one to simplify the parametrization of the initial parton densities.

The Reggeon structure in the two approaches has been discussed in Sect. XIII. However, in the case of the SA those Reggeons are, in a sense, fictitious: they are generated by the fits for the initial parton densities and because of that are present at any x instead of appearing in the asymptotic expressions at $x \rightarrow 0$.

The total resummation of the small- x logarithms is important in the region **B**, but also non-logarithmic contributions are quite essential in the DGLAP region **A**, where they are accounted for to NLO accuracy. Then the interpolating expressions for g_1 are presented in Eqs. (163) and (166). On one hand, they almost coincide with g_1^{DGLAP} in the region **A** and on the other hand, with Eqs. (106,116) in the region **B**, and at the same time do not require the use of the singular parameterizations of the parton densities.

The small- Q^2 region **C** is absolutely beyond the reach of DGLAP. On the other hand, the analysis of the Feynman diagrams contributing to g_1 shows that a shift of Q^2 allows us to extend Eqs. (106,116) into the region **C**. Similarly, Eqs. (163,166) can be extended into the region **D**. Eventually we arrived at the Eqs. (180,181) which are the interpolation expressions which can describe g_1 in the whole region **A** \oplus **B** \oplus **C** \oplus **D**. This was the subject of Sects. XIV-XVI. This shift of Q^2 , given in Eq. (167), inevitably causes the appearance of power $1/Q^2$ -corrections. Q^2 power corrections were found earlier phenomenologically by confronting g_1^{DGLAP} and the experimental data. They were attributed to the impact of higher twists. In Sect. XVII we argued that the role played by the higher twists can be estimated reliably only after accounting for the perturbative power corrections.

Finally, in Sect. XVIII we have used the small- Q^2 description of the singlet g_1 in Eq. (181) for the interpretation of the recent COMPASS data. First we have shown that g_1 in the COMPASS kinematic region does not depend on x , even at very small x . Then, we have suggested that the COMPASS data are compatible with positive gluon densities. We also argued in favor of studying the dependence of g_1 on $2pq$ in the COMPASS experiment rather than on x , in order to estimate the ratio $\delta g/\delta q$.

XX. ACKNOWLEDGMENTS

We are grateful to G. Altarelli, A.V. Efremov, S. Jadach, W. Schafer and O.V. Teryaev for useful discussions. The work is partly supported by Grant RAS 9C237, Russian State Grant for Scientific School RSGSS-3628.2008.2 and by an EU Marie-Curie Research Training Network under Contract No. MRTN-CT-2006-035505 (HEPTOOLS).

APPENDIX A: SIMPLIFICATION OF THE COLOR STRUCTURE OF THE FORWARD SCATTERING AMPLITUDES

We consider below in more detail the color structure of the Born amplitude A^{Born} defined in Eq. (42). As the external partons in A^{Born} are quarks or gluons,

$$A^{Born} = -C^{(col)} 4\pi\alpha_s \frac{\bar{u}(-p_2)\gamma_\mu u(p_1)\bar{u}'(p_1)\gamma_\mu u'(-p_2)}{s + i\epsilon} \quad (A1)$$

where the $SU(3)$ -matrix $C^{(col)}$ describes the color structure of A^{Born} . When all external partons are quarks, $C^{(col)} = t^a t^a$, with t^a ($a = 1, \dots, 8$) being the $SU(3)$ -generators in the fundamental (three-dimensional) representation; when the quarks are replaced by gluons, t^a are replaced by the $SU(3)$ -generators T^a in the vector representation. Each of the initial and final color two-parton states in Eq. (A1) corresponds to a reducible representation of $SU(3)$ and can be expanded into a sum of irreducible states. It is convenient to do it in the t -channel where the amplitude A^{Born} describes the quark-antiquark annihilation $q\bar{q} \rightarrow q'\bar{q}'$ and therefore the irreducible initial $q_i\bar{q}^j$ and final $q_p\bar{q}^q$ color states (with $i, j, p, q = 1, 2, 3$) are the singlet (S) and octet (V). The initial $\mathbf{3} \otimes \mathbf{3}$ color state in the t -channel state is $q_i\bar{q}^j$. It can be expanded into the sum of the singlet and octet, each one is the irreducible state: $\mathbf{3} \otimes \mathbf{3} = \mathbf{1} \oplus \mathbf{8}$. We denote them $(q_i\bar{q}^j)_S$ and $(q_i\bar{q}^j)_V$ respectively. It can be done by applying the projection operators P_S and P_V to the quark-antiquark states:

$$(q_i\bar{q}^j)_S = (P_S)_{ij}^{i'j'} q_{i'}\bar{q}^{j'}, \quad (q_i\bar{q}^j)_V = (P_V)_{ij}^{i'j'} q_{i'}\bar{q}^{j'} \quad (A2)$$

where

$$P_S^{jj'} = \frac{1}{N} \delta_i^{i'} \delta_j^j, \quad P_V^{jj'} = 2(t^a)_i^{i'} (t^a)_j^j. \quad (A3)$$

Obviously, these operators are orthogonal to each other and the factors $1/N$ (with $N = 3$) and 2 in Eq. (A3) are introduced to guarantee the property $P^2 = P$ for each of P_S and P_V . Let us notice that $\|P_S\|^2 = \text{Tr}[P_S^+ P_S] = 1$, $\|P_V\|^2 = \text{Tr}[P_V^+ P_V] = 2NC_F$ where $C_F = (N^2 - 1)/2N$. Applying the projection operators P_S and P_V to the color factor $C^{(col)}$ in Eq. (A1) allows us to write down $C^{(col)}$ as the sum of the scalar $C_S^{(col)}$ and octet $C_V^{(col)}$ color factors:

$$(C^{(col)})_{iq}^{jp} = C_S^{(col)} (P_S)_{iq}^{jp} + C_V^{(col)} (P_V)_{iq}^{jp}, \quad (A4)$$

where

$$C_S^{(col)} = \frac{(P_S)_{jp}^{iq} (t^a)_i^j (t^a)_q^p}{\|P_S\|^2} = \frac{1}{N} \text{Tr}[t^a t^a] = C_F, \\ C_V^{(col)} = \frac{(P_V)_{jp}^{iq} (t^a)_i^j (t^a)_q^p}{\|P_V\|^2} = \frac{2\text{Tr}[t^a t^b t^a t^b]}{2NC_F} = -\frac{1}{2N}. \quad (A5)$$

Substituting Eq. (A4) into Eq. (A1), we rewrite it as

$$A^{Born} = A_S^{Born} P_S + A_V^{Born} P_V, \quad (A6)$$

with

$$A_S^{Born} = -C_S^{(col)} 4\pi\alpha_s \frac{\bar{u}(-p_2)\gamma_\mu u(p_1)\bar{u}'(p_1)\gamma_\mu u'(-p_2)}{s + i\epsilon}, \\ A_V^{Born} = -C_V^{(col)} 4\pi\alpha_s \frac{\bar{u}(-p_2)\gamma_\mu u(p_1)\bar{u}'(p_1)\gamma_\mu u'(-p_2)}{s + i\epsilon}. \quad (A7)$$

When the external quarks in Eq. (A1) are replaced by gluons, generators t^a in the factor $C^{(col)}$ are replaced by the $SU(3)$ -generators T^a in the vector representation. It allows one to generalize Eq. (A7) to the gluons case, expanding the initial t -channel gluon state $\mathbf{8} \otimes \mathbf{8}$ into scalar and octet (see Refs. [10, 11] for detail). The projection operators $P_S^{(gg)}$ and $P_V^{(gg)}$ projecting the two-gluon t -channel state on the scalar and octet states are:

$$P_S^{(gg)} = \frac{1}{N^2 - 1} \delta_{a'b'} \delta_{ab} , \quad P_V^{(gg)} = \frac{1}{N} (T_c)_{a'b'} (T_c)_{ab} . \quad (\text{A8})$$

Strictly speaking, the normalization for projector operators with the gluon-quark transitions can be arbitrary but in order to match DGLAP it can be chosen as follows:

$$\begin{aligned} P_S^{(qq)} &= \frac{1}{N^2 - 1} \delta_i^j \delta_{ab} , & P_V^{(qq)} &= \frac{1}{N} (t_c)_i^j (T_c)_{ab} , \\ P_S^{(gq)} &= \frac{1}{N} \delta_{ab} \delta_{ij} , & P_V^{(gq)} &= 2 (T_c)_{ab} (t_c)_i^j . \end{aligned} \quad (\text{A9})$$

In Eqs. (A8,A9) we have kept the notation i, j for the quark color states while a, b, a', b' denote the gluon states. In contrast to the quark-quark case, the expansion of $\mathbf{8} \otimes \mathbf{8}$ into the sum of the irreducible $SU(3)$ -representations includes the singlet $\mathbf{1}$, the antisymmetric $\mathbf{8}_A$ and symmetric $\mathbf{8}_S$ octets and other contributions which cannot be organized out of the gluon fields and therefore can be left out, so for the gluons $\mathbf{8} \otimes \mathbf{8} = \mathbf{1} \oplus \mathbf{8}_A \oplus \mathbf{8}_S$. The symmetric octet $\mathbf{8}_S$ does not contribute to g_1 with the leading logarithmic accuracy (see Ref. [10] for detail). An additional argument in favor of neglecting the amplitudes with high color dimensions is that they die out quickly with energy.

APPENDIX B: NON-SINGLET CONTRIBUTION TO THE STRUCTURE FUNCTION F_1

The technology for calculating the leading logarithmic contributions to $F_1^{NS}(x, Q^2)$ is quite similar to the one for $g_1^{NS}(x, Q^2)$ (see Refs. [11] for detail). Similarly to g_1^{NS} , F_1^{NS} is expressed through the forward Compton amplitude $T_{NS}^{(+)}$ in the following way:

$$F_1^{NS} = \frac{1}{2\pi} \Im T_{NS}^{(+)} . \quad (\text{B1})$$

The superscript (+) in Eq. (B1) stands for the positive signature. Then it is convenient to define the Mellin amplitude $F_1^{NS}(\omega, y)$ related to $T_{NS}^{(+)}$ through the Mellin transform (34). As a consequence, the IREE for F_1^{NS} is almost identical to Eq. (80):

$$\omega F_1^{NS}(\omega, y) + \frac{\partial F_1^{NS}(\omega, y)}{\partial y} = \frac{1}{8\pi^2} (1 + \lambda_{qq}\omega) L_{qq}^{(+)}(\omega) F_1^{NS}(\omega, y) . \quad (\text{B2})$$

The amplitude $L_{qq}^{(+)}(\omega)$ again corresponds to the quark-quark scattering but its signature is now positive. It should be found independently. Eq. (B2) can be solved similarly to Eq. (80). The only difference between them is replacement of h_{NS} by $h^{(+)}$. The amplitude $h^{(+)}$ obeys the following IREE:

$$\omega h^{(+)} = b^{(+)} + (1 + \lambda_{qq}\omega) (h^{(+)})^2 . \quad (\text{B3})$$

The difference between Eq. (B3) and Eq. (80) is the inhomogeneous term $b^{(+)}$. It is expressed through a_{qq} defined in Eq. (84) and $V_{qq}^{(+)}$:

$$b^{(+)} = a_{qq} + V_{qq}^{(+)} . \quad (\text{B4})$$

Similarly to V_{qq} introduced in Eq. (88), $V_{qq}^{(+)}$ is expressed in terms of m_{qq} defined in Eq. (89) and a new quantity $D^{(+)}$ instead of D :

$$V_{qq}^{(+)} = m_{qq} D^{(+)} \quad (\text{B5})$$

with

$$D(\omega) = \frac{1}{2b^2} \int_0^\infty d\rho e^{-\omega\rho} \ln((\rho + \eta)/\eta) \left[\frac{\rho + \eta}{(\rho + \eta)^2 + \pi^2} - \frac{1}{\rho + \eta} \right]. \quad (\text{B6})$$

So, the expression for F_1^{NS} in region **B** is

$$F_1^{NS}(x, Q^2) = \frac{e_q^2}{2} \int_{-\imath\infty}^{\imath\infty} \frac{d\omega}{2\pi\imath} x^{-\omega} C_{NS}^{(+)}(\omega) \delta q(\omega) e^{h_{NS}^{(+)}(\omega) \ln(Q^2/\mu^2)}. \quad (\text{B7})$$

where

$$C_{NS}^{(+)} = \frac{2\omega}{\omega + \sqrt{\omega^2 - B_{NS}^{(+)}(\omega)}}, \quad (\text{B8})$$

$$h_{NS}^{(+)}(\omega) = (1/2) \left[\omega - \sqrt{\omega^2 - B_{NS}^{(+)}(\omega)} \right] \quad (\text{B9})$$

and

$$B_{NS}^{(+)} = 4(1 + \lambda_{qq}\omega) b_{qq}^{(+)} . \quad (\text{B10})$$

The small- x asymptotics of $F_1^{NS}(x, Q^2)$ is also of the Regge type but the value of the intercept $\Delta_{NS}^{(+)}$ is smaller than the one of g_1^{NS} :

$$\Delta_{NS}^{(+)} = 0.38 . \quad (\text{B11})$$

APPENDIX C: CONVOLUTION OF TWO AMPLITUDES

Let us consider the t - channel convolution of two amplitudes: $Q = A_1^{(p_1)} \otimes A_2^{(p_2)}$ of the scattering amplitudes $A_1^{(p_1)}$ and $A_2^{(p_2)}$ where $p_{1,2} = \pm$ stand for the signatures. It is convenient to describe amplitudes $M_a^{(p_a)}$ in terms of the invariant amplitudes M_a . For example, the invariant amplitude $M^{(\pm)}$ for the quark-antiquark forward annihilation $q(p_1) + \bar{q}(p_2) \rightarrow q(p'_1) + \bar{q}(p'_2)$ are introduced as follows:

$$A^{(\pm)} = \frac{j_\nu j_\nu}{s} M^{(\pm)} \quad (\text{C1})$$

where j_ν are the quark currents. We remind we use the Feynman gauge.

It is also convenient to use the asymptotics of the Sommerfeld-Watson transform (often called the Mellin representation) for each of those amplitudes in the following form:

$$M_a^{(p)}(s, \mu^2) = \int_{-\imath\infty}^{\imath\infty} \frac{d\omega}{2\pi\imath} \left(\frac{s}{\mu^2} \right)^\omega \xi^{(p_a)}(\omega) F_a^{(p_a)}(\omega), \quad (\text{C2})$$

with $a = 1, 2$. The signature factor

$$\xi^{(\pm)}(\omega_a) = -\frac{e^{-\imath\pi\omega} \pm 1}{2} \approx \frac{(1 \pm 1) + \imath\pi\omega}{2} \quad (\text{C3})$$

and the transform inverse to Eq. (C2) is

$$F^{(\pm)}(\omega) = -\frac{1}{\pi\omega} \int_{\mu^2}^\infty \frac{ds}{s} \left(\frac{s}{\mu^2} \right)^{-\omega} \frac{\Im_s M \pm \Im_u M}{2}. \quad (\text{C4})$$

Using Eqs. (C1,C2) and skipping the overall factor $j_\nu j_\nu/s$ allows us to write the convolution Q through the invariant convolution Q_{inv} as

$$Q = \frac{j_\nu j_\nu}{s} Q_{inv}^{p_1 p_2} \quad (\text{C5})$$

with⁷

$$Q_{inv}^{p_1 p_2} = \imath \int_{-\imath\infty}^{\imath\infty} \frac{d\omega_1}{2\pi\imath} \frac{d\omega_2}{2\pi\imath} \xi^{(p_1)}(\omega_1) \xi^{(p_2)}(\omega_2) f_1^{(p_1)}(\omega_1) f_2^{(p_2)}(\omega_2) \int \frac{d^4 k}{16\pi^4} \frac{2k_\perp^2}{(k^2 - m^2 + \imath\epsilon)^2} \left(\frac{s_1}{|k^2|} \right)^{\omega_1} \left(\frac{s_2}{|k^2|} \right)^{\omega_2} \frac{s}{s_1} \frac{s}{s_2} \quad (C6)$$

where the factor $2k_\perp^2$ appears as the result of simplifying the spinor structure, $s_1 = 2p_1 k$, $s_2 = 2p_2 k$. Both of them are understood as $s_{1,2} + \imath\epsilon$.

For integration over k in Eq. (C6) we use the Sudakov variables (15):

$$Q_{inv}^{p_1 p_2} = \frac{\imath}{16\pi^4} \int_{-\imath\infty}^{\imath\infty} \frac{d\omega_1}{2\pi\imath} \frac{d\omega_2}{2\pi\imath} \xi^{(p_1)}(\omega_1) \xi^{(p_2)}(\omega_2) f_1^{(p_1)}(\omega_1) f_2^{(p_2)}(\omega_2) \Psi^{(p_1, p_2)}(\omega_1, \omega_2, s/\mu^2) \quad (C7)$$

with

$$\Psi^{(p_1, p_2)}(\omega_1, \omega_2, s/\mu^2) = \int d\alpha d\beta d^2 k_\perp \frac{k_\perp^2}{(s\alpha\beta - k_\perp^2 + \imath\epsilon)^2} \left(\frac{s\alpha}{|k^2|} \right)^{\omega_1} \left(\frac{s\beta}{|k^2|} \right)^{\omega_2} \frac{s}{s\alpha} \frac{s}{s\beta}. \quad (C8)$$

Let us first integrate Eq. (C8) over α . The integration can be done in the complex plane by applying the Cauchy formula. The singularities in the complex α -plane are the double pole $s\alpha\beta - k_\perp^2 + \imath\epsilon = 0$ and the cut from the Mellin factor $(s\alpha)^{\omega_1}$. The integration yields a non-zero result when the pole and the cut have opposite imaginary parts. The imaginary part of the cut is positive while the imaginary part of the pole is negative provided $\beta > 0$. When $\beta < 0$, both singularities have positive imaginary parts and therefore the integration over α yields zero. Closing up the integration contour in the lower hemi-plane and taking the residue of the pole

$$\alpha = (k_\perp^2 - \imath\epsilon)/s\beta \quad (C9)$$

we perform the integration over α and arrive at

$$\begin{aligned} \Psi^{(p_1, p_2)}(\omega_1, \omega_2, s/\mu^2) &= -2\pi^2 \imath \int_{\mu^2}^s \frac{dk_\perp^2}{k_\perp^2} \left(\frac{s}{k_\perp^2} \right)^{\omega_2} \int_{k_\perp^2/s}^1 d\beta \beta^{\omega_2 - \omega_1 - 1} = \\ &= \frac{-2\pi^2 \imath}{\omega_2 - \omega_1} \int_{\mu^2}^s \frac{dk_\perp^2}{k_\perp^2} \left[\left(\frac{s}{k_\perp^2} \right)^{\omega_2} - \left(\frac{s}{k_\perp^2} \right)^{\omega_1} \right] = \frac{-2\pi^2 \imath}{\omega_2 - \omega_1} \left[\frac{1}{\omega_2} \left(\frac{s}{\mu^2} \right)^{\omega_2} - \frac{1}{\omega_1} \left(\frac{s}{\mu^2} \right)^{\omega_1} \right] \end{aligned} \quad (C10)$$

Therefore we obtain the following expression for Q_{inv} :

$$Q_{inv}^{p_1 p_2} = \frac{1}{8\pi^2} \int_{-\imath\infty}^{\imath\infty} \frac{d\omega_1}{2\pi\imath} \frac{d\omega_2}{2\pi\imath} \xi^{(p_1)}(\omega_1) \xi^{(p_2)}(\omega_2) \frac{f_1^{(p_1)}(\omega_1) f_2^{(p_2)}(\omega_2)}{\omega_2 - \omega_1} \left[\frac{1}{\omega_2} \left(\frac{s}{\mu^2} \right)^{\omega_2} - \frac{1}{\omega_1} \left(\frac{s}{\mu^2} \right)^{\omega_1} \right]. \quad (C11)$$

Eq. (C11) involves two integrations, however one of them can be done easily. The integration lines over $\omega_{1,2}$ in Eq. (C11) are parallel to the imaginary axes and lie to the right of the rightmost singularities of $f_{1,2}$. Let us assume that additionally to it

$$0 < \Re\omega_1 < \Re\omega_2. \quad (C12)$$

The opposite case $\Re\omega_1 > \Re\omega_2$ can be discussed similarly. The integrand of Eq. (C11) includes two similar terms in the squared brackets. Let us focus on integrating the first term, $(s/\mu^2)^{\omega_2}$ and let us integrate this part of Eq. (C11) with respect to ω_1 . In this case closing up the ω_1 -integration contour to the left involves accounting for singularities of $f_1(\omega_1)$. On the contrary, when we close up the ω_1 -contour to the right, the only singularity inside the contour is the pole $1/(\omega_2 - \omega_1)$, so we can do this integration without considering f_1 , just by taking the residue at $\omega_1 = \omega_2$. At the same time, integrating the remaining, proportional to $(s/\mu^2)^{\omega_1}$ part of Eq. (C11) with respect to ω_1 yields zero. Therefore Eq. (C11) is reduced to the simpler form:

$$Q_{inv}^{p_1 p_2} = \frac{1}{8\pi^2} \int_{-\imath\infty}^{\imath\infty} \frac{d\omega}{2\pi\imath} \left(\frac{s}{\mu^2} \right)^\omega \xi^{(p_1)}(\omega) \xi^{(p_2)}(\omega) \frac{f_1^{(p_1)}(\omega) f_2^{(p_2)}(\omega)}{\omega} \quad (C13)$$

⁷ The factor \imath is the product of the overall factor $-\imath$ and $(\pm\imath)^2$ from the t -channel quark or gluon propagators.

Obviously,

$$\xi^{(p_1)}(\omega)\xi^{(p_2)}(\omega) \approx (1/4)[(1 + P_1 P_2) - i\pi\omega(P_1 + P_2)] = \xi^{(p_1)}(\omega) \delta_{p_1 p_2} \quad (C14)$$

where $P_{1,2} = \pm 1$. It means that the leading contribution to $Q_{inv}^{p_1 p_2}$ is diagonal in the signatures. Strictly speaking, this should be checked in advance, with using the Sommerfeld-Watson transform where analytical properties of the involved amplitudes are explicitly accounted for.

APPENDIX D: OFF-SHELL INVARIANT AMPLITUDE M IN EQ. (169)

The invariant amplitude M in Eq. (169) is a generic notation for the following invariant off-shell amplitudes: $M^{NS}(2pk, k^2)$ contributing to the Bethe-Salpeter for g_1^{NS} and the flavor singlet amplitudes $M_{qq}(2pk, k^2)$, $M_{qg}(2pk, k^2)$. They are related to the amplitudes $A_{qq}(2pk, k^2)$, $A_{qg}(2pk, k^2)$ of the forward quark-quark and quark-gluon scattering:

$$\begin{aligned} A_{qq} &= -\frac{\bar{u}(-k)\gamma_\lambda u(p)\bar{u}(p)\gamma_\lambda u(-k)}{(p+k)^2 + i\epsilon} M_{qq}(2pk, k^2), \\ A_{qg} &= -e_\lambda e_\mu^* \frac{\bar{u}(-k)\gamma_\lambda(\hat{p} - \hat{k})\gamma_\mu u(-k)}{(p+k)^2 + i\epsilon} M_{qg}(2pk, k^2). \end{aligned} \quad (D1)$$

The outgoing momenta $-k$ in Eq. (D1) are assigned to the final (upper) off-shell quarks whereas the initial quarks and gluons have momenta p ; e_λ and e_μ are the polarization vectors of the gluons. We remind that the amplitudes $M_{qq}(2pk, k^2)$, $M_{qg}(2pk, k^2)$ are off-shell and therefore they differ from the amplitudes M_{ik} introduced in Eq. (73): M_{qq} and M_{qg} logarithmically depend on two arguments, $2pk$ and k^2 , i.e.

$$M_{qq} = M_{qq}(\rho, z); \quad M_{qg} = M_{q,g}(\rho, z) \quad (D2)$$

where $\rho = \ln(2pk/\mu^2)$, $z = \ln(k^2/\mu^2)$.

It is convenient to introduce the Mellin amplitudes $\varphi_{ik}(\omega, z)$ conjugate to $M_{ik}(\rho, z)$ through Eq. (34). The IREE for $\varphi_{ik}(\omega, z)$ is quite similar to Eqs. (75,76), and we put here all $\lambda_{ik} = 0$ for the sake of simplicity:

$$\begin{aligned} \frac{\partial \varphi^{NS}}{\partial z} + \omega \varphi^{NS} &= \frac{1}{8\pi^2} \varphi^{NS} L_{qq}(\omega), \\ \frac{\partial \varphi_{qq}}{\partial z} + \omega \varphi_{qq} &= \frac{1}{8\pi^2} \varphi_{qq} L_{qq}(\omega) + \frac{1}{8\pi^2} \varphi_{qg} L_{gq}(\omega), \\ \frac{\partial \varphi_{qg}}{\partial z} + \omega \varphi_{qg} &= \frac{1}{8\pi^2} \varphi_{qq} L_{qg}(\omega) + \frac{1}{8\pi^2} \varphi_{qg} L_{gg}(\omega). \end{aligned} \quad (D3)$$

The amplitudes L^{NS} , L_{ik} in Eq. (D3) are on-shell, so in accordance with Eq. (77) they can be expressed in terms of $h^{NS}(\omega) = (1/8\pi^2)L^{NS}(\omega)$, $h_{ik}(\omega) = (1/8\pi^2)L_{ik}(\omega)$ which are obtained in Eqs. (104,95). General solutions to the linear equations (D3) can easily be found (cf Eq. (107)):

$$\begin{aligned} \varphi^{NS} &= \Phi^{NS}(\omega) e^{z[-\omega + h^{NS}]}, \\ \varphi_{qq} &= \Psi_1(\omega) e^{-\omega z + z\Omega(+)} + \Psi_2(\omega) e^{-\omega z + z\Omega(-)}, \\ \varphi_{qg} &= \Psi_1(\omega) \frac{X + \sqrt{R}}{2h_{gq}} e^{-\omega z + z\Omega(+)} + \Psi_2(\omega) \frac{X - \sqrt{R}}{2h_{gq}} e^{-\omega z + z\Omega(-)}, \end{aligned} \quad (D4)$$

with $\Omega_{(\pm)}$, X and R defined in Eqs. (110, 108, 109) respectively whereas $\Psi_{1,2}$ should be specified. Therefore, $E(2pk.k^2)$ used in Eq. (168) can be any of $E^{NS}(2pk.k^2)$, $E_{qq}(2pk.k^2)$, $E_{qg}(2pk.k^2)$ given by the following expressions:

$$\begin{aligned} E^{NS}(2pk.k^2) &= \int_{-\imath\infty}^{\imath\infty} \frac{d\omega}{2\pi\imath} \left(\frac{2pk}{k^2}\right)^\omega \omega \Phi^{NS}(\omega) e^{zh^{NS}}, \\ E_{qq}(2pk.k^2) &= \int_{-\imath\infty}^{\imath\infty} \frac{d\omega}{2\pi\imath} \left(\frac{2pk}{k^2}\right)^\omega \omega \left[\Psi_1(\omega) e^{z\Omega(+)} + \Psi_2(\omega) e^{z\Omega(-)} \right], \\ E_{qg}(2pk.k^2) &= \int_{-\imath\infty}^{\imath\infty} \frac{d\omega}{2\pi\imath} \left(\frac{2pk}{k^2}\right)^\omega \omega \left[\Psi_1(\omega) \frac{X + \sqrt{R}}{2h_{gq}} e^{z\Omega(+)} + \Psi_2(\omega) \frac{X - \sqrt{R}}{2h_{gq}} e^{z\Omega(-)} \right]. \end{aligned} \quad (D5)$$

In order to specify $\Psi_{1,2}$, we use the obvious matching condition:

$$\varphi^{NS}(\omega, z=0) = 8\pi^2 h^{NS}(\omega) , \quad \varphi_{qq}(\omega, z=0) = 8\pi^2 h_{qq}(\omega) , \quad \varphi_{qg}(\omega, z=0) = 8\pi^2 h_{qg}(\omega) . \quad (D6)$$

It immediately fixes φ^{NS} :

$$\varphi^{NS} = 8\pi^2 h^{NS}(\omega) e^{z[-\omega + h^{NS}(\omega)]} \quad (D7)$$

and leads to the explicit expressions for $\Psi_{1,2}$:

$$\Psi_1 = 8\pi^2 \frac{[2h_{qg}h_{gq} - h_{qq}(h_{gg} - h_{qq} - \sqrt{R})]}{2\sqrt{R}} , \quad \Psi_2 = 8\pi^2 \frac{[-2h_{qg}h_{gq} + h_{qq}(h_{gg} - h_{qq} + \sqrt{R})]}{2\sqrt{R}} . \quad (D8)$$

APPENDIX E: CALCULATING THE SMALL- x ASYMPTOTICS OF THE NON-SINGLET g_1 .

Eq. (106) for $g_1^{NS}1(x, Q^2)$ in region **B** can be written as follows:

$$g_1^{NS}(x, Q^2) = \int_{-\infty}^{\infty} \frac{d\omega}{2\pi i} e^{\Phi(\omega, x, Q^2)} \quad (E1)$$

where the phase Φ is

$$\Phi(\omega, x, Q^2) = \omega \ln(1/x) + \ln C_{NS}(\omega) + y h_{NS}(\omega) = \omega \xi + \ln C_{NS}(\omega) - \frac{y}{2} \sqrt{\omega^2 - B_{NS}(\omega)} \quad (E2)$$

where we have used the expression (104) and denoted $\xi = \ln(w/\sqrt{Q^2\mu^2})$. We remind that $y = \ln(Q^2/\mu^2)$. We are going to calculate the asymptotics of g_1^{NS} at $x \rightarrow 0$ and fixed Q^2 , i.e. at fixed Q^2 and $w \rightarrow \infty$. The standard way to calculate asymptotics is to apply the saddle-point method to Eq. (E1). According to it,

$$g_1^{NS} \sim \Pi_{NS}(\omega_0, w, Q^2) e^{\Phi_0(\omega_0, w, Q^2)} , \quad (E3)$$

with the stationary phase $\Phi_0 = \Phi(\omega_0, w, Q^2)$ and the stationary point ω_0 is defined from the requirement $d\Phi/d\omega = 0$, i.e. ω_0 is a solution to the equation

$$\xi + \frac{C'_{NS}(\omega)}{C_{NS}(\omega)} - \frac{y}{4} \frac{(2\omega - B'_{NS}(\omega))}{\sqrt{\omega^2 - B_{NS}(\omega)}} = 0 . \quad (E4)$$

Obviously, Eq. (E4) can have much more the one solution. In this case ω_0 is the solution with the largest $\Re\omega$. It is often called the rightmost stationary point. Substituting the explicit expressions (105) for C_{NS} , we transform Eq. (E4) into

$$\xi \omega B_{NS} \sqrt{\omega^2 - B_{NS}} = (B_{NS} - \omega B'_{NS}/2)(\omega - \sqrt{\omega^2 - B_{NS}}) + \frac{y}{2} \omega B_{NS}(\omega - B'_{NS}/2) . \quad (E5)$$

Obviously this equation cannot be solved analytically. The analytical solution can be found for the particular case when B does not depend on ω (it corresponds to the case of fixed α_s) and $y = 0$. In this case Eq. (E4) can be reduced to the algebraic equation

$$\omega^4 + (2/\rho)\omega^3 - \omega^2 B_{NS} - (2B_{NS}/\rho)\omega - (B_{NS}/\rho^2) = 0 \quad (E6)$$

where $\rho = \ln(w/\mu^2)$. Eq. (E6) has four roots which can be found with using the known from the literature Ferrari formulae but only two of them, namely $\omega = \pm\sqrt{B_{NS}}$ do not go to zero when $w \rightarrow \infty$. Obviously, in this case the rightmost root is $\omega_0 = \sqrt{B_{NS}}$. It is easy to make this conclusion, without solving Eq. (E6). Indeed, Eq. (E6) can be written as

$$\omega^2(\omega^2 - B_{NS}) + (2/\rho)\omega(\omega^2 - B_{NS}) - (B_{NS}/\rho^2) = 0 . \quad (E7)$$

When the terms $\sim 1/\rho^2$ and $\sim 1/\rho$ are dropped, Eq. (E7) can be solved immediately and the rightmost root can easily be found. Applying the same arguments allows one to solve Eq. (E4) at $w \rightarrow 0$ drives us to conclude that the rightmost and non-vanishing at $w \rightarrow \infty$ root of Eq. (E4) does not depend on y and it can be found as the rightmost root of the much simpler equation $\omega^2 = B_{NS}(\omega)$ as is stated in Eq. (125). This leads to the Regge asymptotics of Eq. (124) quite different from the well-known DGLAP asymptotics (132). Let us notice that, in the perfect agreement with the concepts of the phenomenological Regge theory, this root corresponds to the branching point singularity of Eq. (E4).

APPENDIX F: THE DGLAP SMALL- x ASYMPTOTICS

Let us remind how the DGLAP asymptotics of g_1^{NS} in Eq. (132) was obtained. As this topic is well-known, for the sake of simplicity we consider $g_1^{NS}_{DGLAP}$ with the LO accuracy. When the singular term in δq is absent, the small- x asymptotics of $g_1^{NS}_{DGLAP}$ can also be obtained with the saddle-point method. Similarly to Eq. (E1), $g_1^{NS}_{DGLAP}$ can be written as

$$g_1^{NS}_{DGLAP}(x, Q^2) = \int_{-\infty}^{\infty} \frac{d\omega}{2\pi i} e^{\Phi_{DGLAP}(\omega, x, Q^2)} \quad (F1)$$

where the phase Φ_{DGLAP} is

$$\Phi_{DGLAP} = \omega \ln(1/x) + \int_{\mu^2}^{Q^2} \frac{dk_{\perp}^2}{k_{\perp}^2} \frac{\alpha_s(k_{\perp}^2)}{2\pi} \gamma^{(0)}, \quad (F2)$$

with $\gamma^{(0)}$ being given by Eq. (21). The bulk of the integral in Eq. (F1) comes from the region of ω obeying

$$\omega \ln(1/x) \lesssim 1 \quad (F3)$$

because the factor $e^{\omega \ln(1/x)}$ in Eq. (F1) strongly oscillates beyond this region. So, the values of ω mainly contributing to the integral become small when $x \rightarrow 0$. As a consequence, the most important term in $\gamma^{(0)}$ is now the singular in ω term $A_{DGLAP}(Q^2)/\omega$, with

$$A_{DGLAP}(Q^2) = \int_{\mu^2}^{Q^2} \frac{dk_{\perp}^2}{k_{\perp}^2} \frac{\alpha_s(k_{\perp}^2) C_F}{2\pi}. \quad (F4)$$

Therefore, approximately

$$\Phi_{DGLAP} \approx \omega \ln(1/x) + A_{DGLAP}(Q^2)/\omega. \quad (F5)$$

The equation for the stationary point is

$$\Phi'_{DGLAP} = \ln(1/x) - A_{DGLAP}(Q^2)/\omega^2 = 0, \quad (F6)$$

which leads to the stationary point

$$\omega_0^{DGLAP} = \sqrt{A_{DGLAP}(Q^2)/\ln(1/x)} \quad (F7)$$

and eventually to the DGLAP -asymptotic given in Eq. (132). Contrary to the case considered in Appendix E, the DGLAP stationary point depends on $\ln(1/x)$. Eq. (F7) shows that the Q^2 -dependence in the DGLAP asymptotics follows from the DGLAP parametrization $\alpha_s = \alpha_s(k_{\perp}^2)$ and mostly from keeping Q^2 as the upper limit of the integration in Eq. (F4). The latter takes place because of the use the DGLAP ordering (13). However in the small- x region the ordering (13) becomes unreliable and should be replaced by the ordering of Eq. (14) where the upper limit is w . Obviously, the Q^2 -dependence in Eq. (F7) vanishes after replacing Q^2 by w . We remind that the DGLAP asymptotics (132) can be obtained only under the assumption that the initial parton densities are not singular at $x \rightarrow 0$ otherwise the asymptotics (F7) is changed for the Regge asymptotics (149).

APPENDIX G: THE SMALL- x ASYMPTOTICS OF g_1^{NS} WITH THE TRUNCATED SERIES FOR THE COEFFICIENT FUNCTIONS AND ANOMALOUS DIMENSIONS.

We consider here the case where the coefficient functions and anomalous dimensions are calculated in high orders in α_s , however without the total resummation of those contributions. According to Eq. (F3) the essential values of ω in Eq. (F1) are small at $x \rightarrow 0$, so the most important terms in expressions for the non-singlet coefficient functions and anomalous dimensions are the most singular terms in ω , i.e. the double-logarithmic contributions. They can

be obtained, expanding Eqs. (104, 105) into series absolutely in the same way as was done in Eqs. (144, 145). The expansion for the coefficient function in expressions (106) and (20) have the same form

$$C_{NS} = 1 + \frac{a}{4\omega^2} + 2\left(\frac{a}{4\omega^2}\right)^2 + 5\left(\frac{a}{4\omega^2}\right)^3 + \dots \quad (G1)$$

however, with different a . For C_{NS} of Eq. (106)

$$a = B_{NS}(\omega), \quad (G2)$$

with B_{NS} given by Eq. (94). Alternatively, when the DL contributions to C_{NS} are calculated in the DGLAP framework, $a = a_{DGLAP}$:

$$a_{DGLAP} = \alpha_s(Q^2)C_F/(2\pi). \quad (G3)$$

In contrast, the expansions for the exponent in Eq. (17) involves integrations of $\alpha_s(k_\perp^2)$ and therefore those two cases look quite different. As this difference it is not essential for the topic we consider here, we will use the approximation of fixed QCD coupling for the DGLAP description of g_1^{NS} . In this case the most singular, i.e. DL contributions to the DGLAP expression for the anomalous dimension of g_1^{NS} can easily be obtained from the series for H_{NS} . By doing so, we arrive at the following series for the exponent in Eq. (106):

$$\Gamma^{DL} \equiv yH_{NS} = y\left[\frac{a}{4\omega} + \frac{a^2}{16\omega^3} + \frac{a^3}{32\omega^5}\right] + \dots, \quad (G4)$$

with a defined in Eq. (G2) and $y = \ln(Q^2/\mu^2)$, whereas in the DGLAP case the DL contribution to the exponent in Eq. (17) can again be obtained with replacement a by a_{DGLAP} :

$$\Gamma_{DGLAP}^{DL} \equiv \int_{\mu^2}^{Q^2} \frac{dk_\perp^2}{k_\perp^2} \gamma(\omega, \alpha_s) \frac{a_{DGLAP} y}{4\omega} + c_2 \frac{a_{DGLAP}^2 y^2}{\omega^2} + c_3 \frac{a_{DGLAP}^3 y^3}{\omega^3} + \dots \quad (G5)$$

with c_2, c_3 being numerical factors. Therefore, in the n -th order in α_s the most singular contribution to C_{NS} can be written as follows:

$$C_{NS}^{(n)} = c_{(n)} \frac{a^n}{\omega^{2n}} + O(1/\omega^{2n-1}) \quad (G6)$$

where $c_{(n)}$ is a numerical factor. It can be obtained with further expansion of Eq. (105) into series. Similarly, the most singular contributions, $\Gamma^{DL\ n}$ and $\Gamma_{DGLAP}^{DL\ n}$ are

$$\Gamma^{(n)\ DL} = y\tilde{c}_n \frac{a^n}{\omega^{2n-1}}, \Gamma_{DGLAP}^{(n)\ DL} = c_n \frac{a_{DGLAP}^n y^n}{\omega^n}, \quad (G7)$$

with \tilde{c}_n, c_n be numerical factors.

The phase Φ in the Mellin integrals (E1) and (F1) can now be written as follows:

$$\begin{aligned} \Phi &\approx \omega\zeta + \ln C_{NS} + y\tilde{c}_n \frac{a^n}{\omega^{2n-1}}, \\ \Phi_{DGLAP} &\approx \omega \ln(1/x) + \ln C_{NS}^{DGLAP} + c_n \frac{a_{DGLAP}^n y^n}{\omega^n}, \end{aligned} \quad (G8)$$

where we have denoted $\zeta = (1/2) \ln(Q^2/(x^2\mu^2))$. Let us first consider the asymptotics of g_1^{NS} at $Q^2 \sim \mu^2$. In this case the last term in each of the equations in (G8) is zero and the stationary point is determined from the following equation:

$$\zeta + \frac{C'_{NS}}{C_{NS}} = 0. \quad (G9)$$

Obviously, this equation does not have solutions leading to the Regge behavior of g_1^{NS} because all terms in Eq. (G1) are positive.

Let us consider now the case of large Q^2 : $Q^2 \gg \mu^2$. The equations for the stationary points of the phases in Eq. (G8) are:

$$\Phi' = \zeta + \frac{C'_{NS}}{C_{NS}} - y\tilde{c}^{(n)}(2n-1)\frac{a^n}{\omega^{2n}} = 0, \quad (G10)$$

$$\Phi'_{DGLAP} = \ln(1/x) + \frac{C'_{NS}{}^{DGLAP}}{C_{NS}^{DGLAP}} - c_n n \frac{a_{DGLAP}^n y^n}{\omega^{n+1}} = 0.$$

The use of Eq. (G6) for the coefficient function makes easy to see that the term C'_{NS}/C_{NS} and $C'_{NS}{}^{DGLAP}/C_{NS}^{DGLAP}$ are proportional to $1/\omega$, so these terms are much less singular than the last terms in Eq. (G10) and therefore they can be dropped. After that solving Eq. (G10) is easy and we arrive at the following approximate expression for the stationary point:

$$\omega_0 \approx ((2n-1)c^{(n)}a^{(n)}y/\zeta)^{1/2n}, \quad \omega_0^{DGLAP} \approx (nc_n a_{DGLAP}^n y^n / \ln(1/x))^{1/(n+1)} \quad (G11)$$

and leads to the following asymptotics:

$$g_1^{NS} \sim \exp \left[\left(a^{(n)} \right)^{1/2n} y^{1/2n} \zeta^{(1-1/2n)} \right], \quad g_1^{NS}{}^{DGLAP} \sim \exp \left[\left(a_{DGLAP}^n \right)^{1/(n+1)} y^{1/(n+1)} (\ln(1/x))^{(1-1/(n+1))} \right] \quad (G12)$$

Obviously, Eq. (G12) coincides with the LO DGLAP asymptotics (132) at $n = 1$. Eq. (G12) demonstrates explicitly that the asymptotics of $g_1^{NS}{}^{DGLAP}$ always depends on Q^2 and the Regge behavior of g_1^{NS} and $g_1^{NS}{}^{DGLAP}$ cannot be achieved at any fixed n . On the other hand, the Regge behavior of g_1^{NS} and $g_1^{NS}{}^{DGLAP}$ is approached closer and closer when n grows, and is eventually achieved when the total resummation is performed. It is interesting to notice that the "intercept" of $g_1^{NS}{}^{DGLAP}$ in this case could depend on Q^2 through the Q^2 -dependence of $a_{DGLAP}^{(n)}$. Such a dependence originates from the Q^2 -dependence of α_s . However, we have shown in Sect. IV that the parametrization $\alpha_s = \alpha_s(Q^2)$ should not be used at small x .

-
- [1] G. Altarelli and G. Parisi, Nucl. Phys. B126 (1977) 297; V.N. Gribov and L.N. Lipatov, Sov. J. Nucl. Phys. 15 (1972) 438; L.N. Lipatov, Sov. J. Nucl. Phys. 20 (1972) 95; Yu.L. Dokshitzer, Sov. Phys. JETP 46 (1977) 641.
 - [2] M.A. Ahmed and G.G. Ross, Nucl. Phys. B 111 (1976) 441.
 - [3] E.B. Zijlstra and W.L. van Neerven, Nucl. Phys. B 417 (1994) 61, R. Mertig and W.L. van Neerven, J. Phys. C70 (1996) 637; W. Vogelsang, Phys. Rev. D 54 (1996) 2023; R. Hamberg and W.L. van Neerven, Nucl. Phys. B 379 (1992) 143; J. Kodaira, S. Matsuda, K. Sasaki, T. Kematsu, Nucl. Phys. B 159 (1979) 99; J. Kodaira, S. Matsuda, T. Muta, K. Sasaki, T. Kematsu, Phys. Rev. D 20 (1979) 627; M. Anselmino, A. Efremov, E. Leader, Phys. Rep. 261 (1995) 1. Erratum B 426 (1994) 245; W. Furmanski and R. Petronzio, Z. Phys. C 11 (1982) 293; M. Gluck, E. Reya, A. Vogt, Z. Phys. C 48 (1990) 471; M. Gluck, E. Reya, A. Vogt, Phys. Rev. D 45 (1992) 3986; M. Gluck, E. Reya, M. Stratmann, W. Vogelsang, Phys. Rev. D63(1996)4775 (hep-ph/9508347); E.G. Floratos, C. Kounnas and R. Lacaze, Nucl. Phys. B192 (1981) 417.
 - [4] M. Anselmino, A. Efremov, E. Leader, Phys. Rept. 261 (1995) 1, 1995, Erratum-ibid. 281 (1997) 399.
 - [5] G. Altarelli, R.D. Ball, S. Forte and G. Ridolfi, Nucl. Phys. B496 (1997) 337; Acta Phys. Polon. B29(1998)1145.
 - [6] E. Leader, A.V. Sidorov and D.B. Stamenov, Phys. Rev. D73 (2006) 034023; J. Blumlein, H. Botcher, Nucl. Phys. B636 (2002) 225; M. Hirai et al. Phys. Rev. D69 (2004) 054021.
 - [7] V.V. Sudakov, Sov. Phys. JETP 3 (1956) 65.
 - [8] V.N. Gorshkov, V.N. Gribov, G.V. Frolov, L.N. Lipatov, Yad. Fiz. 6(1967)129; Yad. Fiz. 6(1967)361.
 - [9] V.G. Gorshkov, Uspekhi Fiz. Nauk 110(1973)45.
 - [10] B.I. Ermolaev, S.I. Manaenkov, M.G. Ryskin, Z. Phys. C 69 (1996) 259; J. Bartels, B.I. Ermolaev, M.G. Ryskin, Z. Phys. C 70 (1996) 273; J. Bartels, B.I. Ermolaev, M.G. Ryskin, Z. Phys. C 72 (1996) 627.
 - [11] B.I. Ermolaev, M. Greco, S.I. Troyan, Phys. Lett. B579(2004)330; B.I. Ermolaev, M. Greco and S.I. Troyan, Nucl. Phys. B 594 (2001) 71; ibid 571(2000)137.
 - [12] B.I. Ermolaev, M. Greco, S.I. Troyan, Phys. Lett. B522(2001)57.
 - [13] A. Kotlorz and D. Kotlorz, Acta Phys. Polon. B39(2008) 1913.
 - [14] B.I. Ermolaev, M. Greco, S.I. Troyan, Phys. Lett. B622(2005)93.
 - [15] B.I. Ermolaev, M. Greco, S.I. Troyan, hep-ph/0511343.
 - [16] B.I. Ermolaev, M. Greco, S.I. Troyan, Eur. Phys. J. C50(2007)823. B.I. Ermolaev, M. Greco, S.I. Troyan, Eur. Phys. J. C51(2007)859.
 - [17] P.B.D. Collins, An introduction to Regge theory and high energy physics. Cambridge, 1977.
 - [18] A. Sommerfeld, Partial differential equations in physics. Ac. press, 1949; G.N. Watson, Proc. Roy. Soc. 95 (1918) 83.
 - [19] G.M. Prosperini, M. Raciti, C. Simolo, Prog. Part. Nucl. Phys. 58 (2007).

- [20] D.V. Shirkov, I.L. Solovtsov. hep-ph/9604363; Phys.Rev.Lett.79 (1997)1209.
- [21] D.V. Shirkov, I.L. Solovtsov. Theor.Math.Phys.150 (2007)132; A.P. Bakulev, S.V. Mikhailov. arXiv:0803.3013; A.P. Bakulev, S.V. Mikhailov, N.G. Stefanis. Phys.Rev.D72 (2005)074014, Erratum-ibid.D72 (2005)119908; A.P. Bakulev. arXiv:0809.0761; R.S. Pasechnik, D.V. Shirkov, O.V. Teryaev. Phys.Rev.D78:071902,2008.
- [22] S. Brodsky, G.P. Lepage, P. B. Makenzie. Phys. Rev. D 28 (1983) 228.
- [23] Yu.L. Dokshitzer, D.I. Diakonov, S.I. Troyan. Phys.Rep.58(1980)269.
- [24] G.Curci and M. Greco. Phys.Letts. B79 (1978)406; G. Curci, M. Greco, Y Srivastava. Phys.Rev.Letts. 43(1979)834; G.Curci and M. Greco. Phys.Letts. B92 (1980)175
- [25] D. Amati, A. Bassetto, M. Ciafaloni, G. Marchesini, G. Veneziano. Nucl.Phys.B 173(1980)429; A. Bassetto, M. Ciafaloni G. Marchesini. Phys.Rept.100(1983)201.
- [26] Yu.L. Dokshitzer, D.V. Shirkov. Z. Phys. C 67 (1995) 449.
- [27] B.I. Ermolaev, S.I. Troyan. Phys. Lett. B 666(2008)256.
- [28] L.N. Lipatov. Zh.Eksp.Teor.Fiz.82 (1982)991; Phys.Lett.B116 (1982)411.
- [29] R. Kirschner and L.N. Lipatov. ZhETP 83(1982)488; Nucl. Phys. B 213(1983)122.
- [30] B.I. Ermolaev, V.S. Fadin, L.N. Lipatov. Yad. Fiz. 45 (1987) 817.
- [31] B.I. Ermolaev, M. Greco, S.I. Troyan. Acta Physica Pol. B 38 (2007) 2243.
- [32] S.D. Bass, B.L. Ioffe, N.N. Nikolaev, A.W. Thomas. J. Moscow Phys.Soc. 1 (1991) 317.
- [33] B.I. Ermolaev. Sov. J. Nucl. Phys. 49(1989)341.
- [34] M. Chaichian, B. Ermolaev. Nucl. Phys. B 451 (1995) 194.
- [35] V.N. Gribov. Yad. Fiz. 5 (1967) 399.
- [36] B.I. Ermolaev, S.I. Troyan. Proc of 5th Int Workshop on DIS. NY, 1998, p 861.
- [37] J. Soffer and O.V. Teryaev. Phys. Rev.56(1997)1549; A.L. Kataev, G. Parente, A.V. Sidorov. Phys.Part.Nucl 34(2003)20; Nucl.Phys.A666/667(2000)184; A.V. Kotikov, A.V. Lipatov, G. Parente, N.P. Zotov. Eur.Phys.J.C26(2002)51; V.G. Krivohijine, A.V. Kotikov, hep-ph/0108224; A.V. Kotikov, D.V. Peshekhonov hep-ph/0110229.
- [38] N.I. Kochelev, K. Lipka, W.D. Nowak, V. Vento, A.V. Vinnikov. Phys. Rev. D 67 (2003) 074014.
- [39] A. Kotlorz and D. Kotlorz. Acta Phys. Polon. B35 (2004)2503; Eur.Phys.J.C48 (2006)457.
- [40] J. Blumlein, A. Vogt. J. Blumlein, A. Vogt. Acta Phys. Polon. B27 (1996) 1309. J. Blumlein, S. Riemersma, A. Vogt. Nucl.Phys.Proc.Suppl.51C (1996) 30; Acta Phys. Polon. B28 (1997) 577.
- [41] O.Nachtmann. Nucl. Phys. B 63 (1973) 237.
- [42] B. Badelek and J. Kwiecinski. Z. Phys. C 43 (1989) 251; Rev. Mod. Phys. 68 (1996)445; Phys. Lett. B 418 (1998) 229.
- [43] E. Leader, A.V. Sidorov, D.B. Stamenov. hep-ph/0509183; E. Leader, A.V. Sidorov, D.B. Stamenov. Phys. Rev.D 67 (2003) 074017; Phys.Part.Nucl.35 (2004)S38-S43; Phys.Rev.D75 (2007) 074027.
- [44] COMPASS collab (E.S. Ageev et al). Phys.Lett.B633 (2006) 25.
- [45] COMPASS collab (E.S. Ageev et al). Phys.Lett.B647(2007)330.
- [46] B.I. Ermolaev, M. Greco, S.I. Troyan. Eur. Phys. J. C 58 (2008)29.